DISSERTATION

IMMISCIBLE MULTIPHASE FLOW IN GROUND WATER HYDROLOGY: A COMPUTER ANALYSIS OF THE WELL FLOW PROBLEM

Submitted by
Willem Brutsaert

In partial fulfillment of the requirements

for the Degree of Doctor of Philosophy

Colorado State University

Fort Collins, Colorado

May, 1970

COLORADO STATE UNIVERSITY

May 1970

WE HEREBY RECOMMEND THAT THE DISSERTATION PREPARED UNDER

OUR SUPERVISION BY Willem Brutsaert

ENTITLED Immiscible Multiphase Flow in Ground Water Hydrology:

A Computer Analysis of the Well Flow Problem

BE ACCEPTED AS FULFILLING THIS PART OF THE REQUIREMENTS FOR THE DEGREE

OF DOCTOR OF PHILOSOPHY

Committee on Graduate Work

Major Professor

Head of Department

Examination Satisfactory

Committee on Final Examination

Chairman

Permission to publish this dissertation or any part of it must by obtained from the Dean of Graduate School.

ABSTRACT OF DISSERTATION

IMMISCIBLE MULTIPHASE FLOW IN GROUND WATER HYDROLOGY:
A COMPUTER ANALYSIS OF THE WELL FLOW PROBLEM

A mathematical analogue of immiscible multiphase flow in porous media is derived considering three compressible fluids -- two liquids and one gas. Isothermal conditions are assumed so that fluid properties such as compressibility, density, viscosity, and solubility of gas in the liquid are functions of fluid pressure only.

A well flow computer simulator is developed by discretizing the mathematical analogue with fully implicit finite differences. A Newton iteration scheme is utilized to solve the system of non-linear difference equations.

The problem solved in this study is that of free surface gravity well flow, including the effect of partial penetration. A theoretically accurate solution is obtained concluding that unconfined well flow is a multiphase flow phenomenon affecting aquifer response. The importance of capillarity, of air dissolved in water, of water compressibility, as well as the effect of the multiphase flow approach upon the shape of the free surface are discussed. Practically, it is concluded that confined well flow analyses do not apply to free surface gravity well flow problems.

Willem Brutsaert
Department of Civil Engineering
Colorado State University
Fort Collins, Colorado, 80521
May, 1970

ACKOWLEDGEMENTS

The author's advisor and committee chairman, Dr. E. A. Breitenbach, Associate Professor, Civil Engineering Department, Colorado State University, is gratefully acknowledged for constructive comments and encouragement. Dr. D. K. Sunada's guidance during the author's graduate curriculum is deeply appreciated. Thanks are extended to other members of the committee: Dr. H. J. Morel-Seytoux, Department of Civil Engineering, and Dr. J. P. Waltz, Department of Geology.

The author is indebted to Dr. R. A. Wattenbarger of Scientific Software Corporation, Denver, for countless hours of consultation, a most rewarding experience, made possible through Dr. E. A. Breitenbach, President of the Corporation.

Funds were provided by Project 110 of the Colorado State University Experiment Station, to sponsor the author's Graduate Research Assistantship; his sincere thanks are extended. Grants covering computer costs were provided by the University, and were very much appreciated.

Finally, the author is indebted to his wife, Lieve, for her moral support in continual encouragement.

TABLE OF CONTENTS

TABLE OF CONTENTS (Continued)

LIST OF TABLES

LIST OF FIGURES

LIST OF FIGURES (Continued)

1. INTRODUCTION

1.1 Problem Statement

When liquids or gases filter into or through soils, other fluids are displaced or adsorbed. When the fluids are separated by sharp interfaces, the phenomenon is called immiscible multiphase flow. In this study, only immiscible fluids are considered; this phenomenon will simply be called multiphase flow.

The general multiphase flow system of this study consists of a ground water reservoir with air overlaying fresh water, the fresh water in its turn overlaying brine, or of a petroleum reservoir with gas overlaying oil, the oil in its turn overlaying water or brine. The gaseous phase on top will never be in contact with the lowest liquid phase, such that the middle phase, oil or fresh water, will be the dependent phase. A pumped well will produce the dependent phase, oil or fresh water. In the petroleum technology, this is a typical coning problem where gas and water are coning into the oil phase under the effect of pumping, usually a confined system. In ground water hydrology, generally it can be a free surface gravity well flow problem, where air and salt water are coning into the pumped fresh water phase; more simply, when the air phase is missing, it can be a fresh water-salt water confined coning problem; when the salt water phase is missing, it can be an unconfined free surface gravity well flow problem. It is this last problem which is of interest in this study.

To present, the problem of multiphase unconfined free surface gravity well flow is unsolved. Mathematical complexity is the obstacle. The multiphase flow process is represented by a system

of non-linear partial differential equations, one for each phase, resulting from a combination of the continuity principle with Darcy's law. Avoiding the mathematical complexity of multiphase flow, a non-linear unconfined one phase flow equation can be obtained, assuming that the flow is horizontal and that all storage comes from the immediate drawdown at the free surface. To date, even this relatively simple equation is not known to have an analytical solution, so that solutions of a linear confined horizontal flow equation were extended to the unconfined flow case.

The only hope for solving the multiphase flow system is by numerical techniques. In the past, the numerical solution of the multiphase flow equation in radial flow coordinates was a very difficult and uneconomical problem, with computer time often exceeding real flow time. Therefore, very little numerical work, and only under confined flow conditions, has been done in radial coordinates. The main problem was computational instability near the well which resulted from high flow velocities in this region, and at the same time from the explicit evaluation (at the old time level) of coefficients in an implicit (at the new time level) difference scheme. In multiphase flow, these coefficients consist of highly non-linear saturation dependent functions. The completely implicit treatment of the finite difference equations is a way to avoid this computational instability but results in the simultaneous solution of a system of non-linear equations -- a difficult problem in itself. It is the fully implicit scheme which will be explored in the numerical approach of this study.

The study of multiphase free surface well flow is important in the light of aquifer test analysis. It appears from the literature

that the practice of analyzing unconfined aquifer data with confined flow analytical solutions to obtain aquifer characteristics is highly questionable. It is the author's belief that fully saturated confined and free surface well flow are two totally different flow phenomena. Under some circumstances, especially in finer materials such as silt and clay aquifers, capillarity becomes important. A considerable portion of the unconfined flow phenomenon may take place in the cone of depression. This may affect the aquifer response to drainage or pumping. Also, when a well is pumped, the pressure declines around the well bore. Air dissolved in the water may evolve from solution and occupy space, decreasing the effective permeability to water. At first, the liberated air exists as small isolated bubbles, but may become continuous when a critical air saturation is attained. At this point, air would start to flow. If the well is pumped at a constant pressure, its discharge will decline.

It is concluded that the free surface well flow problem is a multiphase flow phenomenon and should be treated accordingly. In the light of an ever increasing fresh water demand, the proper evaluation of unconfined aquifer characteristics is of utmost importance. It is hoped that with this study a contribution is made toward better management of the total water resource.

1.2 Objectives

This dissertation is concerned with the question whether unconfined well flow is a multiphase flow phenomenon affecting aquifer response. An answer is pursued by:

(1) Development of a two-dimensional three-phase mathematical simulator of the well flow problem, by approximating the fundamental flow equations with finite differences.

(2) Development of a completely implicit difference analogue for solving the flow equations, attempting to make multiphase radial well flow models economically feasible.

(3) Evaluation of the multiphase flow approach by comparing solutions obtained in this study with previous analytical approaches.

2. HISTORY OF MULTIPHASE FLOW

2.1 Multiphase Flow and Ground Water Hydrology

Multiphase flow in porous media is not a new concept. Petroleum engineers have been concerned with the simultaneous flow of liquids and gases for several decades; to date, through laboratory studies and mathematical simulation, three-dimensional three-phase flow problems are fairly well understood.

Soil physicists and drainage and irrigation engineers, concerned with the infiltration and the distribution of water in the upper soil profile, realized as early as 1907 (Buckingham, 14) that in unsaturated soils, water will flow from points of higher head to points of lower head, causing differences in moisture content. To date, all analytical, numerical, and laboratory work in this field is still centered around the thesis of Richards, published in 1931 (47). He assumed that no flow occurs in the air phase, in other words, no pressure gradients, and that the movement of the water may be defined without reference to the other fluids (air) contained in the pores.

As opposed to the abundant literature on multiphase flow in the petroleum industry, and on the Richards approach in the field of irrigation and drainage, literature on this subject in ground water hydrology is completely lacking. To date, all problems in ground water hydrology have been treated solely from a one phase flow point of view. In other words, the porous medium is always fully saturated with water and the flow or displacement of air is totally disregarded. It was realized, however, that the free surface flow problem is not a phenomenon in which water is instantaneously released from storage. This

assumption was used in all analytical studies of confined flow and was applied to unconfined flow problems.

Physical aspects of multiphase flow such as capillarity, the extension of Darcy's law to unsaturated porous media, and the concept of relative permeability are beyond the scope of this study. They were previously discussed by i.a. Muskat (43), Scheidegger (49), Childs (15), Morel-Seytoux (42), Corey (18), and Bear et al. (1).

2.2 Radial Multiphase Flow Simulation

For extensive treatments of multiphase reservoir simulation the reader is referred to i.a. Breitenbach et al. (9, 10, 11), Dougherty and Mitchell (21), Earlougher (24), Fagin and Stewart (25), and Odeh (45). Because of numerical difficulties, very little simulation has been done in radial coordinate systems such as well flow problems and coning studies. The reasons for these numerical difficulties stem from the very nature of the radial coordinate system. Since detailed pressure and saturation distributions are required around the well bore, grid blocks near the well bore should be small, resulting in anisotropy in the geometry of the grid block configuration. Moreover, steep pressure gradients leading to high flow velocities do occur in the vicinity of the well bore. Also, due to the highly non-linear saturation dependent functions of the multiphase flow system, severe computational instability in the form of saturation oscillations in the grid blocks near the well bore often occurs. To retain stability, time steps are to be reduced considerably, often to the point where computer time exceeds real flow time. Hence, these studies became economically unfeasible. It is evidenced by the literature that

instability may result when the highly non-linear saturation dependent coefficients of the finite difference equations are evaluated at the beginning of a time step and held constant throughout that time step. This technique is sometimes called "implicit-explicit" or also "mixed".

Welge and Weber (71) studied single well coning behavior with two-phase, two-dimensional, incompressible fluid flow equations, solved by the alternating direction implicit procedure. Several examples of water and gas coning calculations, including studies in both laboratory models and producing wells, are presented. They experienced the above described oscillation near the well bore, which they described as a drastic fluctuation yielding meaningless results.

Blair and Weinaug (3) demonstrated the oscillatory behavior in a coning problem by comparing a fully implicit scheme with an implicit-explicit scheme. In the fully implicit scheme, all quantities in the distance difference are evaluated at the new time level. For the same size time step, the fully implicit scheme gave a stable solution, whereas the mixed technique wildly fluctuated. By using the fully implicit scheme, they experienced an increase in computer time of two-to-threefold as compared to the mixed techniques. The following advantages were mentioned: (1) The implicit difference equation is stable in cases where the mixed equation is not. (2) The implicit equation has lower time truncation than the mixed equation, permitting longer time steps to be taken.

Spivak and Coats (55) state that in coning problems the numerical instability is due to the explicit handling of saturation dependent transmissibilities (transmissibility in their study is defined by the coefficients of the discretized flow equations) and production terms

in the finite difference solution of the flow equations. Their examples show that the implicit handling of production terms alone can result in a fivefold increase in permissible time step for a coning simulation with virtually no increase in computing time per time step. Updating the production terms without updating transmissibilities is questionable, although their concern of eliminating the instability encountered in coning simulation without introducing the complexity of the fully implicit scheme is well founded.

From the above studies on modeling of coning problems it appears that the fully implicit finite difference scheme offers a great challenge for solving non-linear muliphase well flow problems. Unfortunately, the fully implicit scheme results in a set of non-linear difference equations to be solved simultaneously.

Newton's method, also called the Newton iteration process or Newton linearization, is mathematically the most preferable of the several known methods for the solution of systems of non-linear equations because of its quadratic convergence (64). Practically, however, a very important limitation on Newton's method and, in fact, on all of the so-called functional iteration methods, is that it does not generally converge to a solution from an arbitrary starting point. Thus Newton's method may fail to converge if the initial estimate is not sufficiently close to the root. Its theory and extension to n-dimensional vector spaces appears in a number of standard textbooks on functional analysis or numerical analysis (27, 28, 35, Appendix A).

Blair and Weinaug (3) demonstrated the applicability of Newton's method in coning problems. They concluded that the Newton method is entirely practical for multiphase flow problems. In their approach the

flow equations were solved simultaneously. In this study, however, it is thought that advantage can be taken of the quasi-linear nature of the pressure dependent functions. This can be done by reducing the three flow equations into a single equation in terms of pressure of one of the phases, and three saturation equations. The newton linearization process is first performed on the pressure equation which is then solved for pressures. Subsequently, the saturation equations are Newton-linearized and iterated upon, until saturations are compatible with the first pressure iterate. This process is called a 'Newtonian iterate' and is repeated until a convergence criterion is met. It is felt that a more efficient Newtonian iteration scheme can be obtained by using this separation technique. One Newtonian iterate on pressure should often lead sufficiently close to the final answer. A similar separation technique of the flow equations is very popular in reservoir simulation. The pressure equation is obtained in a manner which eliminates all time derivatives, or differences, of saturations. The resulting pressure equation is then solved implicity, followed by an explicit updating of saturation; this separation principle was proposed independently by Stone et al. (61) and by Sheldon et al. (51) in 1960.

It is apparent from this short literature survey that the numerical solution of the radial multiphase flow equations may have become economically feasible and that existing methods can possibly be improved upon.

3. MATHEMATICAL ANALOGUE OF MULTIPHASE FLOW

Mathematically, multiphase flow can be very conveniently described in terms of equations. The principle of continuity (mass balance) is combined with Darcy's law and with thermodynamic relationships which describe the pressure-volume-temperature behavior. For each of the different phases, a set of non-linear partial differential equations of the parabolic type will result, commonly called the fundamental flow equations. Complete derivations of these equations can for example be found in Muskat (43) and Breitenbach et al. (10).

The following derivation is valid for isothermal three-phase, two-dimensional flow. The isothermal condition is assumed for simplicity. The derivation is done in a general way such that either rectangular (vertical cross sections) or radial coordinates apply, depending upon the definition of cross-sectional area of flow in Darcy's law, and pore volume. The two dimensions considered in this study are the horizontal and the vertical. Radial symmetry is assumed. The three phases considered are two liquids and one gas. For convenience, the two liquids are given specific names, oil and water, with the understanding that they could have been any two other immiscible liquids. The gas phase will be in contact only with one of the liquids, oil in this case. Consequently, gas dissolves in the oil, but not in the water and also, only the gas-oil and oil-water capillary pressure relationships are to be considered. The two-phase air-water abstraction, as will be used in this study, is easily deduced from this general three-phase flow case, i.e., all characteristics and assumptions of the oil and gas

phases can be simply translated upon the air-water system, disregarding the third phase (water) in the general three-phase model.

Because of the isothermal assumption, the fluid properties such as viscosity, density and gas-liquid solubility will only depend upon pressure.

3.1 The Mass Balance Equations

The mass balance in its simplest form for the differential element of Figure 1 states that for any of the phases the mass flow out of the

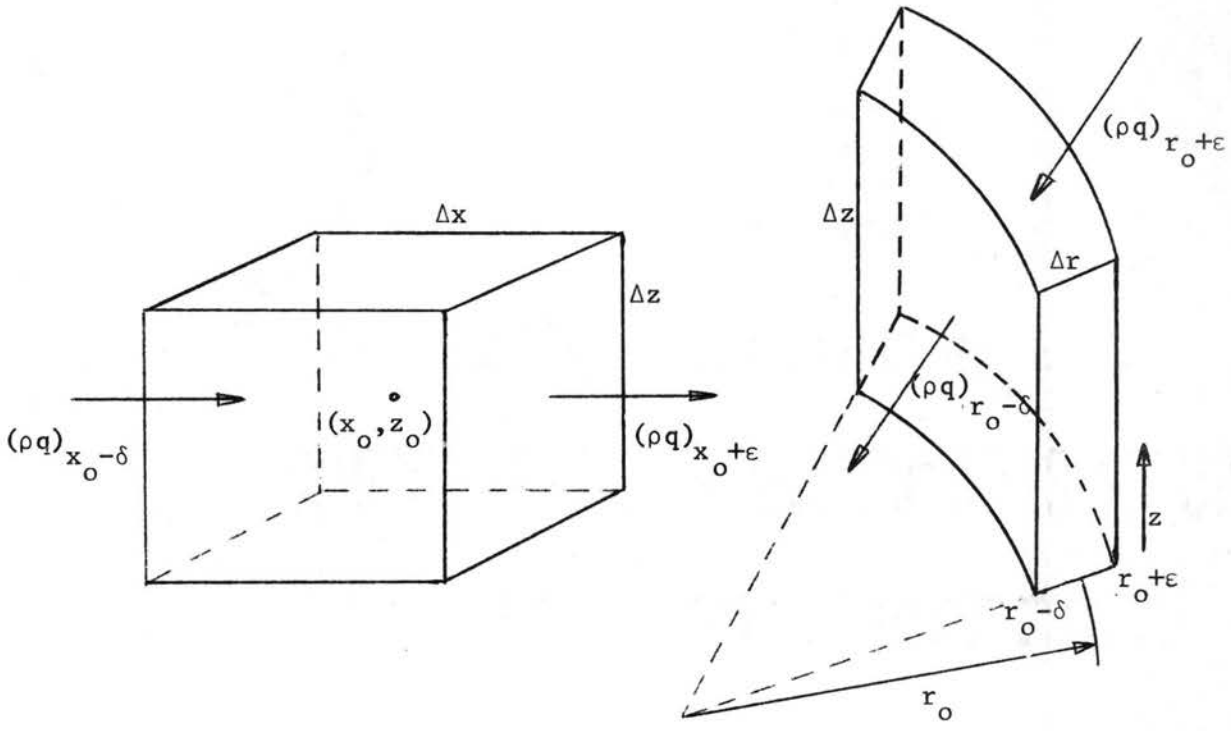

1.a 1.b

Figure 1. Differential element for developing the mass balance equations.

element subtracted from the mass flow into the element is the rate change of mass (change in storage), at aquifer conditions, i.e.:

$$(\rho_A\, q_A)_{out} - (\rho_A\, q_A)_{in} = -\frac{\partial}{\partial t}\ (\rho_A\, V_b\, \phi S) \qquad (1)$$

in which: ρ_A = fluid density at aquifer conditions

q_A = flow rate at aquifer conditions (FT^3/day)

V_b = bulk volume of differential element

ϕ = porosity

S = fluid saturation.

Proceeding now for one of the phases, say oil, it can be also said that the net mass flow or the left hand side of equation 1 is the mass rate of depletion (MROD) of the differential element:

$$(MROD)_o = (\rho_{oA}\, q_{oA})_{x_o+\varepsilon} - (\rho_{oA}\, q_{oA})_{x_o-\delta} \pm \rho_o\, q_{op} \qquad (2)$$

in which: x_o = center of mass of differential element

q_{op} = flow rate sink (+) or source (-), commonly called the production term

subscript o = oil phase

δ = distance of left face of element to center of mass

ε = distance of right face of element to center of mass.

Considering the mass flow function as a continuously differentiable function in time and space, it can be expanded about the center of mass (x_o) of the differential element by Taylor series:

$$(\rho_{oA}\, q_{oA})_{x_o-\delta} = (\rho_{oA}\, q_{oA})_{x_o} - \frac{\partial}{\partial x}\ (\rho_{oA}\, q_{oA})_{x_o}\ (\delta) + \frac{1}{2!}\frac{\partial^2}{\partial x^2}\ (\rho_{oA}\, q_{oA})(\delta)^2 - \ldots \qquad (3)$$

and also:

$$(\rho_{oA}\, q_{oA})_{x_o+\varepsilon} = (\rho_{oA}\, q_{oA})_{x_o} + \frac{\partial}{\partial x}(\rho_{oA}\, q_{oA})_{x_o}(\varepsilon) + \frac{1}{2!}\frac{\partial^2}{\partial x^2}(\rho_{oA}\, q_{oA})(\varepsilon)^2 + \ldots \tag{4}$$

In the limit, when Δx goes to zero, the second order terms and higher of equations 3 and 4 can be neglected. This argument holds only when deriving a differential equation. When deriving finite differences, however, by Taylor series expansion, second and higher order terms cancel because of the linearity principle between nodes in the discretization process. After subtracting equation 3 from equation 4, and substituting the result into equation 2, the following expression for MROD is obtained (note: $\varepsilon + \delta \equiv \Delta x$)

$$(\text{MROD})_o = \frac{\partial}{\partial x}(\rho_{oA}\, q_{oA})_{x_o}\, \Delta x \pm \rho_o\, q_{op} \tag{5}$$

The complete mass balance equation then in two dimensions for oil flow under aquifer conditions becomes

$$\frac{\partial}{\partial x}(\rho_{oA}\, q_{oA})_{x_o}\Delta x + \frac{\partial}{\partial z}(\rho_{oA}\, q_{oA})_{z_o}\Delta z \pm \rho_o\, q_{op} = -\frac{\partial}{\partial t}(\rho_{oA}\, V_b\, \phi\, S_o) \tag{6}$$

It is practical to translate equation 6 to surface conditions or atmospheric conditions. For this purpose it will suffice to define a factor B, commonly called formation volume factor (F.V.F.) in the petroleum technology; it is a ratio which relates aquifer volumes to surface volumes, hence, a fluid compressibility factor. If it is further assumed that the bulk volume, V_b, is invariable, that the porosity is constant in time, and that during a time step the surface (atmospheric) pressure is invariant in space and time, the mass balance equation finally becomes:

$$\frac{\partial}{\partial x}\left(\frac{q_{oA}}{B_o}\right)\Delta x + \frac{\partial}{\partial z}\left(\frac{q_{oA}}{B_o}\right)\Delta z = V_b\,\phi\,\frac{\partial}{\partial t}\left(\frac{S_o}{B_o}\right) \pm q_{op} \qquad (7)$$

The assumption of constant porosity in time can create serious problems in subsiding unconfined aquifers. The problem of subsidence is not considered in this study.

Analogously, the mass balance equation for water would be:

$$\frac{\partial}{\partial x}\left(\frac{q_{wA}}{B_w}\right)\Delta x + \frac{\partial}{\partial z}\left(\frac{q_{oA}}{B_o}\right)\Delta z = V_b\phi\,\frac{\partial}{\partial t}\left(\frac{S_w}{B_w}\right) \pm q_{wp} \qquad (8)$$

To obtain the gas balance equation, two separate mass flows are to be considered, (1) mass flow of free gas, and (2) mass flow of gas in solution in the oil. With the definition of Rs , the solution gas ratio, to relate a standard volume of gas dissolved in a standard volume of liquid (oil) at aquifer conditions, the gas balance equation can be conveniently written as:

$$\frac{\partial}{\partial x}\left(\frac{q_{gA}}{B_g} + \frac{Rs}{B_o}\,q_{oA}\right)\Delta x + \frac{\partial}{\partial z}\left(\frac{q_{gA}}{B_g} + \frac{Rs}{B_o}\,q_{oA}\right)\Delta z = V_b\,\phi\,\frac{\partial}{\partial t}\left(\frac{S_g}{B_g} + \frac{Rs\;S_o}{B_o}\right) \pm q_{gp} \qquad (9)$$

in which q_{gp} is the total gas production term (free gas plus solution gas).

3.2 The Fundamental Flow Equations

To obtain the fundamental flow equations from the mass balance equations 7, 8 and 9, it suffices to accept the validity of Darcy's law under multiphase flow conditions, in which for each of the phases permeability is now a function of saturation. Rigorous discussions of the validity of this postulate were made previously in the literature

(15, 43, 44, 49). The flow potential involves a pressure force, a capillary pressure force and a gravitational force. Capillary pressure conveniently relates pressures of the different phases. This relationship is:

$$p_c = p_{nw} - p_w \tag{10}$$

in which p_c = capillary pressure

p_{nw} = pressure in the nonwetting phase

p_w = pressure in the wetting phase.

Discussions of the phenomenon of capillarity, its dependence on saturation and its importance in multiphase flow are numerous (15, 18, 42, 43). Unfortunately, capillary pressure is not a single valued function of saturation but is affected by hysteresis (1, 15, 42). In this study of gravity drainage of an aquifer by a pumped well, a single valued capillary pressure versus saturation relationship obtained under draining conditions applies.

With Darcy's law, the capillary pressure relation, and using the oil pressure as the reference pressure, the volumetric flux terms "q" become:

$$q_{oA} = - A \frac{k\ kro}{\mu_o} (\nabla p_o + \rho_{oA} g \nabla h) \tag{11}$$

$$q_{gA} = - A \frac{k\ krg}{\mu_g} (\nabla p_o + \nabla p_{cog} + \rho_{gA} g \nabla h) \tag{12}$$

$$q_{wA} = - A \frac{k\ krw}{\mu_w} (\nabla p_o - \nabla p_{cow} + \rho_{wA} g \nabla h) \tag{13}$$

in which: p_o = oil pressure

p_{cog} = capillary pressure between the oil and gas phases

p_{cow} = capillary pressure between the water and oil phases

ρ = fluid density

h = elevation above a reference plane

k = permeability (intrinsic)

kr = relative permeability (fraction of k)

A = cross-sectional area of flow

μ = fluid viscosity

g = acceleration of gravity

∇ = gradient

Subscript A = aquifer conditions.

Substituting equations 11, 12 and 13 into equations 7, 8, and 9, the fundamental flow equations result

$$\frac{\partial}{\partial x}\left(\frac{k\ kro}{B_o\ \mu_o} A_x \frac{\partial \Phi_o}{\partial x}\right)\Delta x + \frac{\partial}{\partial z}\left(\frac{k\ kro}{B_o\ \mu_o} A_z \frac{\partial \Phi_o}{\partial z}\right)\Delta z = V_b\ \phi\ \frac{\partial}{\partial t}\left(\frac{S_o}{B_o}\right) \pm q_{op} \qquad (14)$$

$$\frac{\partial}{\partial x}\left(\frac{k\ krw}{B_w\ \mu_w} A_x \frac{\partial \Phi_w}{\partial x}\right)\Delta x + \frac{\partial}{\partial z}\left(\frac{k\ krw}{B_w\ \mu_w} A_z \frac{\partial \Phi_w}{\partial z}\right)\Delta z = V_b\ \phi\ \frac{\partial}{\partial t}\left(\frac{S_w}{B_w}\right) \pm q_{wp} \qquad (15)$$

$$\frac{\partial}{\partial x}\left(\frac{k\ krg}{B_g\ \mu_g} A_x \frac{\partial \Phi_g}{\partial x} + Rs\ \frac{k\ kro}{B_o\ \mu_o} A_x \frac{\partial \Phi_o}{\partial x}\right)\Delta x + \frac{\partial}{\partial z}\left(\frac{k\ krg}{B_g\ \mu_g} A_z \frac{\partial \Phi_g}{\partial z} + Rs\ \frac{k\ kro}{B_o\ \mu_o} A_z \frac{\partial \Phi_o}{\partial z}\right)\Delta z$$

$$= V_b \phi\ \frac{\partial}{\partial t}\left(\frac{S_g}{B_g} + \frac{Rs\ S_o}{B_o}\right) \pm q_{gp} \qquad (16)$$

in which:

$$\Phi_o = p_o + \rho_{oA}\, g\, h \tag{17}$$

$$\Phi_g = p_o + p_{cog} + \rho_{gA}\, g\, h \tag{18}$$

$$\Phi_w = p_o - p_{cow} + \rho_{wA}\, g\, h \tag{19}$$

Equations 14, 15, and 16 are non-linear parabolic partial differential equations, each having the two dependent variables, pressure and saturation. They are linked by the following saturation relationship:

$$S_o + S_g + S_w = 1.0 \tag{20}$$

Together with equation 20, they constitute the mathematical analogue of three-phase flow in porous media. To date, numerical methods are the only means for solving them.

To summarize the above derivation the important assumptions and conditions under which the equations hold are listed below. Their significance is given in the previous text.

- Two dimensional flow (x,z or r,z directions with radial symmetry)
- Three-phase flow (oil, gas, water): phases immiscible
- Isothermal flow (fluid properties only function of pressure)
- Darcy's law applies under multiphase flow conditions
- The gas phase is in contact with the oil phase only, and therefore only dissolves in oil
- Gas dissolved in the oil retains its molecular identity (no chemical bounding)
- Surface conditions are invariant in space and time
- Pore volume is incompressible.

4. COMPUTER SIMULATION OF MULTIPHASE FLOW

The construction of the computer simulator requires the flow region (vertical cross section) to be superimposed by a discrete grid system. Figure 2 shows an isolated grid block (central block) together with its neighboring grid blocks, or cells, and (i,j) indexing.

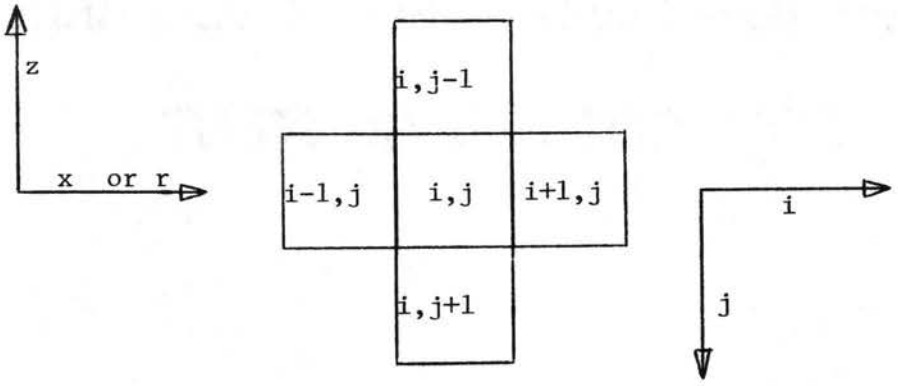

Figure 2. Grid system used for discretization of the continuous equations.

The network of reservoir elements, or the computation grid, conforms to the geometry of the actual reservoir system. The fundamental flow equations 14, 15 and 16 in discretized form apply to each of the individual elements; in other words, a mass balance is performed on each of the blocks.

4.1 The Finite Difference Form of the Flow Equations

The finite differences used to discretize the differentials of equations 14, 15 and 16 will be of a fully implicit nature, which means

that the flow equations are discretized at the new time level. Using centered finite differences, the r-component of the oil equation in the grid configuration of Figure 1 becomes

$$\frac{\partial}{\partial r}\left(\frac{k\ kro}{B_o\ \mu_o} A_r \frac{\partial \Phi_o}{\partial r}\right) \Delta r \simeq \left(\frac{k\ kro}{B_o\ \mu_o} A_r\right)_{i-1/2,j} \frac{\Phi_{o_{i-1,j}} - \Phi_{o_{i,j}}}{\Delta r} + \left(\frac{k\ kro}{B_o\ \mu_o} A_r\right)_{i+1/2,j} \frac{\Phi_{o_{i+1,j}} - \Phi_{o_{i,j}}}{\Delta r} \tag{21}$$

The subscript $i+1/2,j$ means that the function $\left(\frac{k\ kro}{B_o \mu_o} Ar\right)$ is to be representative for both cells (i,j) and $(i+1,j)$, which is explained in section 4.2.

To conveniently write the rather lengthy finite difference forms of the flow equations, the following notations will be defined and adhered throughout this dissertation.

$$\frac{k\ kro\ b_o}{\mu_o} A = CO$$

$$\frac{k\ krg\ b_g}{\mu_g} A = CG \tag{22}$$

$$\frac{k\ krw\ b_w}{\mu_w} A = CW$$

in which $b = \frac{1}{B}$.

The subscripts $i-1/2$, $i+1/2$, $j-1/2$, and $j+1/2$ will be respectively replaced by the letters W, E, N, and S, the idea being the West, East, North and South side of a cell. A difference operator is defined

as follows

$$\Delta\overline{CO}\ \Delta\Phi_o = \overline{CO}_W \left(\Phi_{o_{i-1,j}} - \Phi_{o_{i,j}}\right) + \overline{CO}_N\left(\Phi_{o_{i,j-1}} - \Phi_{o_{i,j}}\right) + \overline{CO}_E\left(\Phi_{o_{i+1,j}} - \Phi_{o_{i,j}}\right)$$
$$+ \overline{CO}_S \left(\Phi_{o_{i,j+1}} - \Phi_{o_{i,j}}\right) \qquad (23)$$

Note that $\overline{CO}$, $\overline{CG}$, and $\overline{CW}$ stem from the contraction of CO, CG, and CW with the spatial increment Δr or Δz in the denominator of the spatial differences of equation 21.

With the above definitions in mind the fundamental flow equations in discretized form become

$$\Delta\overline{CO}^{n+1}\ \Delta\Phi_o^{n+1} = \frac{V}{\Delta t}\left[(b_o\ S_o)^{n+1} - (b_o\ S_o)^n\right] + q_o \qquad (24)$$

$$\Delta\overline{CG}^{n+1}\ \Delta\Phi_g^{n+1} + \Delta Rs\ \overline{CO}^{n+1}\Delta\Phi_o^{n+1}$$
$$= \frac{V}{\Delta t}\left[(b_g\ S_g)^{n+1} - (b_g\ S_g)^n + (Rs\ b_o\ S_o)^{n+1} - (Rs\ b_o\ S_o)^n\right] + q_g \qquad (25)$$

$$\Delta\overline{CW}^{n+1}\ \Delta\Phi_w^{n+1} = \frac{V}{\Delta t}\left[(b_w\ S_w)^{n+1} - (b_w\ S_w)^n\right] + q_w \qquad (26)$$

The superscripts n and n+1 respectively refer to the present and new time level. The coefficients $\overline{CO}$, $\overline{CG}$, and $\overline{CW}$ are seen to be written at the new time level and since they are pressure and saturation

dependent, equations 24, 25 and 26 constitute a system of non-linear equations to be solved simultaneously.

4.2 The Flow Coefficients of the Discretized Flow Equations

The flow coefficients $\overline{CO}$, $\overline{CG}$, and $\overline{CW}$ of the flow equations determine the ability of flow between any two cells, and hence they should involve the medium and fluid properties of both cells.

In Figure 3, two cells (cell 1 and 2) in the r-direction of a radial coordinate system are considered.

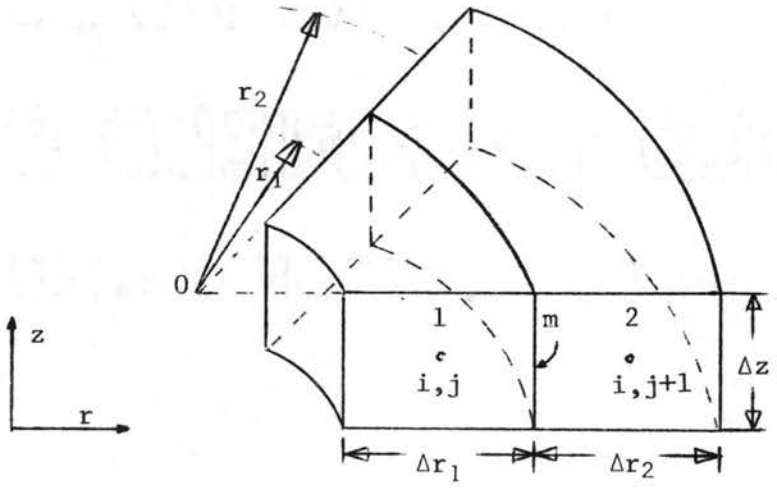

Figure 3. Segment of annulus, showing blocks in radial coordinate system.

Let m represent the face (vertical) between cell 1 and 2. At any point in the r-direction, the rate of flow of any of the phases is defined by Darcy's law:

$$q = \left(\frac{k\ kr\ b}{\mu}\right)\quad 2\pi r\quad \Delta z\quad \frac{\partial \Phi}{\partial r} \tag{27}$$

Since fluid and medium properties are constant in space within any one cell, it is possible to integrate the differential equation 27 from the center of cell 1 to its face m to come up with an expression of flow between these two points:

$$q_{1-m} = \left(\frac{k\ kr\ b}{\mu}\right)_1 \frac{2\pi\ \Delta z_1}{\ell n\left(\frac{r_1 + \frac{\Delta r_1}{2}}{r_1}\right)} (\Phi_m - \Phi_1) \tag{28}$$

Likewise,

$$q_{m-2} = \left(\frac{k\ kr\ b}{\mu}\right)_2 \frac{2\pi\ \Delta z_2}{\ell n\left(\frac{r_2}{r_2 - \frac{\Delta r_2}{2}}\right)} (\Phi_2 - \Phi_m) \tag{29}$$

and by continuity

$$q_{1-m} = q_{m-2} = q \tag{30}$$

From equation 28 and 29 one obtains:

$$\Phi_m - \Phi_1 = \frac{q\ \ell n\left(\frac{r_1 + \frac{\Delta r_1}{2}}{r_1}\right)\left(\frac{\mu}{b}\right)_1}{2\pi\ k_1\ kr_1\ \Delta z_1} \tag{31}$$

$$\Phi_2 - \Phi_m = \frac{q\ \ell n\left(\frac{r_2}{r_2 - \frac{\Delta r_2}{2}}\right)\left(\frac{\mu}{b}\right)_2}{2\pi\ k_2\ kr_2\ \Delta z_2} \tag{32}$$

Adding equation 31 and 32 and rearranging, an expression of the flow between two blocks is obtained

$$q = \frac{2\pi(k\ kr\ \Delta z)_1\ (k\ kr\ \Delta z)_2}{\left[\left(\frac{\mu}{b}\right)_1 (k\ kr\ \Delta z)_2\ \ell n\left(\frac{r + \frac{\Delta r}{2}}{r}\right)_1\right] + \left[\left(\frac{\mu}{b}\right)_2 (k\ kr\ \Delta z)_1\ \ell n\left(\frac{r}{r - \frac{\Delta r}{2}}\right)_2\right]} (\Phi_2 - \Phi_1) \tag{33}$$

If discontinuities in permeabilities are allowed to occur at the nodes of the cells, so that permeabilities would change from node to node, if the relative permeability is assigned at the cell from which the flow emanates (upstream block), and if the pressure dependent functions b and μ are averaged over the two blocks, then equation 33 simplifies to give

$$q = c\ kr_U \left(\frac{b}{\mu}\right)_{1-2} \frac{2\pi(k\ \ \Delta z)_1}{\ell n\ \frac{r_2}{r_1}}\ \ (\Phi_2 - \Phi_1) \tag{34}$$

The subscript U stands for upstream and the constant c is a conversion factor depending upon the units of p, k and μ. Finally, the flow coefficients of the oil phase in an (i,j) configuration in the r-direction can be defined as:

$$\overline{CO_W} = c\ kro_U \left(\frac{b_o}{\mu_o}\right)_W \frac{2\pi(k\Delta z)_{i,j}}{\ell n\ \frac{r_{i,j}}{r_{i-1,j}}} \tag{35}$$

$$\overline{CO}_E = c\ kro_U \left(\frac{b_o}{\mu_o}\right)_E \frac{2\pi\ (k\Delta z)_{i,j}}{\ell n \frac{r_{i+1,j}}{r_{i,j}}} \tag{36}$$

Following an analogous procedure the flow coefficients in the z-direction become

$$\overline{CO}_N = c\ kro_U \left(\frac{b_o}{\mu_o}\right)_N \frac{k_{i-1,j}\ \pi\left(r^2_{i+1/2,j} - r^2_{i-1/2,j}\right)}{\left(\frac{\Delta z_{i,j} + \Delta z_{i,j-1}}{2}\right)} \tag{37}$$

$$\overline{CO}_S = c\ kro_U \left(\frac{b_o}{\mu_o}\right)_S \frac{k_{i,j}\ \pi\left(r^2_{i+1/2,j} - r^2_{i-1/2,j}\right)}{\left(\frac{\Delta z_{i,j} + \Delta z_{i,j+1}}{2}\right)} \tag{38}$$

4.3 The Solution Process with Newton Linearization

The Newton linearization is an iterative technique, a general discussion of which in n-dimensonal vector spaces is given in Appendix A. In this section only the pertinent aspects of the Newton method, as they fit into the following solution scheme, will be explained.

The "residual" approach is taken to solve the system of equations; a description of the residual approach is given in Appendix B. The main reason for following the residual approach is that the final algebra of the equations comes out to be very simple due to cancellation of a number of terms which is characteristic of the Newton technique when

applied to the residual system. Moreover, when this process is done with a combination of single and double precision, extreme accuracy can be obtained when desired. In this study, single precision was utilized throughout because of the large mantissa length (60 bits) of the CDC 6400 computer used in this study.

The innovation in the proposed technique of this study is the fact that the Newton process is applied separately to one pressure equation and three saturation equations, whereas in earlier work (2) the Newton process was applied simultaneously to pressure and saturations of the system of equations 24, 25 and 26. By separating the pressure equation from the saturation equations advantage is taken of the quasi-linear behavior of the pressure dependent functions in the flow coefficients. With respect to saturations, however, the problem is highly non-linear. Very often, one Newtonian iterate on pressures will lead sufficiently close to the new time step values of pressures and hence a more efficient Newtonian process is attained.

4.3.1 The pressure equation - The first step in the solution process is to combine equations 24, 25 and 26 into one equation with oil pressure as the only dependent variable. Saturations are evaluated at the present iteration level in obtaining an improved pressure solution from this pressure equation.

Suppose that along the iteration process the k-th estimate of equations 24, 25 and 26 is obtained:

$$\overline{\Delta CO}^{k} \Delta\Phi_o^k - \frac{V}{\Delta t} \left[(b_o S_o)^k - (b_o S_o)^n \right] - q_o = r_o^k \qquad (39)$$

$$\Delta\overline{CG}^{k}\Delta\Phi_{g}^{k} + \Delta Rs\ \overline{CO}^{n+1}\ \Delta\Phi_{o}^{n+1} - \frac{V}{\Delta t}\left[(b_g S_g)^{k} - (b_g S_g)^{n} + (Rs\ b_o S_o)^{k} - (Rs\ b_o S_o)^{n}\right] - q_g = r_g^{k} \tag{40}$$

$$\Delta\overline{CW}^{k}\Delta\Phi_{w}^{k} - \frac{V}{\Delta t}\left[(b_w S_w)^{k} - (b_w S_w)^{n}\right] - q_w = r_w^{k} \tag{41}$$

The terms r_o^k, r_g^k, and r_w^k are defined as the residual errors. Subtracting equation 39 from 24, 40 from 25, and 41 from 26, assuming that gravity and capillary pressure terms at the k-th and (n+1)-th level are approximately the same, and that the pressure dependent functions of the coefficients $\overline{CO}$, $\overline{CG}$, and $\overline{CW}$ can be evaluated at time level n, the following equations in terms of oil pressure are obtained

$$\Delta\overline{CO}\Delta p_o^{*} - \frac{V}{\Delta t}\left[(b_o S_o)^{n+1} - (b_o S_o)^{k}\right] = - r_o^{k} \tag{42}$$

$$\Delta\overline{CG}\ \Delta p_o^{*} + \Delta Rs\ \overline{CO}\ \Delta p_o^{*} - \frac{V}{\Delta t}\left[(b_g S_g)^{n+1} - (b_g S_g)^{k} + (Rs\ b_o S_o)^{n+1} - (Rs\ b_o S_o)^{k}\right] = - r_g^{k} \tag{43}$$

$$\Delta\overline{CW}\ \Delta p_o^{*} - \frac{V}{\Delta t}\left[(b_w S_w)^{n+1} - (b_w S_w)^{k}\right] = - r_w^{k} \tag{44}$$

in which $p^{*} = p^{n+1} - p^{k}$.

The pressure dependent functions of the coefficients $\overline{CO}$, $\overline{CG}$ and $\overline{CW}$ are evaluated at time level n, because of their nearly constant behavior with respect to pressure throughout a time step. Also, Newton linearizing these coefficients is not fruitful because of the nearly linear pressure dependent functions involved; moreover, it adds to the

complexity of the problem without noticeable improvement. It can be shown that if the coefficients were linearized with respect to pressure neglecting second order terms, $(p^*)^2$, the term $\Delta\overline{CO}\ \Delta p_o^*$ of equation 42 would become $\Delta\left(\frac{\partial\overline{CO}}{\partial p}\ p^k\right)\Delta\ p_o^*$; the derivative term between parentheses is constant for all practical purposes throughout a time step for nearly linear functions. Variations in time of pressure and hence of pressure dependent functions can be considerable, and, therefore, the non-linear pressure dependent terms of the right hand side of equations 42, 43 and 44 are linearized by the Newton linearization process. For the oil equation as an example, the right hand side is approximated as follows

$$[(b_o\ S_o)^{n+1} - (b_o\ S_o)^k] \simeq S_o^{n+1}\left(b_o^k + \frac{\partial b_o}{\partial p_o}\ p_o^*\right) - (b_o\ S_o)^k \tag{45}$$

and if it is temporarily assumed that $S_o^{n+1} - S_o^k = S_o^*$ is negligibly small, the expression for the right hand side becomes

$$[(b_o\ S_o)^{n+1} - (b_o\ S_o)^k] \simeq S_o^k\ \frac{\partial b_o}{\partial p_o}\ p_o^* \tag{46}$$

To distinguish all linearized terms from other difference terms, they will be left in partial differential notation, with the understanding that in a finite difference scheme they should be written as $\Delta b/\Delta p$ evaluated at k.

Analogous expressions are obtained for the water and gas phase functions. The solution gas terms, however, in the right hand side of equation 43 are second order non-linear. The approximation is performed as follows

$$[(Rs\ b_o\ S_o)^{n+1}-(Rs\ b_o\ S_o)^k] \simeq \left(Rs^k + \frac{\partial Rs}{\partial p_o}\ p_o^*\right)\left(b_o^k + \frac{\partial b_o}{\partial p_o}\ p^*\right) S^{n+1}-(Rs\ b_o\ S_o)^k \tag{47}$$

Neglecting second order terms and again temporarily assuming S_o^{n+1} approximately equal to S_o^k (or $S_o^* \simeq 0$), equation 47 becomes

$$[(Rs\ b_o\ S_o)^{n+1}-(Rs\ b_o\ S_o)^k] \simeq S_o^k\ Rs^k\ \frac{\partial b_o}{\partial p_o} + S_o^k\ b_o^k\ \frac{\partial Rs}{\partial p_o}\ p_o^* \tag{48}$$

Incorporating the ideas of equations 46 and 48 into equations 42, 43 and 44, the following "linear" equations with respect to p^* are obtained

$$\Delta\overline{CO}\ \Delta p_o^* - \frac{V}{\Delta t}\ S_o^k\ \frac{\partial b_o}{\partial p_o}\ p_o^* = - r_o^k \tag{49}$$

$$\Delta\overline{CG}\ \Delta p_o^* + \Delta Rs\ \overline{CO}\ \Delta p_o^* - \frac{V}{\Delta t}\left[S_g^k\left(\frac{\partial b_g}{\partial p_g}\right) + S_o^k\left(Rs^k\ \frac{\partial b_o}{\partial p_o} + b_o^k\ \frac{\partial Rs}{\partial p_o}\right)\right]\ p_o^* = - r_g^k \tag{50}$$

$$\Delta\overline{CW}\ \Delta p_o^* - \frac{V}{\Delta t}\ S_w^k\ \frac{\partial b_w}{\partial p_w}\ p_o^* = - r_w^k \tag{51}$$

To obtain these equations the same assumption regarding capillary pressure as made for obtaining equations 42, 43 and 44 was made.

At this point, it is rather clear that the Newton linearization process as applied in this study leads to a much better approximation of the time derivative. As a matter of fact, truncation due to large time step size is practically annihilated. To make this point clear,

consider a continuous function of pressure, represented in Figure 4 by linear splines from the data tables.

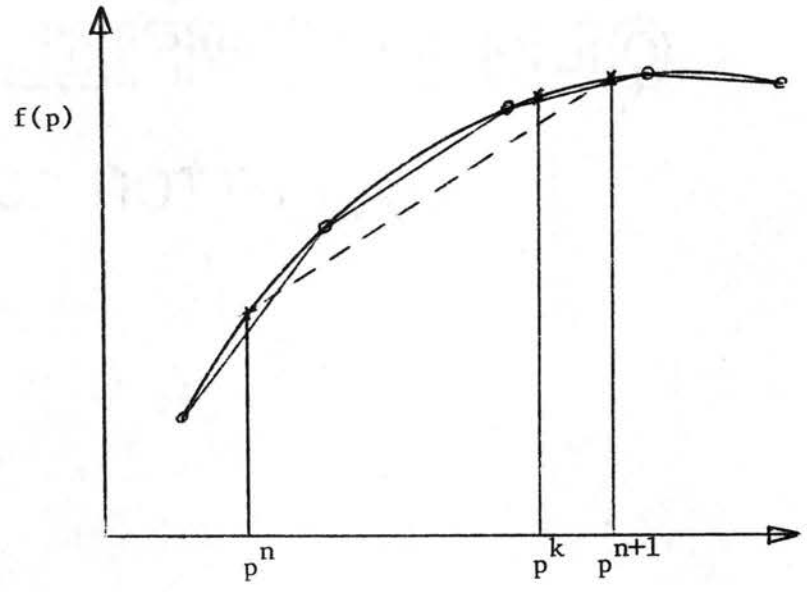

Figure 4. Example of truncation error due to time step size.

The abscissa shows the position of pressures at the present time level n, at the new time level n+1, and also at an intermediate level somewhere along the iteration process. To represent the time derivative, i.e., $\frac{p^{n+1} - p^n}{\Delta t}$, no longer cords from position n to n+1 are taken, as shown by the dashed line, but an improved value of p^k is obtained by adding the derivative of the function to its present value. It is the above consideration which makes the Newton method such a powerful tool for highly non-linear equations.

For convenience, equation 49 is multiplied by Rs and subtracted from equation 50. After having multiplied equation 49 by $\left(\frac{1}{b_o^k}\right)_{i,j}$, equation 50 by $\left(\frac{1}{b_g^k}\right)_{i,j}$ and equation 51 by $\left(\frac{1}{b_w^k}\right)_{i,j}$, these three

equations are added to each other to obtain one linear equation in p_o^*, the correction term for oil pressure.

$$\frac{1}{b_{o}^{k}}_{i,j} \Delta\overline{CO}\,\Delta p_o^* + \frac{1}{b_{g}^{k}}_{i,j} \Delta Rs.\,\overline{CG}\,\Delta p_o^* + \frac{1}{b_{g}^{k}}_{i,j} \Delta\overline{CG}\,\Delta p_o^* + \frac{1}{b_{w}^{k}}_{i,j} \Delta\overline{CW}\,\Delta p_o^*$$

$$- \frac{V}{\Delta t}\left(\frac{S_o\, b'_o}{b_o} + \frac{S_g\, b'_g}{b_g} + \frac{S_o\, b_o}{b_g} R's + \frac{S_w\, b'_w}{b_w}\right)_{i,j} p^*_{o\,i,j}$$

$$= \left[- \frac{1}{b_o^k} r_o^k - \frac{1}{b_g^k}(r_g^k - Rs^k\, r_o^k) - \frac{1}{b_w} r_w^k\right]_{i,j} \qquad (52)$$

in which the prime denotes a derivative.

This equation can also be written in a simple way as

$$A_O\, p^*_{i,j} - A_W\, p^*_{i-1,j} - A_N\, p^*_{i,j-1} - A_E\, p^*_{i+1,j} - A_S\, p^*_{i,j+1} = - R^k_{i,j} \qquad (53)$$

where

$$R^k = -\left(\frac{1}{b_o^k}\right)_{i,j} r_o^k - \left(\frac{1}{b_g^k}\right)_{i,j} (r_g^k - Rs^k\, r_o^k) - \left(\frac{1}{b_w^k}\right)_{i,j} r_w^k \qquad (54)$$

$$A_O = A_W + A_N + A_S + A_E + \frac{V}{\Delta t}\left[\left(S_o \frac{b'_o}{b_o}\right)^k + \left(S_g \frac{b'_g}{b_g}\right)^k + \left(S_w \frac{b'_w}{b_w}\right)^k + \left(\frac{S_o\, b_o Rs'}{b_g}\right)^k\right] \qquad (55)$$

$$A_W = \left(\frac{1}{b_o^k}\right)_{i,j} \overline{CO}_W + \left(\frac{1}{b_g^k}\right)_{i,j} (Rs^n_W - Rs^k_{i,j})\,\overline{CO}_W + \left(\frac{1}{b_g^k}\right)_{i,j} \overline{CG}_W + \left(\frac{1}{b_w^k}\right)_{i,j} \overline{CW}_W \qquad (56)$$

with analogous expressions for A_E , A_N and A_S . The residual error terms r_o , r_g and r_w are defined by equations 39, 40 and 41.

In matrix notation, equation 53 becomes

$$Ap^* = - R \quad . \tag{57}$$

In a two dimensional problem the A matrix is a sparce five diagonal matrix (11). After having solved this system for p^* , the correction vector, then the new pressures are simply computed from the following algorithm

$$p^{n+1} = p^k + p^*$$

The above linear system can be solved by any classical matrix solver or by iterative processes applicable to parabolic equations. Anisotropy, mainly resulting from the grid configuration of this radial flow problem makes the alternating direction implicit iterative method very unsuitable.

The method used in the model of this study is a Corrected Line Successive Over Relaxation (LSORC). This LSORC was recently developed by Watts (69) and was presented at the Annual Meeting of Reservoir simulation of the Society of Petroleum Engineers, February 1970, Denver. The algorithm of the method as used in this model was developed by Dr. R. A. Wattenbarger of Scientific Software Corporation, Denver. The LSORC method converges sufficiently fast that the proper choice of a relaxation parameter is not too critical. It was shown by Watts to be particularly suitable for highly anisotropic cases. The power of the method lies in the fact that a correction is made to a whole column at a time so as to annihilate the total residual of the column which is

most efficient when the columns are oriented in the direction of the isotropy of the problem.

Thus, in matrix terminology, the elements of an estimated solution vector, on the whole, are brought closer to their correct values. This "column correction" must be coupled in some way with an iterative matrix inversion method, for which the successive overrelaxation (LSOR) with the lines oriented along the correction columns, seems to be the most suitable one.

4.3.2 The saturation equations - After having obtained an improved pressure estimate from equation 53, the next step in the solution process is to substitute these improved pressures into equations 24, 25 and 26, and Newton iterate on saturations until compatible with the new pressure solution. This is the very non-linear part of the problem and usually several iterations are required for the saturation solution to converge to the latest pressure level. The Newton linearizations are performed on the kr(S) functions in the same manner as described in the previous section. Hence, relative permeabilities and also capillary pressures follow up the saturations by one iterate. The $p_c(S)$ relationships are thus not Newton linearized because relative permeability and capillary pressure are physically interrelated (18).

Extracting the kr(S) functions out of the coefficients $\overline{CO}$, $\overline{CG}$ and $\overline{CW}$, equations 24, 25 and 26 can be rewritten as follows

$$\Delta kro(S_o^{n+1})\ \overline{CO}'\ \Delta\Phi_o^{n+1} = \frac{V}{\Delta t}\left[(S_o\ b_o)^{n+1} - (S_o\ b_o)^n\right] + q_o \qquad (58)$$

$$\Delta\ krg(S_g^{n+1})\ \overline{CG}'\ \Delta\Phi_g^{n+1} + \Delta\ kro(S_o^{n+1})\ Rs\ \overline{CO}'\ \Delta\Phi_o^{n+1} = \frac{V}{\Delta t}[(S_g\ b_g)^{n+1} - (S_g\ b_g)^n + (S_o\ Rs\ b_o)^{n+1} - (S_o\ Rs\ b_o)^n] + q_g \quad (59)$$

$$\Delta\ krw(S_w^{n+1})\ \overline{CW}'\ \Delta\Phi_w^{n+1} = \frac{V}{\Delta t}\ [(S_w\ b_w)^{n+1} - (S_w\ b_w)^n] + q_w \quad (60)$$

where $\overline{CO}'$, $\overline{CG}'$, and $\overline{CW}'$ are $\overline{CO}$, $\overline{CG}$ and $\overline{CW}$ as defined before, except for the relative permeability terms.

Suppose that the k-th saturation iterate of equations 58, 59 and 60 is obtained.

$$\Delta\ kro(S_o^k)\ \overline{CO}'\ \Delta\Phi_o^{n+1} - \frac{V}{\Delta t}\left[S_o^k\ b_o^{n+1} - S_o^n\ b_o^n\right] - q_o = u_o^k \quad (61)$$

$$\Delta\ krg(S_g^k)\ \overline{CG}'\ \Delta\Phi_g^k + \Delta kro(S_o^k)\ Rs\ \overline{CO}'\ \Delta\Phi_o^{n+1} - \frac{V}{\Delta t}\left[S_g^k\ b_g^k - S_g^n\ b_g^n + S_o^k\ (Rs\ b_o)^{n+1} - S_o^n\ (Rs\ b_o)^n\right] - q_g = U_g^k \quad (62)$$

$$\Delta\ krw(S_w^k)\overline{CW}'\ \Delta\Phi_w^{n+1} - \frac{V}{\Delta t}\left(S_w^k\ b_w^{n+1} - S_w^n\ b_w^n\right) - q_w = u_w^k \quad (63)$$

Again, the terms u_o , u_g , and u_w are the residual errors. Note that the gas potential Φg is superscripted with a k because its capillary pressure term is saturation dependent and hence, also the gas pressure. Assuming again that p_c^{n+1} is approximately equal to p_c^k , then subtracting the k-th iterate from the (n+1)-th solution, one

obtains

$$\Delta\,[kro(S_o^{n+1}) - kro(S_o^k)]\;\overline{CO}'\Delta\Phi_o^{n+1} - \frac{V}{\Delta t}\;b_o^{n+1}\;S_o^* = -\,u_o^k \tag{64}$$

$$\Delta[krg(S_g^{k+1}) - krg(S_g^k)]\;\overline{CG}'\;\Delta\Phi_g^{n+1} + \Delta\,[kro(S_o^{n+1}) - kro(S_o^k)]\;Rs\;\overline{CO}'\;\Delta\Phi_o^{n+1}$$

$$- \frac{V}{\Delta t}\,[b_g^{n+1}\;S_g^* + (Rs\;b_o)^{n+1}\;S_o^*] = -\,u_g^k \tag{65}$$

$$\Delta[krw(S_w^{n+1}) - krw(S_w^k)]\;\overline{CW}'\;\Delta\Phi_w^{n+1} - \frac{V}{\Delta t}\;b_w^{n+1}\;S_w^* = -\,u_w^k \tag{66}$$

where $S^* = S^{n+1} - S^k$.

The $kr(S^{n+1})$ functions are approximated by the Newton linearization as follows

$$kr(S^{n+1}) \simeq kr(S^k) + \frac{\partial kr}{\partial S}\;S^*$$

hence,

$$kr(S^{n+1}) - kr(S^k) \simeq \frac{\partial kr}{\partial S}\;S^*$$

Incorporating this idea into equations 64, 65 and 66, one obtains

$$\Delta\left(\frac{\partial\,kro}{\partial\,s_o}\right)^k S_o^*\;\overline{CO}'\;\Delta\Phi_o^{n+1} - \frac{V}{\Delta t}\,b_o^{n+1}\;S_o^* = -\,u_o^k \tag{67}$$

$$\Delta\left(\frac{\partial\,krg}{\partial S_g}\right)^k S_g^*\;\overline{CG}'\;\Delta\Phi_g^{n+1} + \Delta\left(\frac{\partial\,kro}{\partial S_o}\right)^k S_o^*\;\;Rs\;\;\overline{CO}'\;\Delta\Phi_o^{n+1}$$

$$- \frac{V}{\Delta t}[b_g^{n+1}\;S_g^* + (Rs\;b_o)^{n+1}\;S_o^*] = -\,u_g^k \tag{68}$$

$$\Delta\left(\frac{\partial\, krw}{\partial S_w}\right)^k S_w^* \quad \overline{CW}' \; \Delta\Phi_w^{n+1} - \frac{V}{\Delta t} \; b_w^{n+1} \; S_w^* = - \; u_w^k \tag{69}$$

The residual errors u_o , u_g and u_w are defined by equations 61, 62 and 63.

Equations 67, 68 and 69 are linear equations in S^* , which is the correction to be added to S^k to obtain improved values of saturations. The solution process proceeds then in reevaluating relative permeabilities and capillary pressures to obtain improved coefficients of the flow equations from which a still better estimate of saturations results, until convergence.

As mentioned in the section on flow coefficients to determine the flow between two blocks, the relative permeability is evaluated at the block from which the fluid emanates (upstream block). In a fully implicit scheme this is justifiable since the flow direction does no longer rely on data from the beginning of a time step, as is the case in an implicit-explicit scheme, with possibility of a reversed flow picture at the end of a time step. Moreover, in a fully implicit scheme, the upstream approach for flow towards a well makes it possible to solve for saturations simultaneously, a column at a time, since saturations in a particular column will only depend upon the saturations upstream. Hence, if the columns are oriented parallel to the well bore and starting the solution process with the exterior column, a tridiagonal matrix per column and per phase will result. These tridiagonal matrices are easily solved by Gauss elimination using the Thomas Algorithm.

From equations 67, 68 and 69, the following algorithms are obtained.

$$\overline{DO}_O \, S^*_{o_{i,j}} - \overline{DO}_N \, S^*_{o_U} - \overline{DO}_S \, S^*_{o_U} = \overline{RO}_{i,j} \tag{70}$$

$$\overline{DG}_O \, S^*_{g_{i,j}} - \overline{DG}_N \, S^*_{g_U} - \overline{DG}_S \, S^*_{g_U} = \overline{RG}_{i,j} \tag{71}$$

$$\overline{DW}_O \, S^*_{w_{i,j}} - \overline{DW}_N \, S^*_{w_U} - \overline{DW}_S \, S^*_{w_U} = \overline{RW}_{i,j} \tag{72}$$

The structure of the coefficients $\overline{DO}$, $\overline{DG}$ and $\overline{DW}$ will depend upon the flow picture. Figure 5 demonstrates the two extreme flow pictures possible for a block. The East (E) and West (W) flows will always be as shown in Figure 5 for flows towards a well located westward.

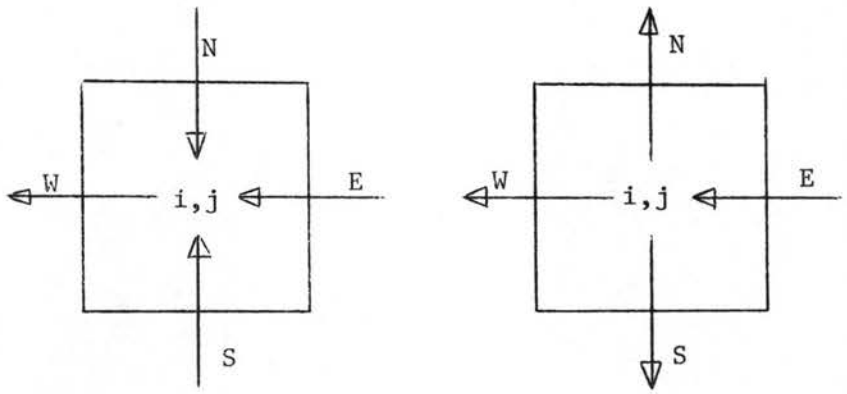

5a 5b

Figure 5. Possible flow pictures at any block for defining the coefficients of equations 70, 71, and 72.

However, the North (N) and South (S) flows will be either all into the block (Figure 5a) or all out of the block (Figure 5b) or any combination of into or out of. The decision on the direction of flow is based on

the magnitude of the potentials. For example, if the flow is toward the block (Figure 5a), then the North and South blocks are both upstream ones and the North and South coefficients are defined as follows

$$\overline{DO}_N = \overline{CO}'_N \left(\Phi_{o_{i,j-1}}^{n+1} - \Phi_{o_{i,j}}^{n+1} \right) \left(\frac{\partial\, kro}{\partial S_o} \right)_{i,j}^{k} \tag{73}$$

$$\overline{DO}_S = \overline{CO}'_S \left(\Phi_{g_{i,j+1}}^{n+1} - \Phi_{g_{i,j}}^{n+1} \right) \left(\frac{\partial\, kro}{\partial S_o} \right)_{i,j}^{k} \tag{74}$$

with analogous expressions for gas and water, if the directions are the same.

If the flow is all out of the blocks (Figure 5b), then the block (i,j) itself becomes an upstream block with respect to both North and South flows, and the magnitudes of the North and South coefficients are added into the central (main diagonal) coefficients $\overline{DO}_O$, $\overline{DG}_O$, and $\overline{DW}_O$. Naturally, for this case the off diagonal elements of the tri-diagonal matrix are zero. Practically, a combination of the above extreme cases almost always occurs.

Except for the possible addition of North and South coefficients, the main diagonal coefficients are defined as

$$\overline{DO}_O = \frac{V}{\Delta t} \left(b_o^{n+1} \right)_{i,j} - \overline{CO}'_W \left(\Phi_{o_{i-1,j}}^{n+1} - \Phi_{o_{i,j}}^{n+1} \right) \left(\frac{\partial\, kro}{\partial S_o} \right)_{i,j}^{k} \tag{75}$$

$$\overline{DG}_O = \frac{V}{\Delta t} \left(b_g^{n+1} \right)_{i,j} - \overline{CG}'_W \left(\Phi_{g_{i-1,j}}^{n+1} - \Phi_{g_{i,j}}^{n+1} \right) \left(\frac{\partial\, krg}{\partial S_g} \right)_{i,j}^{k} \tag{76}$$

$$\overline{DW}_O = \frac{V}{\Delta t} \left(b_w^{n+1} \right)_{i,j} - \overline{CW}'_W \left(\Phi_{w_{i+1,j}}^{n+1} - \Phi_{w_{i,j}}^{n+1} \right) \left(\frac{\partial\, krw}{\partial S_w} \right)_{i,j}^{k} \tag{77}$$

Finally, the right hand sides of equations 70, 71 and 72 are

$$\overline{RO}_{i,j} = \overline{CO}'_E \left(\Phi_{o}^{n+1}{}_{i+1,j} - \Phi_{o}^{n+1}{}_{i,j}\right) \left(\frac{\partial\, kro}{\partial S_o} S_o^*\right)_{i+1,j}^{k+1} + u_o^k \tag{78}$$

$$\begin{aligned}\overline{RG}_{i,j} = {} & \overline{CG}'_E \left(\Phi_{g}^{n+1}{}_{i+1,j} - \Phi_{g}^{n+1}{}_{i,j}\right) \left(\frac{\partial\, krg}{\partial S_o} S_g^*\right)_{i+1,j}^{k+1} + u_g^k - \frac{V}{\Delta t} (Rs\, b_o)_{i,j}^{n+1} S_o^*{}_{i,j} \\ & + Rs_W \overline{CO}'_W \left(\Phi_{o}^{n+1}{}_{i-1,j} - \Phi_{o}^{n+1}{}_{i,j}\right) \left(\frac{\partial\, kro}{\partial S_o} S_o^*\right)_{i,j} \\ & + Rs_S \overline{CO}'_S \left(\Phi_{o}^{n+1}{}_{i,j+1} - \Phi_{o}^{n+1}{}_{i,j}\right) \left(\frac{\partial\, kro}{\partial S_o} S_o^*\right)_{U} \\ & + Rs_N \overline{CO}'_N \left(\Phi_{o}^{n+1}{}_{i,j-1} - \Phi_{o}^{n+1}{}_{i,j}\right) \left(\frac{\partial\, kro}{\partial S_o} S_o^*\right)_{U} \\ & + Rs_E \overline{CO}'_E \left(\Phi_{o}^{n+1}{}_{i+1,j} - \Phi_{o}^{n+1}{}_{i,j}\right) \left(\frac{\partial\, kro}{\partial S_o} S_o^*\right)_{i+1,j}\end{aligned} \tag{79}$$

$$\overline{RW}_{i,j} = \overline{CW}'_E \left(\Phi_{w}^{n+1}{}_{i+1,j} - \Phi_{w}^{n+1}{}_{i,j}\right) \left(\frac{\partial\, krw}{\partial S_w} S_w^*\right)_{i+1,j}^{k+1} + u_w^k \tag{80}$$

Saturations are solved this way for all three phases separately as opposed to what is often done, solve for saturations of two phases and obtain the saturation of the third phase from the saturation relationship, equation 20. The reason for doing it this way is that otherwise slightly incorrect fluid volumes, resulting from solving the system for fairly large time steps (overshoot), could never be corrected for by adjusting pressures on a volumetric error basis. In other words, after having obtained saturations compatible with the latest pressure

estimate, one Newton iteration cycle is completed, and the next step now is to readjust pressures. The best way is to do it on a volumetric basis with the following condition

$$1.0 - S_o - S_g - S_w = 0.0 \tag{81}$$

If this condition does not hold, there is either too much or too little fluid in a block and the phases will have to be compressed or expanded accordingly.

A time step is finally solved for when the residuals of both the pressure equation and the saturation equations are annihilated. In practice, the convergence criterion is not so strongly stated; convergence is satisfied when pressures and saturations vary less than a given value.

4.4 Initial and Boundary Conditions

4.4.1 The grid system - From comparisons with analytical solutions (one phase fully saturated flow, confined flow, fully penetrating well), the grid configuration of Figure 6 was shown to approximate the well bore pressures very well (see also Figure 8).

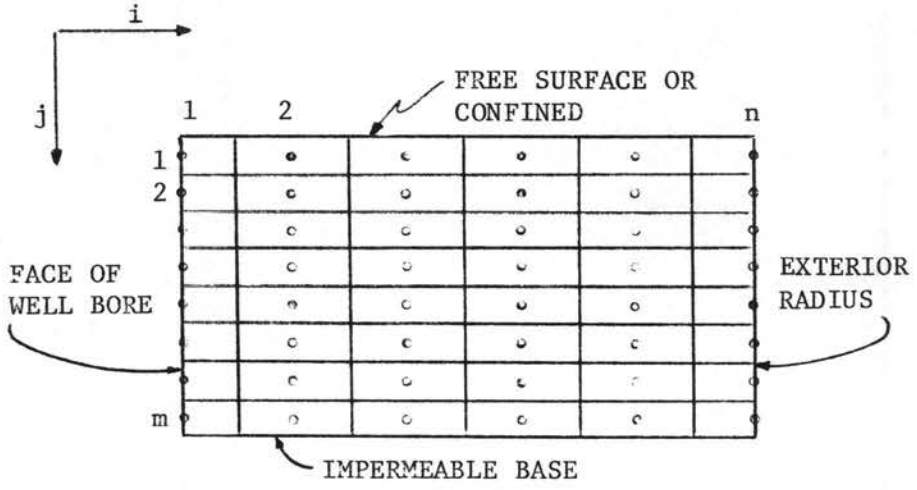

Figure 6. Grid system used in this study.

The first and the last column of pressures are respectively right at the edge of the well bore and right at the exterior boundary. Since pressures away from the well vary logarithmically with distance (approximately for unsteady multiphase flow), the radii from the well bore center to the center of the cells are logarithmically distributed so that $\log(\Delta r)$ is a constant. For numerical convenience only half Δr is taken at the well bore and at the outside boundary.

The system is set up as a closed one (no flow across boundaries) and from there the different type boundary conditions will be constructed. From a programming point of view, the no flow boundary condition is very conveniently satisfied by assigning zero values to the flow coefficients across the boundary.

4.4.2 Possible boundary conditions - Since the reservoir is overlaying an impermeable base, the lower boundary is taken care of throughout by a no flow condition. Mathematically, the potential gradient normal to the boundary is zero; in terms of the numerical model, the south coefficients of the lower row are all zero.

At the exterior radius boundary, the well bore boundary and along the top of the aquifer, the following possible conditions may exist:

1. No flow boundary conditions.
2. Pressure boundary conditions.
3. Flow rate boundary conditions.

4.4.2.1 Well bore boundary conditions - At the well bore, a combination of conditions one and two or conditions one and three are possible depending upon which portion of the well is perforated (screened).

As the computer program is presently written, the no flow condition is automatically taken care of.

The flow rate boundary condition is easy to incorporate, i.e., a value is assigned to the production terms "q" of equations 24, 25 and 26. In practice, an oil production is assigned. The gas and water productions are computed from the following relationships.

$$q_g = q_w \left(\frac{krg\ b_g/\mu_g}{kro\ b_o/\mu_o} + Rs \right) \tag{82}$$

$$q_w = q_o \left(\frac{krw\ b_w/\mu_w}{kro\ b_o/\mu_o} \right) \tag{83}$$

These relationships show that production will depend upon the ratios of the mobilities of the phases, which is true if the magnitude of the potential drops in the different phases are the same. By mobility in the petroleum technology is meant the term kr/μ . In practice, this condition of equal potential drops in the different phases very closely holds. The gas production of course, is composed of two terms: free gas and solution gas.

Since gas and water productions are saturation dependent they are taken up in the Newton linearization scheme and readjusted after each saturation iterate as follows

$$q_g^{k+1} = q_o^{n+1} \left(\frac{krg\ b_g/\mu_g}{kro\ b_o/\mu_o} + \frac{1}{kro} \frac{\Delta\ krg}{\Delta\ S_g} S_g^* + Rs \right)^k \tag{84}$$

$$q_w^{k+1} = q_o^{n+1} \left(\frac{krw\ b_w/\mu_w}{kro\ b_o/\mu_o} + \frac{1}{kro} \frac{\Delta\ krw}{\Delta\ S_w} S_w^* \right)^k \tag{85}$$

This way, convergence is considerably accelerated.

The pressure boundary condition does not create any problems with regard to solving the pressure equation. Except for the main diagonal of equation 53, which is set equal to 1.0, all coefficients and the right hand side of this equation are set equal to zero for all the perforated blocks where a pressure is assigned. The pressure solution thus shows a flow towards or away from the well bore, but due to the fact that mathematically a no flow condition exists at the well bore, the saturation solution shows an accumulation or a depletion of fluids in those blocks. This accumulation (or depletion) then is the basis for estimating the magnitude of fluid production terms compatible with the pressure solution; it is considered as a volumetric correction rate, Δq , to be added to the latest estimate of q. The total volumetric correction rate can be expressed as follows

$$\frac{\Delta q_o}{b_o} + \frac{\Delta q_g}{b_g} + \frac{\Delta q_w}{b_w} = - \frac{V}{\Delta t} (1.0 - S_o - S_g - S_w) \qquad (86)$$

Again the different phases will produce according to the mobility ratios. Therefore, substituting equations 82 and 83 into equation 86, and after rearranging, the following expression is obtained for Δq_o

$$\Delta q_o = \frac{- \frac{V}{\Delta t} (1.0 - S_o - S_g - S_w)}{\left[\frac{1}{b_o} + \frac{1}{b_g} \left(\frac{krg\ b_g/\mu_g}{kro\ b_o/\mu_o} + Rs \right) + \frac{1}{b_w} \left(\frac{krw\ b_w/\mu_w}{kro\ b_o/\mu_o} \right) \right]} \qquad (87)$$

After having computed Δq_o first, the correction is added to the latest estimate of q_o with which q_g and q_w are computed from equations 82 and 83.

Obviously, equation 87 becomes invalid as soon as kro is zero. The oil phase is no longer producing at this moment. As long as krg and krw are not zero, however, gas and water can still be produced and if the well is not yet shut down, q_g and q_w can be computed with an equation obtained similarly to equation 87, i.e.

$$\Delta q_g = \frac{-\frac{V}{\Delta t}(1.0 - S_o - S_g - S_w)}{\left[\frac{1}{b_g} + \frac{1}{b_w}\left(\frac{krw\ b_w/\mu_w}{krg\ b_g/\mu_g}\right)\right]} \tag{88}$$

$$q_w = q_g \left(\frac{krw\ b_w/\mu_w}{krg\ b_g/\mu_g}\right) \tag{89}$$

The third possibility is that both krg and kro are zero, but krw not; the expression for Δq_w becomes

$$\Delta q_w = b_w \left[-\frac{V}{\Delta t}(1.0 - S_o - S_g - S_w)\right] \tag{90}$$

This process of computing production terms implicitly requires a double sweep of the last column (well column) in each saturation iterate, the first sweep to detect an accumulation (or depletion) of fluids, the second sweep to annihilate the accumulation (or depletion) of fluids by considering it as a volumetric correction rate.

4.4.2.2 Boundary conditions along top of aquifer - In case of a confined aquifer, the no flow condition holds and is automatically taken care of.

In case of an unconfined aquifer the north side is physically open to the atmosphere, but mathematically closed. The boundary condition is one of constant atmospheric air pressure. This case is very

analogous to the well pressure condition and hence it can be expected to be treated in a similar way. A depletion, however, rather than an accumulation of fluids in the upper row blocks is now taking place, so that the q values assume negative signs and are to be considered as recharge.

The "free surface", if it can be defined in this multiphase flow model, would be defined by the line of atmospheric pressure in the liquid phase. For modeling the "free surface" the method just described was behaving perfectly. The computational work, however, because of the double saturation sweep, as explained in section 4.4.2.1, is a little longer but the cumulative material balance error remained very small throughout (10^{-5} FT^3).

4.4.2.3 The exterior radius boundary conditions - At the exterior radius boundary, a no flow condition was assigned throughout this study. Boundary effects are minimized by taking the outside radius large enough (10,000 ft). Boundary conditions two (pressure) and three (flow rate) at the exterior boundary are incorporated in the model, but were not used.

4.4.3 Initial conditions - As mentioned earlier, all runs of this study were made using the oil-gas phases to represent an air-water system. A hydrostatic pressure distribution was assumed as the initial condition. Above a region completely saturated with water, a region partly saturated with water existed in equilibrium with the assigned Pc (S) relationship.

Since compressibility factors are included in this study it is rather difficult to compute a perfectly equilibrated initial condition. Therefore, to allow the fluids to settle, the first few time steps were

run without pumping. Very slow convergence was noticed, though, in the pressure equation, since this is a near steady state condition leading up to a nearly elliptic pressure equation. The diagonal dominancy of the coefficient matrix is diminished.

4.5 The Computer Program

The computer program was coded in FORTRAN IV EXTENDED for a CDC 6400 computer with a core memory consisting of 64,000 storage locations. A careful arrangement of storage for this two-dimensional, three phase model was imperative. For this purpose, the program was segmented into computational entities. In each segment the exact amount of core was specified by reallocating only the needed variables for that segment. With this tremendous storage saving technique grid systems as large as 30 by 30 are being handled. Tape and disk are extensively used for temporary storage.

All two-dimensional variables were stored in one-dimensional arrays which is, from a computing point of view, an enormous time saving: it takes some computing time to locate variables in a two-dimensional array, whereas a simple algorithm in the program easily identifies two-dimensional variables from the one-dimensional array.

The treatment of input data is considered an important part of the program in terms of saving man hours. All input data are read in at once in the beginning on a separate tape or disk unit. The first four columns of each data card carry a mnemonic name (see Appendix C) making it possible to go back on tape and search for any single bit of information and bringing it in central memory. If the data do not satisfy a check on correctness or if they are found to be out of order,

an error message is printed. Depending upon the seriousness of the incorrectness it can be decided to discontinue the run. The input data are separated into single point data, array data, pressure and saturation dependent data, and time step data such as new boundary conditions and time step size. Appendix C shows how pressure and saturation dependent data are organized in the form of interpolation tables. Linear interpolation is used throughout, which is accurate if enough data points are used. Experience showed (11) that higher order interpolation did not give significantly better results besides being very time consuming. That this is an important factor in multiphase flow is easily understood since for each block of the grid system all pressure and saturation dependent functions have to be evaluated for each phase and at each iteration. To speed up the process of interpolation a latest entry point index is kept in central memory since it is very likely that the next entry will be close, if not the same, to the previous entry; it minimizes searching time tremendously.

The overall structure of the program is diagrammatically shown in Figure 7. Each segment shown operates independently.

4.6 Validity of the Simulator

An analytical solution of the multiphase flow equations does not exist; also, a rigorous proof of convergence of the finite difference solution does not exist. Hence, no direct way of showing the correctness of the simulator is available. Its verification will thus mainly depend upon argumentation based on correctness of equations, and on model performance.

The first step in this syllogistic proof is to accept the flow equations as the true mathematical analogue of multiphase flow. They

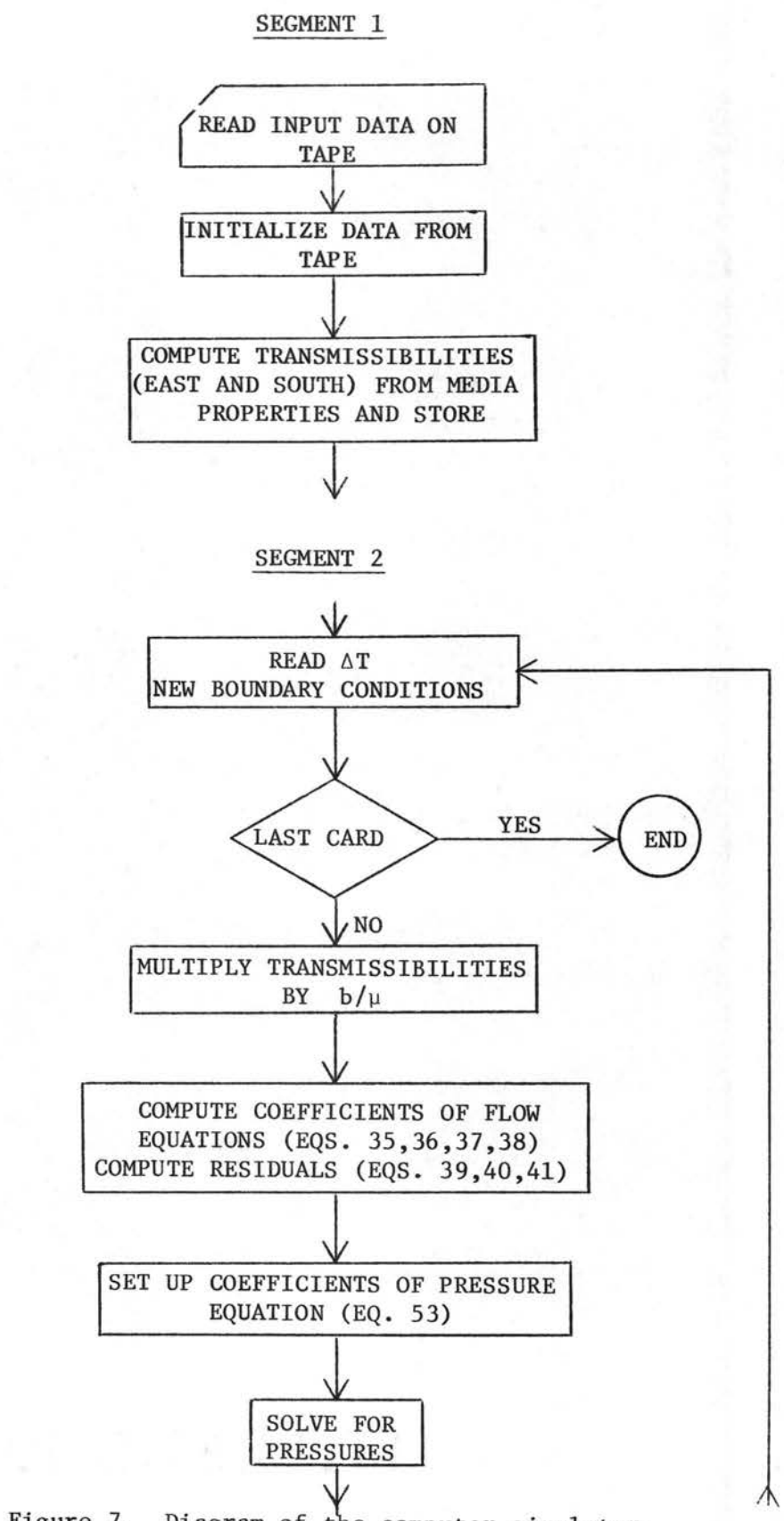

Figure 7. Diagram of the computer simulator.

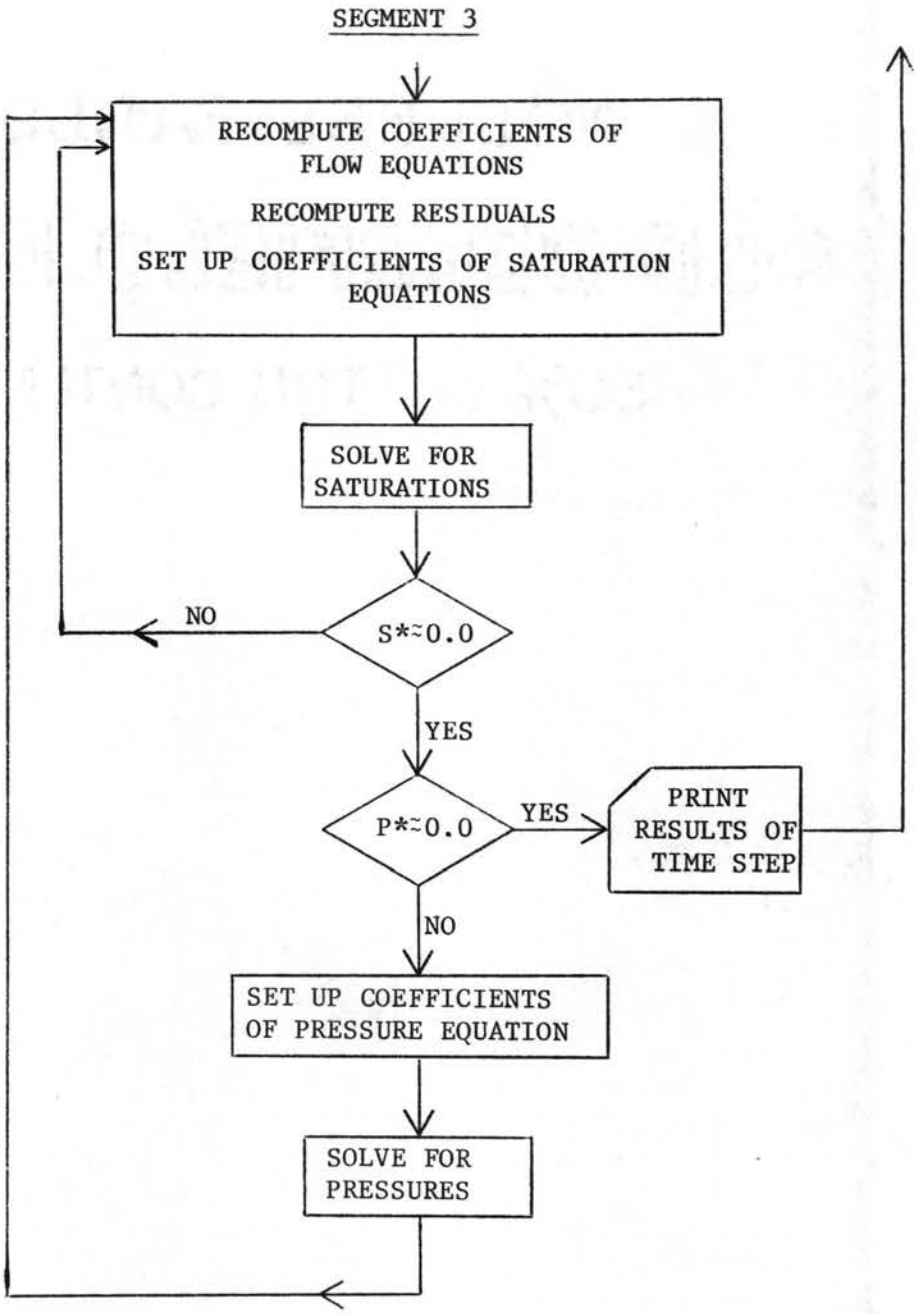

Figure 7. (Continued) Diagram of the computer simulator.

are derived from a true statement of continuity. Their validity will depend upon the validity of Darcy's law as the force law. As stated earlier, evidence of the validity of Darcy's law is rather plentiful under the assumptions stated. This leads to the acceptance of the correctness of the equations. The flow equations have further been checked with experimental results both from laboratory tests and from field tests (Welge and Weber, Soengkowo, Blair and Peaceman, and many others).

Next, the question arises as to how good is the solution that is obtained by the proposed computational algorithm. Obviously, a considerable amount of ingenuity is involved in the construction of a finite difference scheme. As long as the discretization used does not violate the continuity principle, i.e., as long as mass is conserved, a good finite difference scheme to represent the continuous partial differential equations is obtained. It was further proved analytically by different numerical analysts (Douglas, Smith, Lees, Rose) that, as the grid spacing approaches zero, convergence to the actual solution is obtained, by using finite differences for solving linear parabolic partial differential equations in rectangular regions. Similar proofs are not available for discretized non-linear partial differential equations when applied to systems which are not rectangular or which have variable grid spacing. Nevertheless, based on experience of many researchers (10, 21, 22) it can be concluded that finite difference methods for solving non-linear equations do give good results. The correctness of these results mainly depends upon truncation errors which stem from the discretization process. Space truncation errors are usually not significant if a sufficiently small mesh spacing is used.

Time truncation errors, however, are usually rather severe, because of the tendency to take as large a time step as possible for economical reasons. This, indeed, is a problem in the classical mixed techniques (implicit-explicit) in which the flow coefficients are time truncation dependent apart from the time derivative itself. This time truncation error is practically annihilated with the fully implicit scheme as applied in this study (cf. section 4.3.1). Finally, the numerical solution obtained is a good solution of the finite difference equations, since in the solution process residuals are indeed vanishing.

The last step in this heuristic proof of validity is based on qualitative and quantitative performance of the model. Test runs can be set up for which intuitively the answers are known; or also, limiting cases can be checked for agreement with theory. For example, a test run was made modeling a confined homogeneous and isotropic aquifer with a fully penetrating pumped well. Gravity was neglected and the aquifer was fully saturated with one of the wetting phases. Exact analytical solutions for this strictly horizontal radial case with flow rate boundary conditions (62) do exist. The numerical solution behaved as was predicted by the analytical solution. Results of the flow rate boundary condition case are shown in Figure 8. The storativity factor, S, needed to obtain the analytical solution was computed from the compressibility factor, β , which in its turn was obtained from the formation volume factor (F.V.F.) data as used in the numerical model. All physical characteristics appear on Figure 8. The relationship between storativity and compressibility derived by several authors (1) is

$$S = \rho g(\alpha + n\beta)b$$

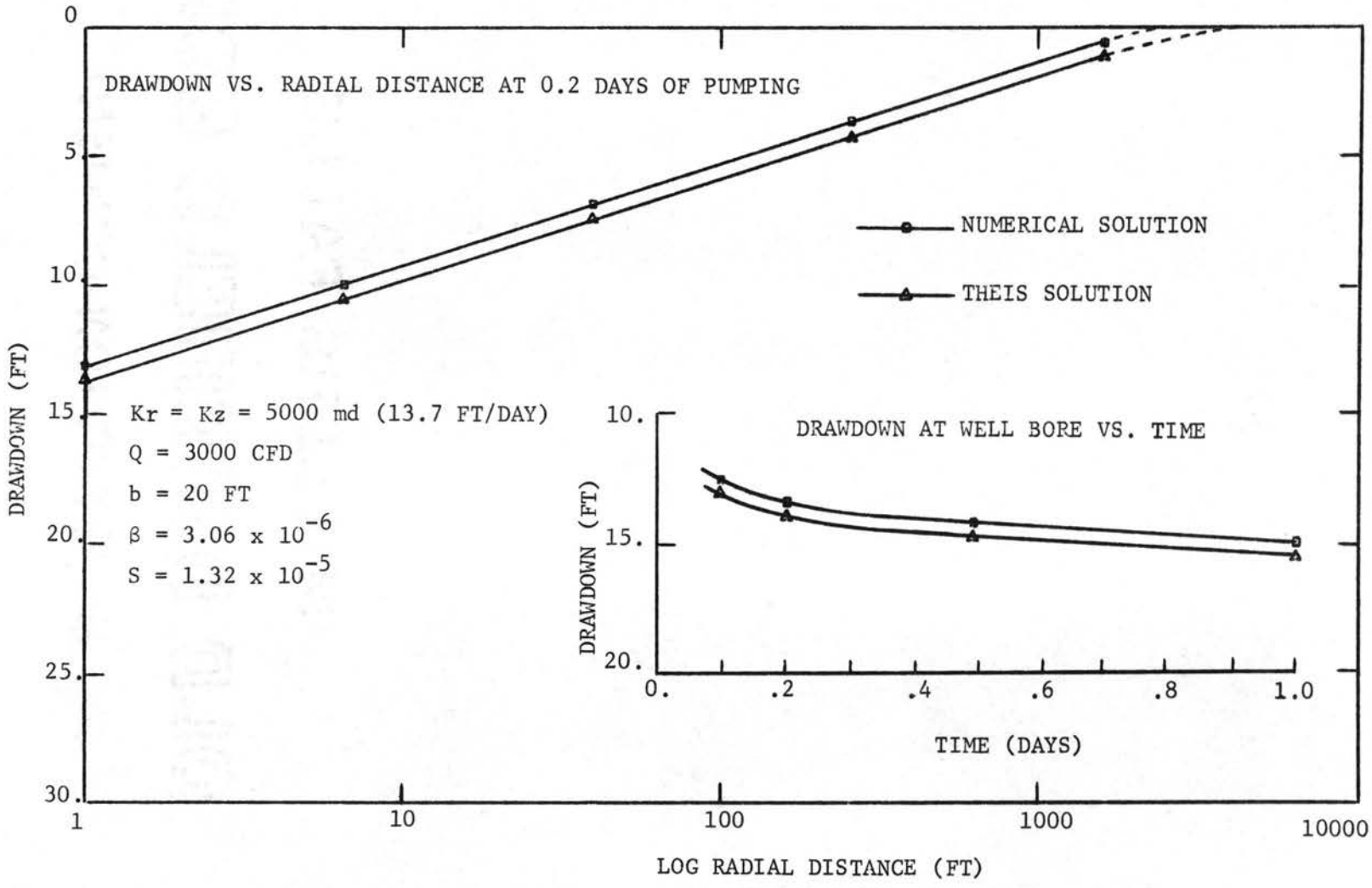

Figure 8. Confined flow comparison of Theis solution and numerical solution.

in which n is the porosity, α is the aquifer compressibility factor which is zero in this case, and b is the aquifer thickness. Very close agreement is obtained, realizing that only six grid blocks were utilized to model an aquifer with well radius of one foot and exterior radius of 10,000 feet. The results of the numerical simulator only differ by 0.3 percent from the Theis solution if both solutions were applied to an artesian aquifer with piezometric head of 200 feet of water. These results also indicate the validity of the Theis solution very close to the line sink. Conversely, the results also indicate that pressure at the well bore is well represented with the grid block configuration as used in this study (cf. section 4.4.1).

Several multiphase flow cases for which there are no analytical solutions were run and analysed with respect to their behavior. In one case, a gravity-less confined medium was modeled without any pumping. Pressure and saturation distributions, initially uniform throughout, did not vary after a time step as would be expected.

Good test runs, particularly useful for debugging purposes, are the ones that exploit the conditions of symmetry. Several of these were run. Other test runs involved the effects of capillarity and gravity. The following test case was of particular interest in the petroleum technology; gas, oil, and water were overlaying each other in a confined reservoir. The well was screened only in the middle of the oil phase. Gas and water were coning into the oil phase. The usefulness of this case lies in the fact that optimum schedules may be derived at to obtain maximum withdrawal of oil.

It is concluded that, based on the above heuristic argumentation, the simulator is considered to be a valid multiphase flow solver under the conditions and assumptions stated.

5. RESULTS AND DISCUSSION

The discussion of the results of this study is centered around the "free surface" gravity well flow problem. As long as the flow is confined in a fully saturated medium, analytical solutions assuming horizontal flow predict the behavior well; these solutions are very adequate for confined aquifer test analysis. Because of the lack of analytical solutions of unconfined free surface flow, unconfined aquifer data are always analysed from a confined flow point of view. With respect to this approach, Stallman (59) concludes one of his papers on aquifer test analysis as follows:

> "Analysis of pumping tests made in unconfined aquifers should be a fertile field for anyone slightly inclined toward pessimism".

The results of this study, obtained from the most complete 'free surface' well flow analogue to date will show why indeed the analysis of data of unconfined aquifers, when fitted with confined flow analytical solutions, is so controversial and leads to so many contradictory conclusions.

The solution obtained from the two-phase "free surface" gravity flow model differs in many aspects from confined (artesian) flow analytical solutions. Therefore, the results of this study will be compared as much as possible with these solutions and evaluated with respect to aquifer test analysis. To better appreciate this comparative discussion a brief account of analytical solutions used with underlying assumptions follows.

5.1 Brief Account of Analytical Solutions

Present theories of aquifer tests are all more or less based on solutions of the one-dimensional radial confined flow equation (1, 32, 62, 63). Some of these solutions account for the effect of partial penetration (30), others account for delayed yield from storage (7). Notwithstanding its restrictions, the Theis solution is most generally used. The basic assumptions, underlying the Theis solution are:

(1) Confined flow of infinite areal extent.

(2) Instantaneous release from storage.

(3) All flow is horizontal (no vertical flow components).

(4) Fully penetrating well.

(5) The well is considered to be a sink (infinitesimally narrow well).

(6) Constant aquifer thickness, b.

(7) No gravity effect.

(8) Homogeneous, isotropic medium.

When applied to a water table aquifer, the Theis solution becomes subject to the Dupuit-Forchheimer assumptions, which also implies that the free-water surface is the streamline bounding the flow region and that a linear relationship exists between flow rate and aquifer thickness.

Important aspects arising in unconfined aquifers, not or only partially considered in analytical analyses, but often realized by ground water hydrologists (59), are:

(1) Effect of vertical flow components on drawdown.

(2) Storage release by expansion of water.

(3) Variable specific yield (delayed yield from storage) and role of the capillary zone with this respect, i.e., flow in the "cone of depression".

(4) Partial penetration of wells under free surface flow conditions

The numerical model is not restricted by any of the above four aspects. Hence, a fair chance exists to evaluate their magnitude of importance.

5.2 Case Study

Two unconfined well flow cases were run:

Case 1: Low permeability aquifer (13.7 FT/DAY) with medium characteristics of a Columbia sandy loam (see Appendix C for detailed aquifer and fluid properties).

Case 2: High permeability aquifer (219.2 FT/DAY) with medium characteristics of an unconsolidated sand (see Appendix C).

It was felt that within the objectives of this study these two cases would suffice to demonstrate the original solution obtained. The availability of funds for this one man project was a major factor in determining the number of cases to be studied.

Specification of property	Case 1	Case 2
Medium	Columbia sandy loam	unconsolidated sand
Permeability	13.7 FT/DAY = 5000 Milli-Darcies	219.2 FT/DAY = 80,000 Milli-Darcies
Porosity	0.5	0.5
Residual water saturation	20 percent	10 percent
Initial saturated thickness	136 feet	139 feet
Well screen (percent of initial saturated thickness)	Lower 45 percent of aquifer thickness	Lower 43 percent of aquifer thickness
Pumping rate	43,200 FT^3/DAY	86,400 FT^3/DAY
Grid system	6 columns, 8 rows	6 columns, 8 rows
Total time of analysis	7.780 DAYS	6.675 DAYS
Computer time (central processor)	560 seconds	840 seconds

Table 1. Summary of important characteristics of Case 1 and Case 2.

Table 1 summarizes the most important characteristics of Case 1 and Case 2. Each case is run at a constant pumping rate until a definite flow pattern has developed.

5.3 Analysis of Case 1

5.3.1 Equipotential lines, isopiestic lines, and flow pattern -

After nearly eight days of pumping a definite flow pattern had developed with little change taking place in the potential and free surface profiles. This eight day period seemed long enough to analyse all aspects of the results. The potentiometric map of an r-z cross-section is plotted in Figure 9, on semi-log paper, the r-direction (abscissa) being the log scale. In order not to misinterpret Figure 9, the potentiometric map is also plotted on normal scale paper in Figure 10, diagrammatically showing a few flow lines as well.

It is readily seen from this flow pattern that tremendous volumes of water emanate from a distance away from the well and that very little flow is contributed from near the well bore, above the screen. Two factors seem to interact in determining this flow configuration: gravity and the radial nature of flow. That the flow pattern is very much affected by gravity is readily observed from the flow diagram. It is admitted that the vertical flow component becomes small at, say, 250 feet away from the well; however, at the same time it should be realized that the cross-sectional area of flow in the horizontal plane increases by a factor of radius squared as one moves away from the well.

The dashed line on Figures 9 and 10 is the line of atmospheric pressure which corresponds to the definition of the free surface. A point of inflection is noticed along this curve. In time, this point of inflection moves away from the well bore and the rate of drawdown near

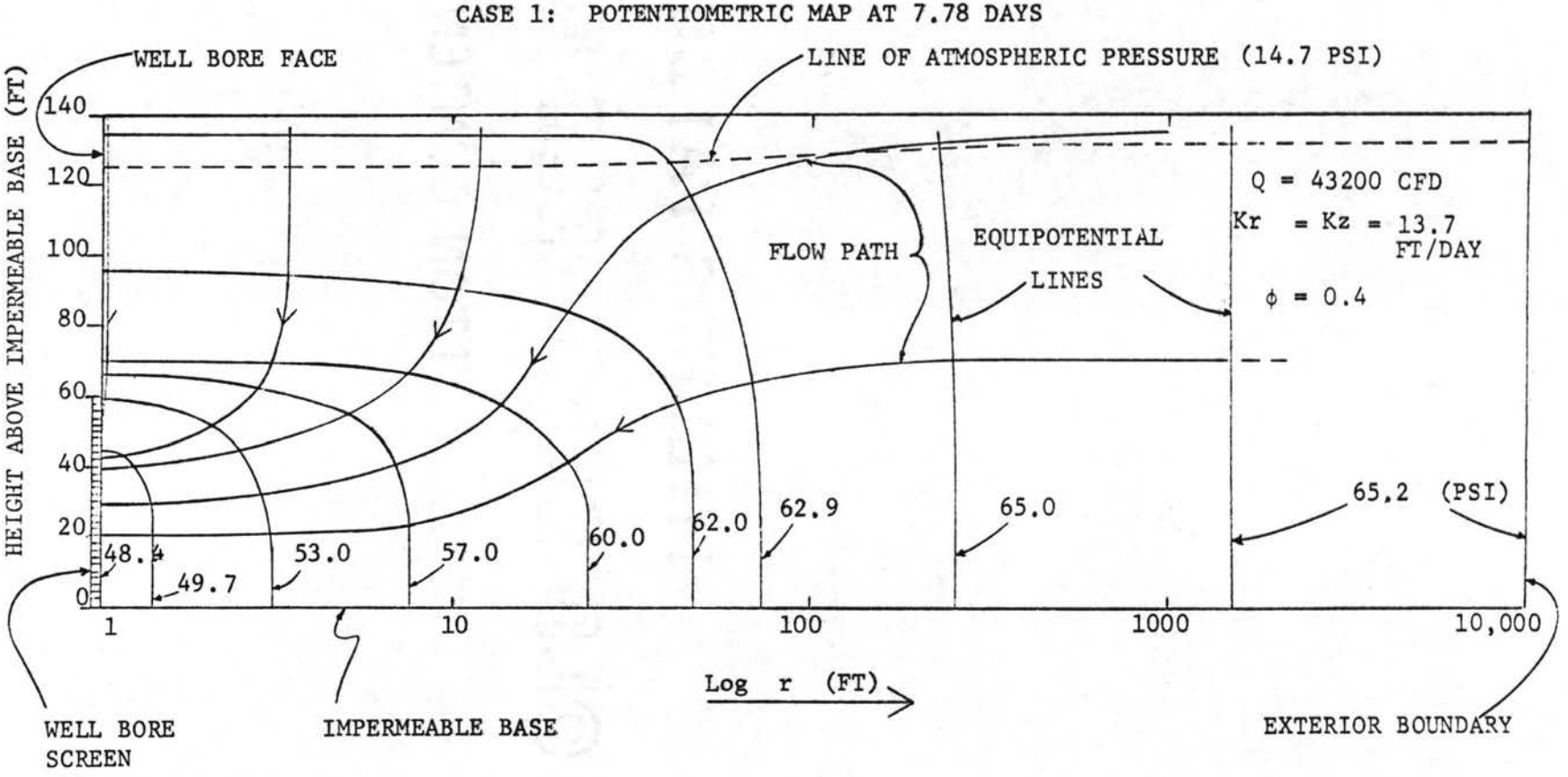

Figure 9. Potentiometric map and flow lines of Case 1: logarithmic distance scale.

CASE 1: POTENTIOMETRIC MAP AT 7.78 DAYS

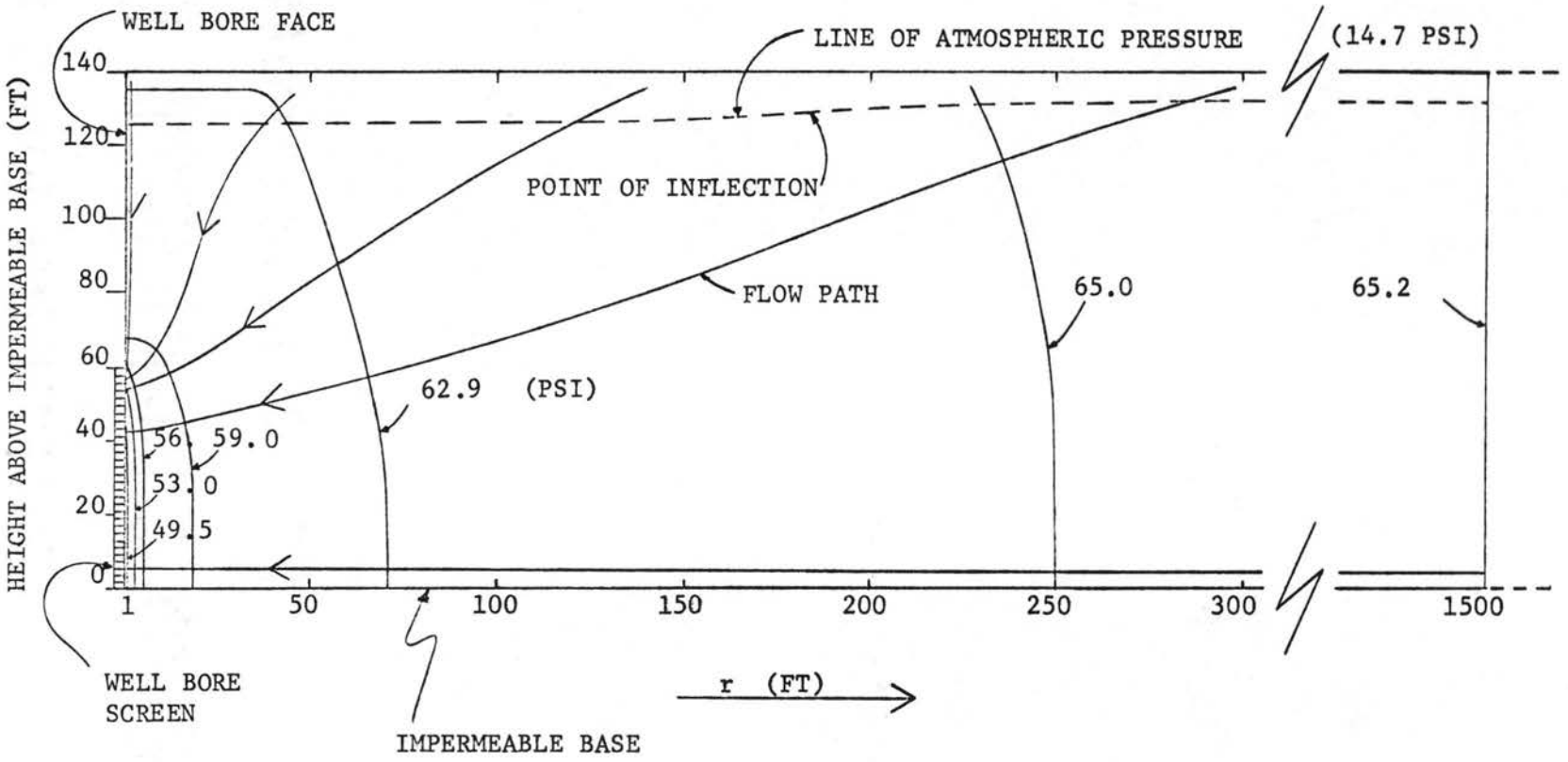

Figure 10. Potentiometric map and flow lines of Case 1: normal distance scale.

the well bore becomes smaller and smaller (under constant pumping conditions). This curve in no way corresponds to what is often seen as the free surface profile around well bores, suggested by the Theis solution, corrected or not for the effect of partial penetration.

All lines of equal pressure (see pressure map, Appendix D) ending above the well screen have the same physical appearance as the dash lines of Figures 9 and 10; however, equal pressure lines ending below the top of the screen cone down. Therefore it seems clear that fully screened wells, if they occur, should behave very much like partially penetrating wells; the flux across the well screen is not a constant and is largest near the pump (usually bottom of aquifer) where suction head is greatest. Moreover, the moment a fully penetrating well is pumped, the effective portion of the screen (effective area of flow) is very rapidly much less than its original fully penetrating length. Equipotentials will still look as before. A possible flow field for a fully penetrating well is suggested in Figure 11 applicable to a two-phase flow system.

In summary, the last paragraph, by induction, says that so called fully penetrating wells operate as if they were partially penetrating. The difference between fully and partially penetrating wells would then be the dip of the line of atmospheric pressure very close to the well bore until it becomes a seepage face, affecting very little the overall free surface, radial gravity flow phenomenon.

This solution in no way agrees with the horizontal flow concept of analytical analyses of confined flow, in which the flux through the screen is a constant and in which the full length of the screen is always exposed to the entire aquifer thickness.

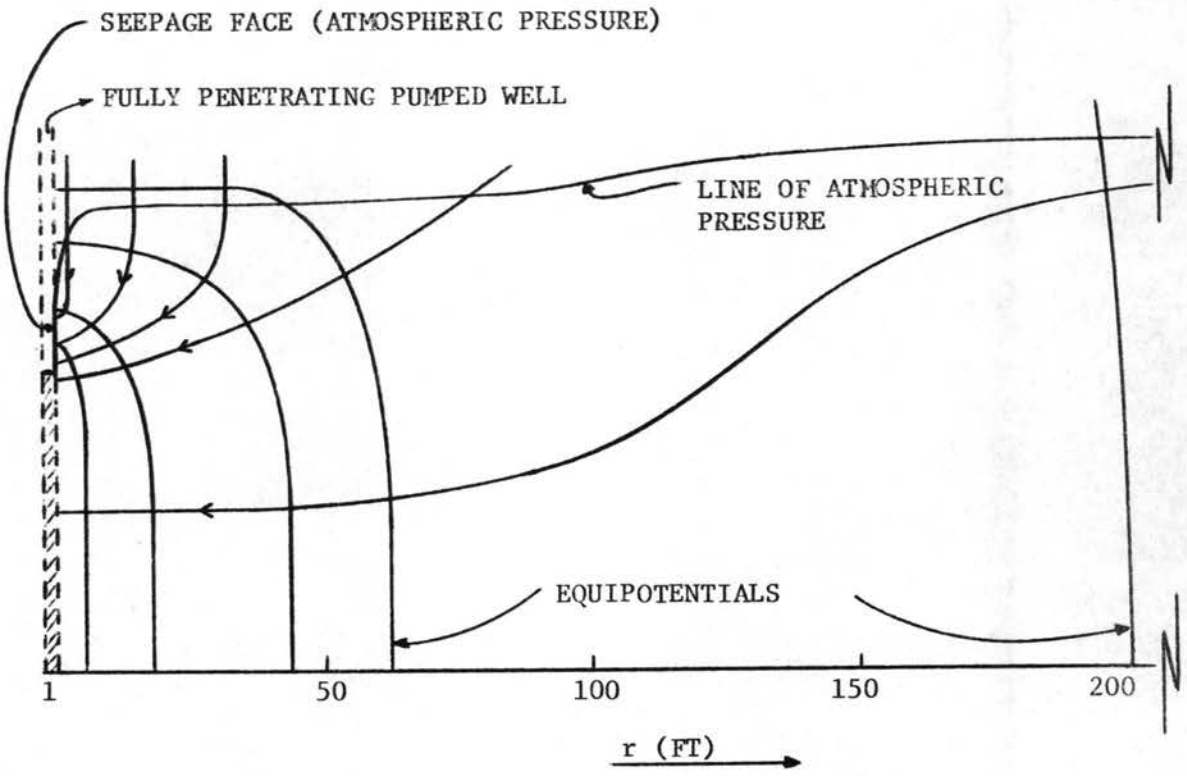

Figure 11. Possible flow field of a fully penetrating well.

It is important to point out again that the analytical analysis is good as long as the flow is confined and fully saturated, but as soon as it is applied to free surface flow it becomes subject to the absurdities introduced by the Dupuit-Forchheimer assumptions. The Theis solution, whether or not corrected for the effect of partial penetration, cannot be visualized as the solution for the position of the free surface. In the Dupuit-Forchheimer context, the free surface is a streamline, all flow below it being horizontal. Researchers who realized the importance of gravity in free surface flow problems attempted to visualize the flow picture as shown in Figure 12 by combining the Theis solution "free surface", a streamline, with a set of streamlines emanating from it.

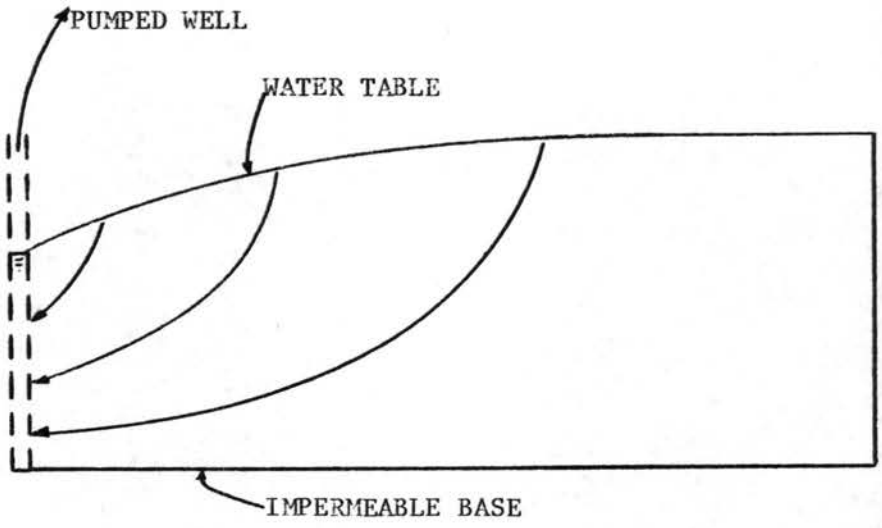

Figure 12. Unconfined gravity flow as visualized in the literature.

5.3.2 Potential distribution along bottom of aquifer - A very significant result is obtained when the potential behavior of the model of this study along the bottom of the aquifer (horizontal flow) is compared with the piezometric head obtained from the Theis solution corrected for partial penetration (Hantush, 1962). In the analytical analysis the effect of partial penetration is negligible at a distance away from the well bore approximately equal to 1.5 the aquifer thickness. Figures 13, 14 and 15 demonstrate the analogous behavior of the analytical solution and the potential distribution along the bottom of the model aquifer. At 0.49 days (Figure 13) the line representing the analytical solution lies slightly above the line of the numerical solution. At 3.49 days (Figure 14) the line of the analytical solution lies below the line of the numerical solution. As time goes on these two solutions remain parallel but seem to move further apart (compare Figure 13 with 14). In Figure 14, this behavior was also compared along a horizontal line 13.5 feet below the original position of the free

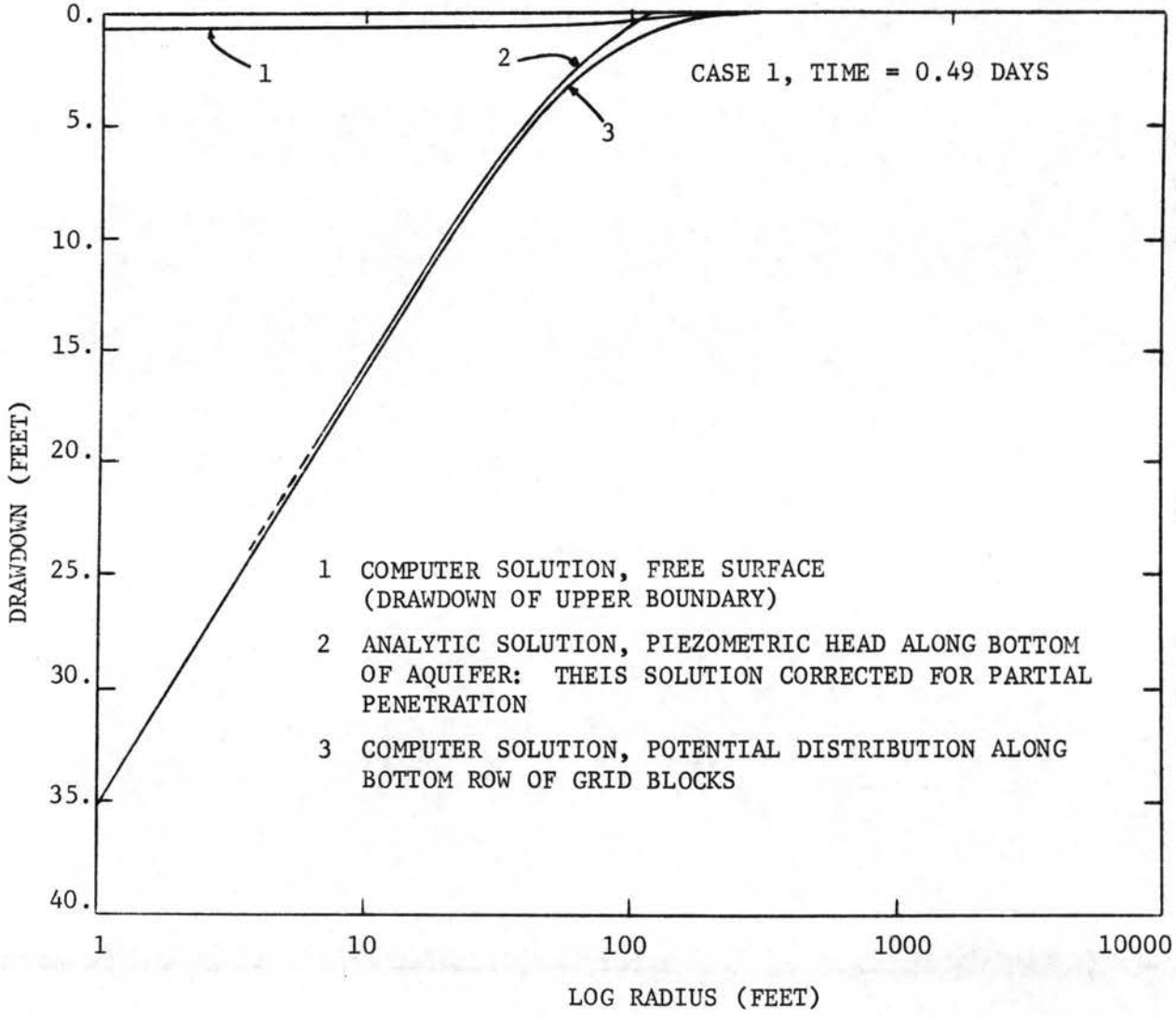

Figure 13. Potential distribution along bottom of aquifer compared with Theis solution corrected for partial penetration at 0.49 days; Case 1.

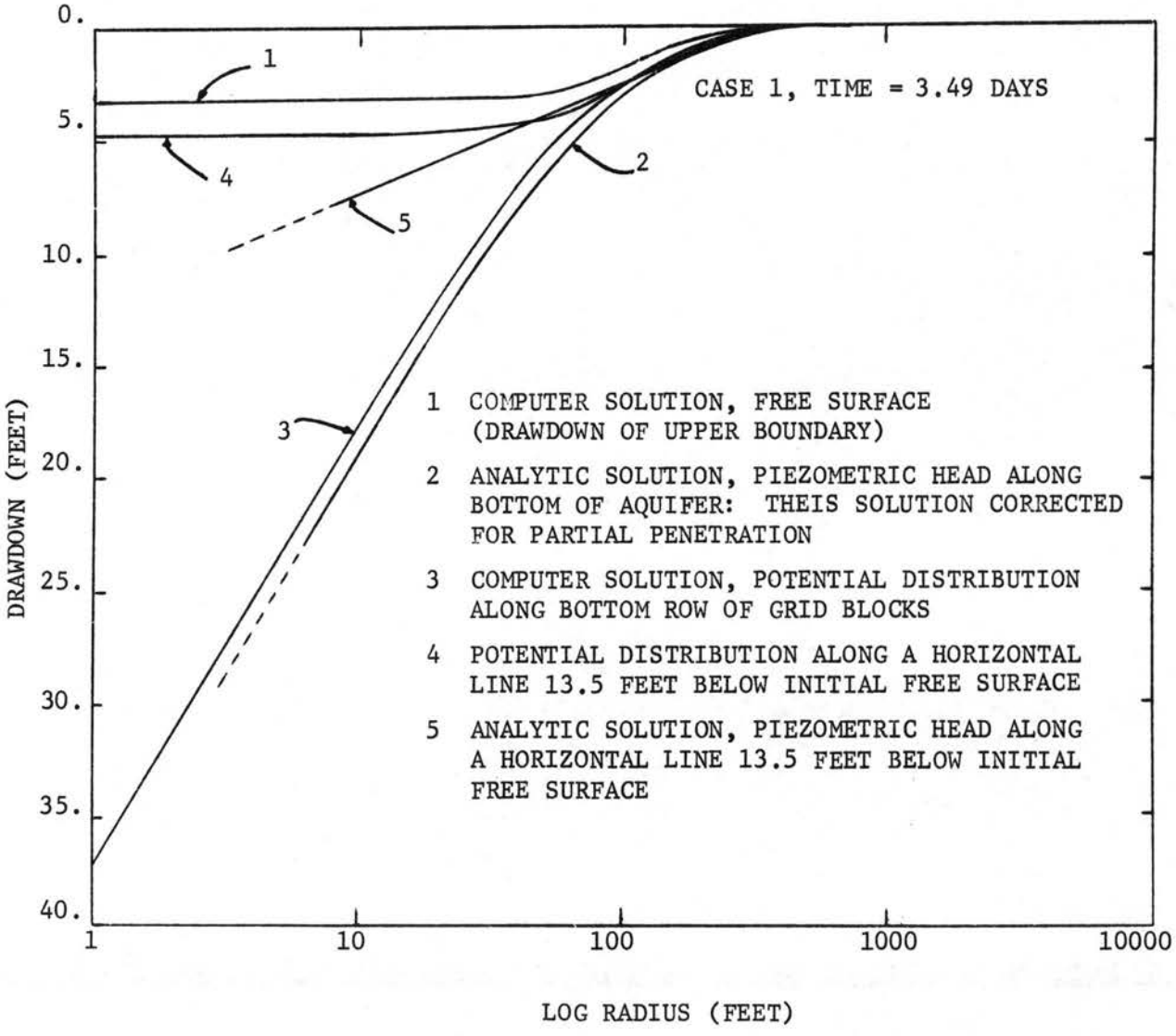

Figure 14. Potential distribution along bottom of aquifer compared with Theis solution corrected for partial penetration at 3.49 days; Case 1.

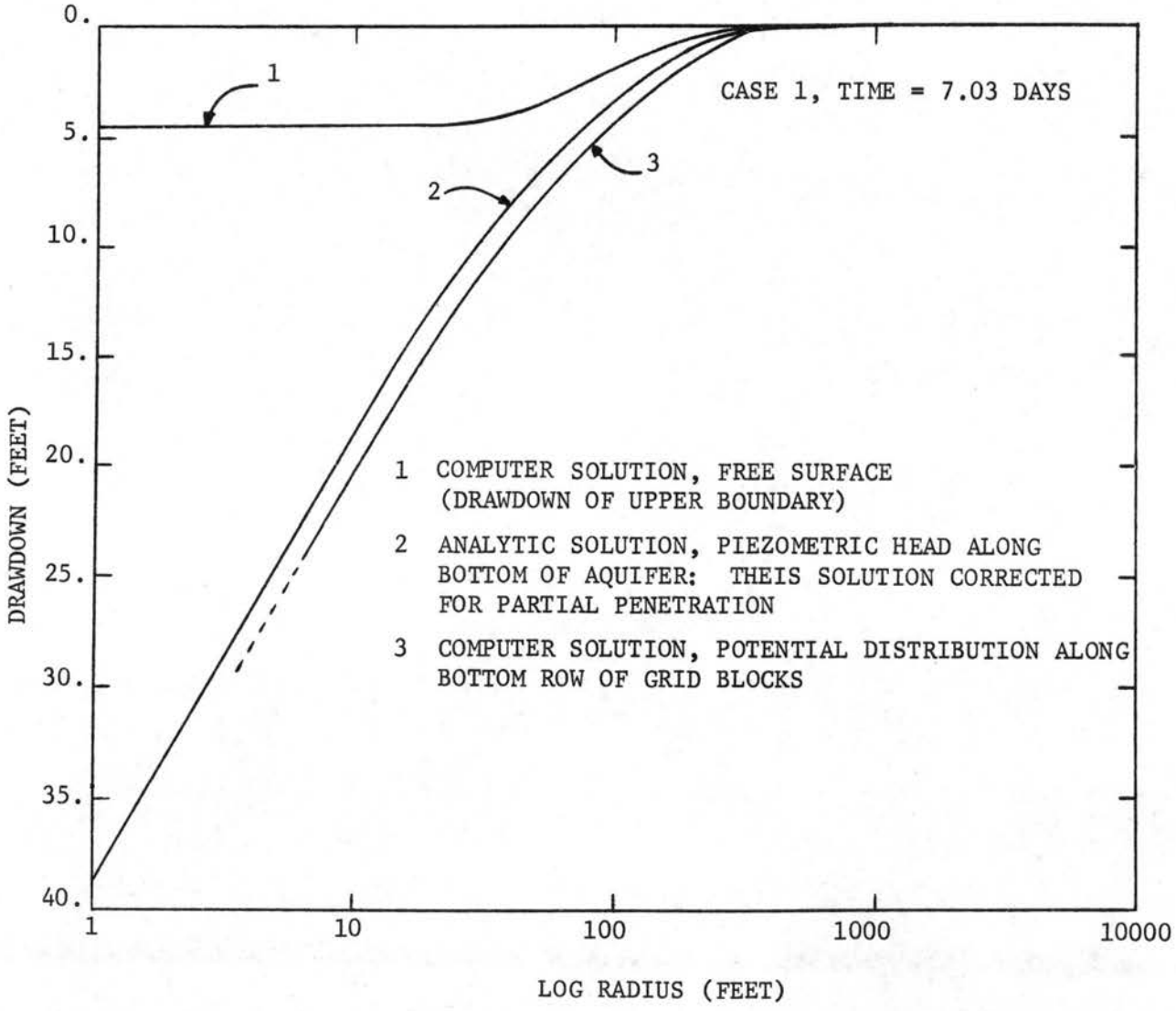

Figure 15. Potential distribution along bottom of aquifer compared with Theis solution corrected for partial penetration at 7.03 days; Case 1.

surface. The similarity in behavior is no longer true. For comparative purposes the definition of free surface as used in Figures 13, 14 and 15 deviates a little from the line of atmospheric pressure and is simply obtained from converting the saturation in a block to a water level in the block; for example, a 10 feet high block with a saturation of 60% and a residual of 20% means a water level at 5 feet in the block.

The significance of this result is that analytical solutions for confined aquifers represent the piezometric head in the confined aquifer but cannot be used to fit free surface data obtained from unconfined aquifers. Moreover, the analytical solution of partial penetrating wells in confined aquifers does not apply near the free surface in unconfined aquifers.

5.3.3 Potential distribution in time - Potential drops at different values of radii are plotted versus the logarithm of time in Figures 16, 17 and 18. At any time, these figures better explain the relative position of the curves then explained in Figures 13, 14 and 15. where they get closely together.

The potential distribution curves as well as the free surface drawdown curves, although to a smaller extent, have a relatively steep portion, a flatter portion with a point of inflection and again a steeper portion. This inflection curve is also observed when drawdown is plotted versus the logarithm of r^2/t as demonstrated in Figure 19. Regarding the above behavior of the numerical results, a quotation of Stallman (59) follows:

> "Commonly plots of the logarithm of observed drawdown versus the logarithm of t/r^2 show a steep slope after pumping begins, then a relatively flat segment, then a steep slope. The last

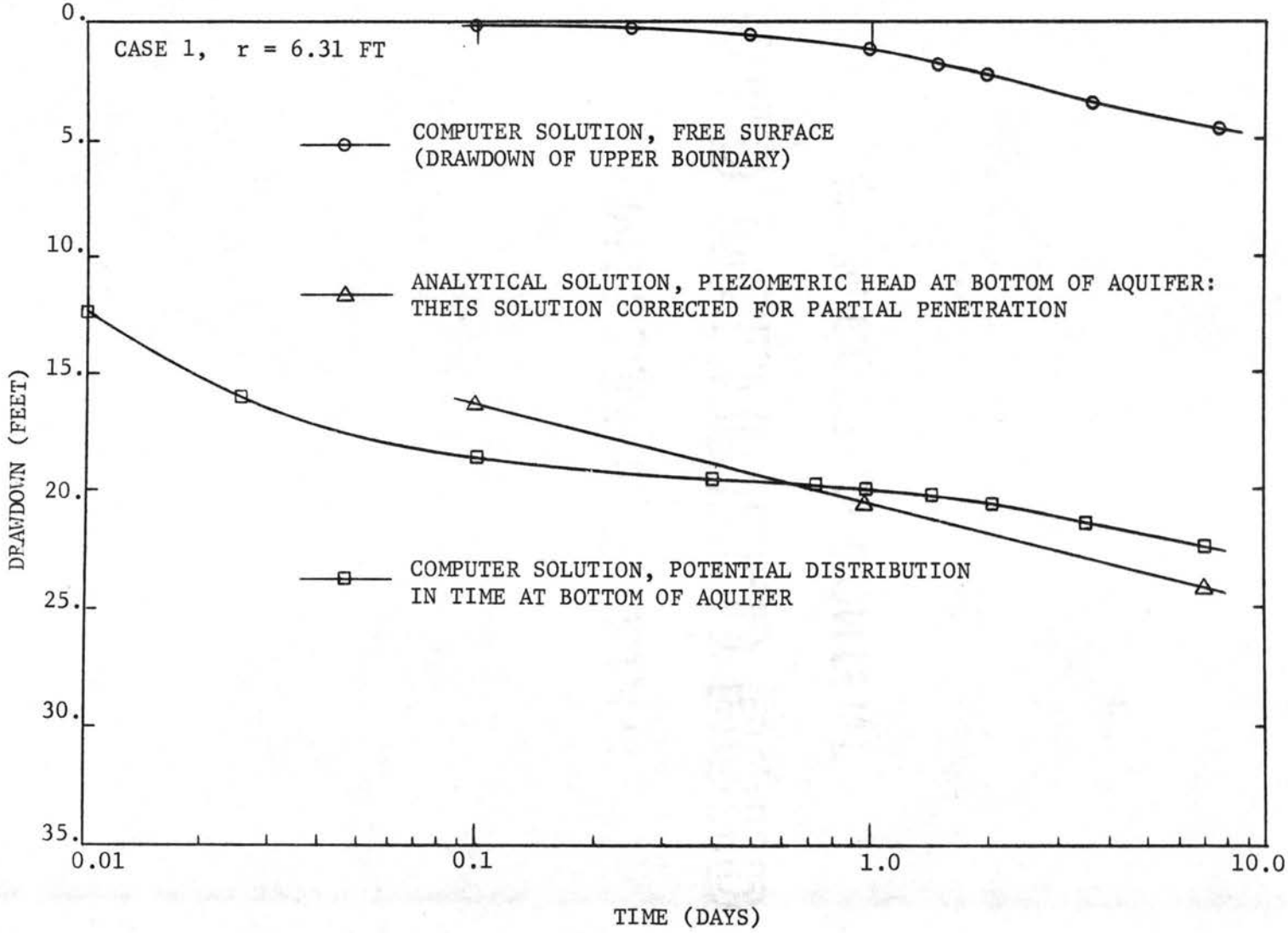

Figure 16. Potential distribution in time at bottom of aquifer at r = 6.3 feet, compared with analytic solution; Case 1.

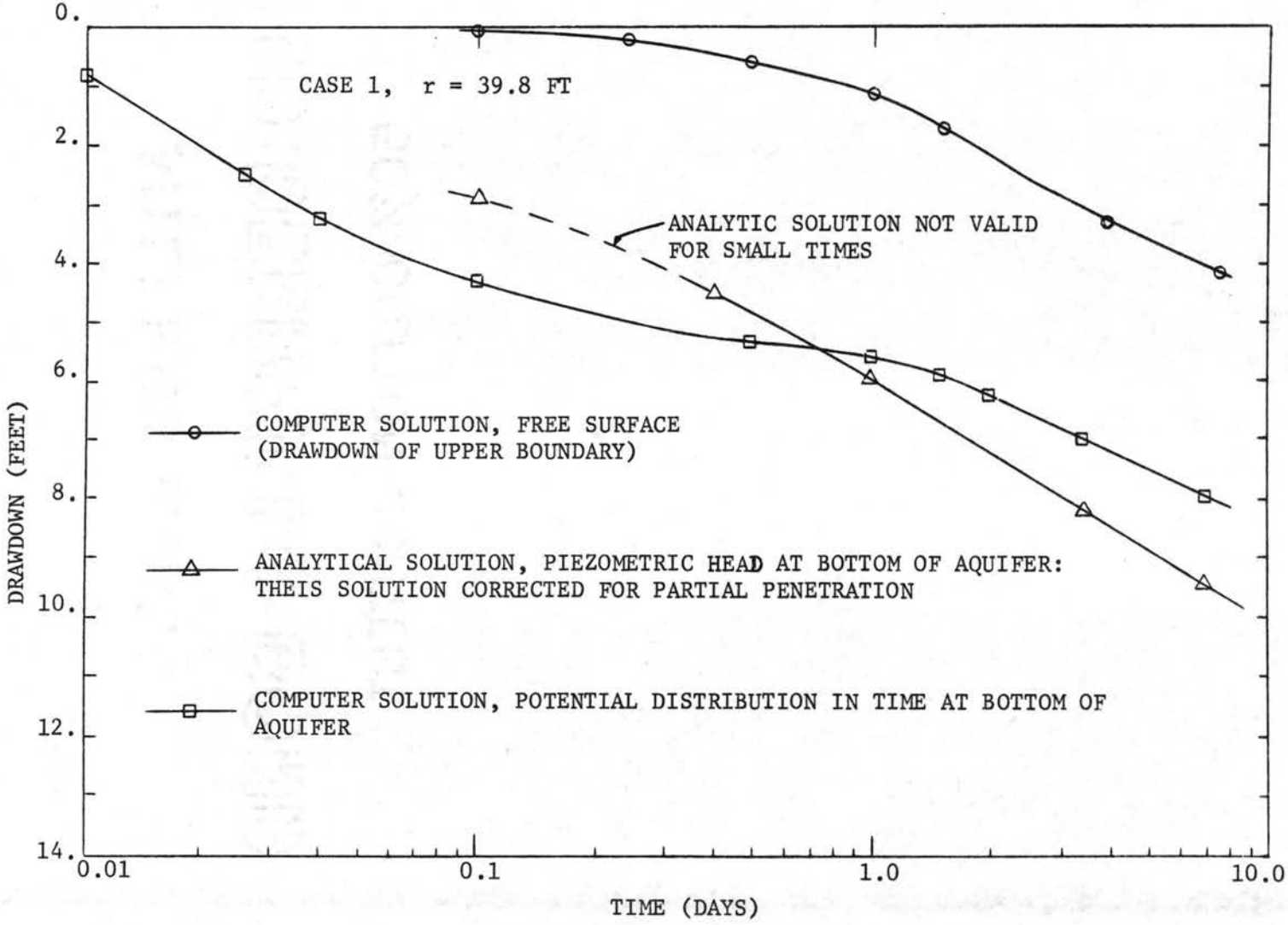

Figure 17. Potential distribution in time at bottom of aquifer at r = 39.8 feet, compared with analytic solution; Case 1.

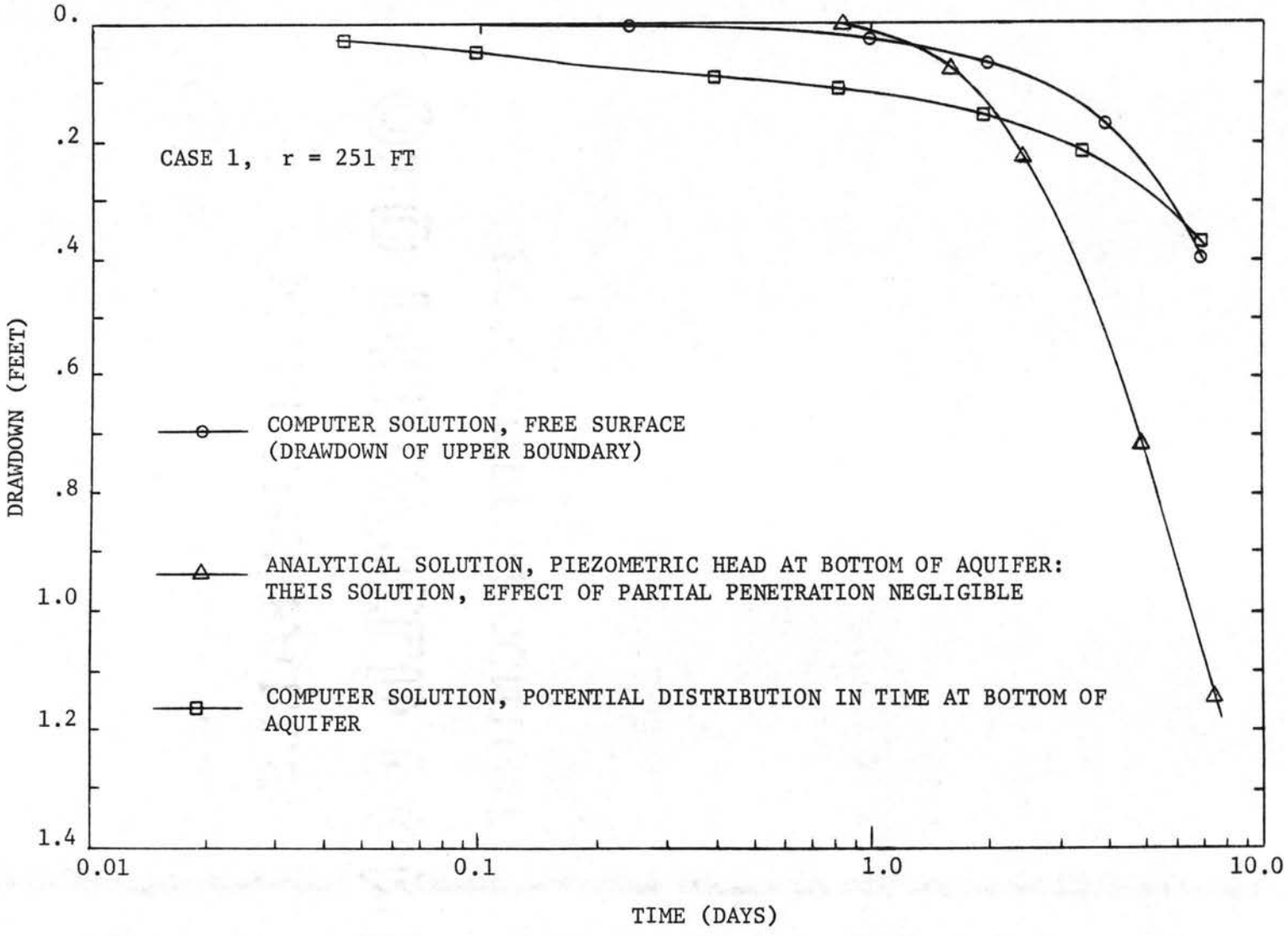

Figure 18. Potential distribution in time at bottom of aquifer at r = 251 feet, compared with analytic solution; Case 1.

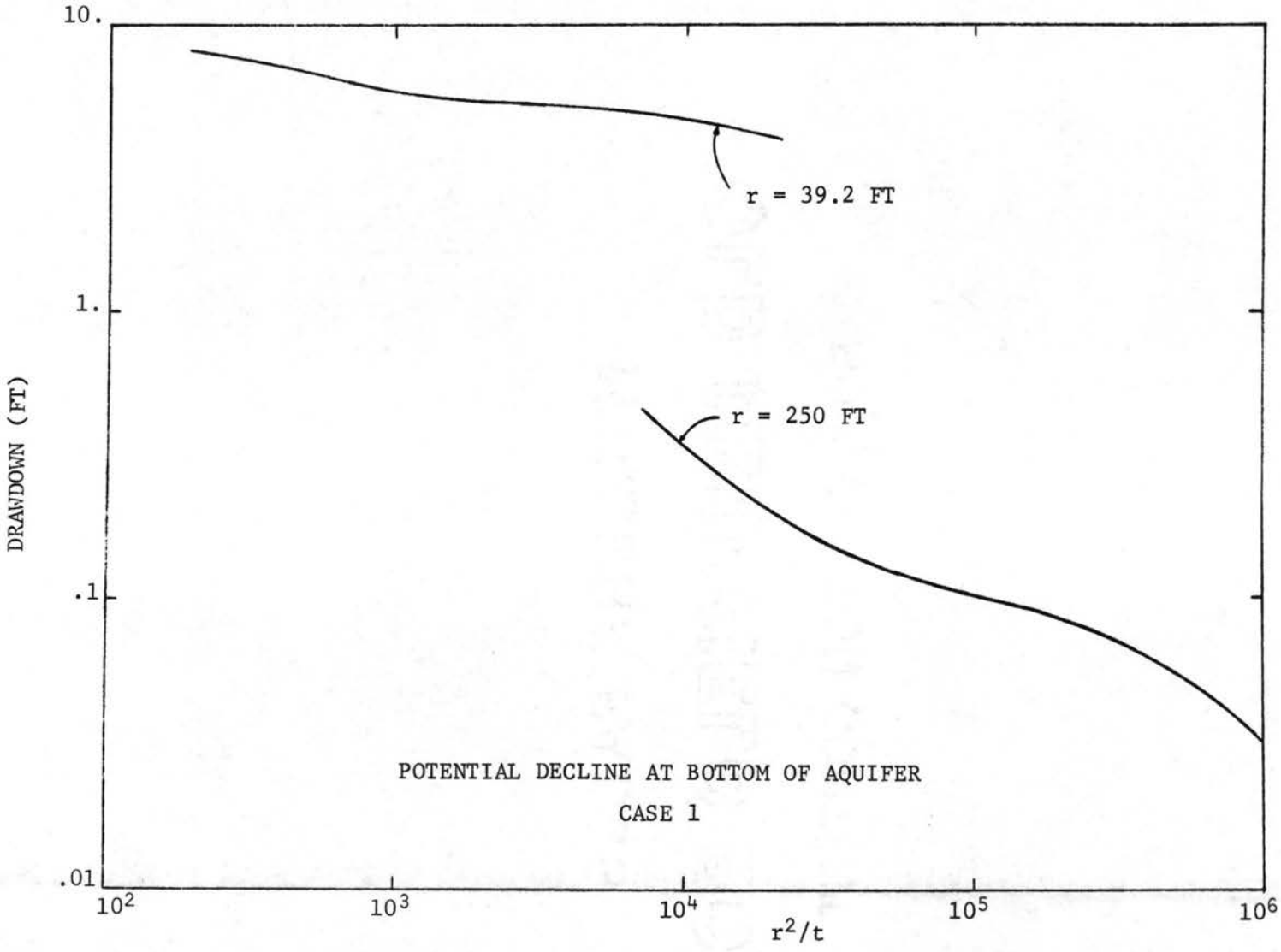

Figure 19. Drawdown versus $\log(r^2/t)$; Case 1.

segment of data generally yields sensible values of specific yield if equations of artesian flow are used for analysis. The shape of the first parts of the data plots depends upon the items that follow, which generally are not accounted for in analysis of test data from unconfined aquifers: (1) variable effective specific yield; (2) artesian release from storage below the water table; (3) vertical flow components; (4) thinning of the saturated zone as drawdown increases; (5) observation well characteristics; (6) heterogeneity."

The writer of this study feels that, in the light of this two phase, compressible fluid, gravity flow model, the above inflecting behavior is almost entirely accounted for by storage release by expansion of water for the following reasoning. Figures 16, 17 and 18, and also Figure 13, show that the initial drop in potential along the bottom of the aquifer, right after pumping starts, is greater in the numerical model than predicted by the analytical solution. The curve representing the numerical solution gradually becomes less steep until it inflects at about 0.7 days. Beyond the point of inflection this curve tends to become parallel, but not quite, with the curve representing the analytical solution. Physically, this means that after the initial pressure drop due to a sudden pumping effect, water pumped comes mainly from storage release by expansion of water in the aquifer. In a radial flow system this phenomenon is considerable since tremendous volumes of water are involved a short distance away from the well bore.

Beyond the inflection point this phenomenon of "artesian" storage release is diminishing but not disappearing, because a pressure decline, albeit small after the initial pressure drop, is continuously going on.

It is important to notice that the effect of water release by expansion is being felt at approximately the same time in the aquifer: compare Figure 16 (at r = 6.31 feet) with Figure 18 (at r = 251 feet) with respect to the occurrence of the point of inflection.

In a real field situation, aquifer compressibility may be considerable. It is quite understandable that aquifer compressibility then will play a role in a sense that it may accentuate the above described behavior.

5.3.4 Results obtained strictly related to multiphase flow

5.3.4.1 Effect of capillarity - It has been observed quite frequently that calculations of specific yield made with data obtained in the beginning of an aquifer test differed considerably from calculations made with data of the end of the test (59, 72). Wenzel (72), as an example, computed a specific yield of 0.01 just after pumping started, 0.1 after 50 minutes of pumping, and about 0.22 after 48 hours of pumping. In the light of past fully saturated flow analyses this variable effective specific yield was explained as "delayed yield from storage". When confined flow analysis is applied to unconfined flow, it is assumed that all contributions from storage come from the immediate lowering of the water table, but field observations indicate that porous materials do not drain instantaneously as water levels are lowered. Capillarity is the phenomenon responsible for this field observation.

Since capillary forces are accounted for in this multiphase numerical model, the effect of the so called "delayed yield from storage" should be observable when comparing results to analytical solutions which do not account for delayed yield from storage. Not much

though, is revealed by the curves of Figures 16, 17 or 18. They show that at any given distance from the well bore the pumping effect is felt much earlier in the numerical model (curve of potential distribution) than predicted by the analytical model (curve of piezometric head), but that the analytical model soon catches up and bypasses the numerical model with respect to drawdown. However, interaction with the phenomenon of storage release by expansion of water makes it difficult to exactly evaluate "delayed yield from storage". As time goes on and as the pumping effect is felt farther and farther with drawdowns becoming very small, the effect of capillarity should gradually become smaller and smaller too. Indeed, computations of specific yield at different times show that a limiting value is approached when times grow large. Note that the analytical solution is not a valid criterion for evaluating delayed yield from storage by comparing its solution with the numerical results of this study, mainly because confined flow behaves differently than unconfined flow.

Capillarity is not the object of detailed analysis in this study. Although its effect is incorporated on a macro-scale, it is realized that a detailed distribution of saturation above the water table cannot be obtained, the vertical dimension of the blocks being the same order of magnitude of the capillary effect under hydrostatic conditions.

5.3.4.2 Effect of air dissolved in water - Data for the amount of air dissolved in water under aquifer conditions were taken from Dodson and Standing (2). These data behave corresponding to Henry's law, i.e., a linear law for gases dissolved in liquid solvents as a function of pressure. The data (see Appendix C) show that at atmospheric pressure 0.0338 cubic feet of air are dissolved in water.

It is realized that under certain circumstances the above amount of dissolved air might be either overestimated or underestimated. However, practically all ground water originates as surface water; the following situation is quite possible. Consider an aquifer continuously pumped and recharged. During the process of recharging considerable amounts of air may be trapped and eventually partly dissolve with increasing pressure in the water body, which would lead to a larger amount of air dissolved in the water than the amount assumed in this study. The assumed amounts are certainly not exaggerated but rather reflect average aquifer conditions.

Before showing the results regarding air dissolved in water, it may be useful to describe the following mechanism. When an aquifer is suddenly being pumped, the pressure in the aquifer will sharply drop in the vicinity of the well bore. This causes air to evolve from solution first as small isolated bubbles, and to occupy space which was previously occupied by the water. As the pressure keeps dropping, more air will evolve from solution and at the same time expand, until the bubbles coalesce and continuous filaments of air are being formed. This is the so called residual air saturation (critical gas saturation in the petroleum technology) at which air starts to flow. It is easily seen that during this process the permeability to water significantly decreases.

Figure 20 shows what occurred in time in this two-phase, free surface gravity flow simulator. The water desaturation curve in the bottom block adjacent to the well screen goes with the left ordinate; the pressure curve of the same block goes with the right ordinate. Pressure is seen to sharply drop the moment pumping begins (time zero)

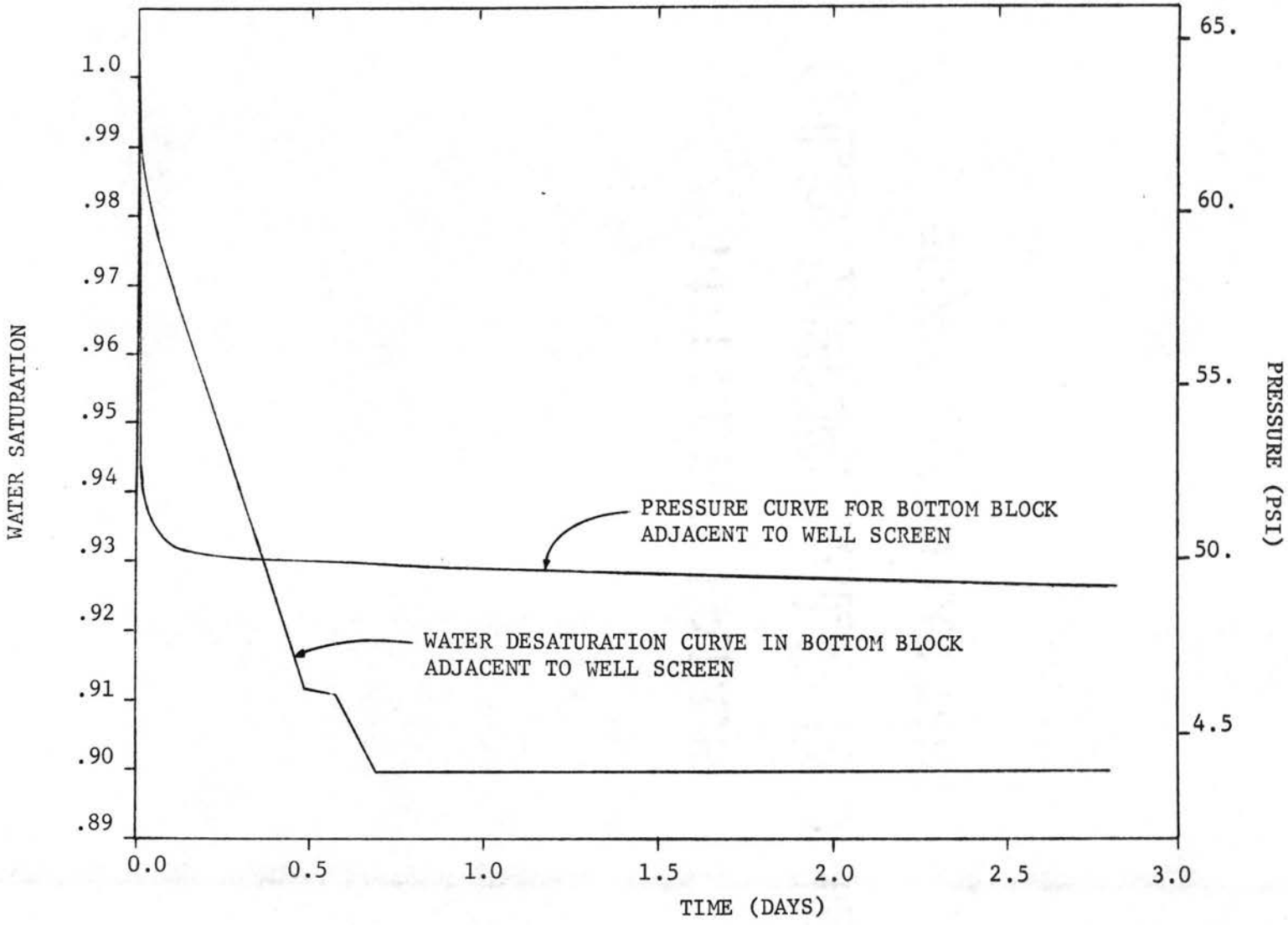

Figure 20. Water desaturation curve and pressure curve in bottom block adjacent to well screen; Case 1.

and then more gradually. The air saturation is seen to gradually increase (water saturation decreases) until it reaches residual saturation (Sa = 0.10, Sw = 0.90). At this moment (0.7 days) the air in this block becomes a continuous phase and starts flowing. All air coming out of solution or expanding after 0.7 days, which is very little because of the slow pressure drop, readily flows out; physically, this is easily understood because of the very low resistance to flow of air. Hence, air saturation remains constant after 0.7 days. The saturation results show that beyond 0.7 days the air phase saturation is building up in the block next to the one adjacent to the well bore, but very slowly (Sa = 0.047 after 7.78 days of analysis).

The significance of the above result may be summarized as follows: first, the effective permeability near the well bore is significantly affected by air evolving from solution; relative permeability has dropped from 1.0 to 0.875 (see Appendix C, input data of Case 1). Secondly, this drop in effective permeability in turn affects the potential distribution around the well bore, in a way that the pumping effect will extend further away from the well bore than it would if no gas evolved from solution, simply to overcome the lower permeability near the well bore.

5.3.4.3 The free surface boundary condition - Two phase flow is not uniquely responsible for the shape of the free surface. The effect of partial penetration of the well and gravity seem to be the governing factors in determining the shape of the free surface around the well bore (see Dagan, page 1060, Figure 1). Two-phase flow, however, will allow one to locate the line of atmospheric pressure (free surface) and also to study the effect of capillarity as related to the problem of delayed yield from storage.

The nature of the behavior of the drawdown curve in time and space, however, reveals that flow in the so called cone of depression (unsaturated zone, capillary zone) is insignificant with respect to the total flow phenomenon and hence that delayed yield from storage as explained by capillarity, has very little bearing upon the solution. It should be clear by now that confined flow analysis does not apply to unconfined free surface gravity flow. There is a variety of undetermined factors involved when confined flow analysis is applied to unconfined flow, and adjusting the confined flow solutions to fit unconfined flow data is highly questionable.

Noteworthy of mentioning is the computation of air flow into the upper row of blocks, intimately related to the treatment of the free surface boundary condition (cf. section 4.4.2.2). With a pumping rate at the well bore of 43,200 CF/DAY, the rate of air flow into the upper row of blocks is expected to be nearly the same. This result is indeed obtained (see Appendix D, sample computer output: gas production map). Difference in volume of water at aquifer conditions and water at surface (atmospheric) conditions accounts for the slight discrepancy. Differences in air and water rates are sometimes larger, however, than explainable by compressibility of water; these differences can easily be understood when it is realized that the convergence criterion on saturations is 0.0001 (i.e. maximum allowable value of S^* , cf. Chapter 4). Grid blocks a distance away from the well are quite large with tremendous pore volumes. The grid block with radius of 251 feet, for example, has a pore volume of 4×10^7 FT^3, so that a value of S_w^* , say 0.00005, satisfying the convergence criterion is equivalent to 2.0×10^3 FT^3 of water.

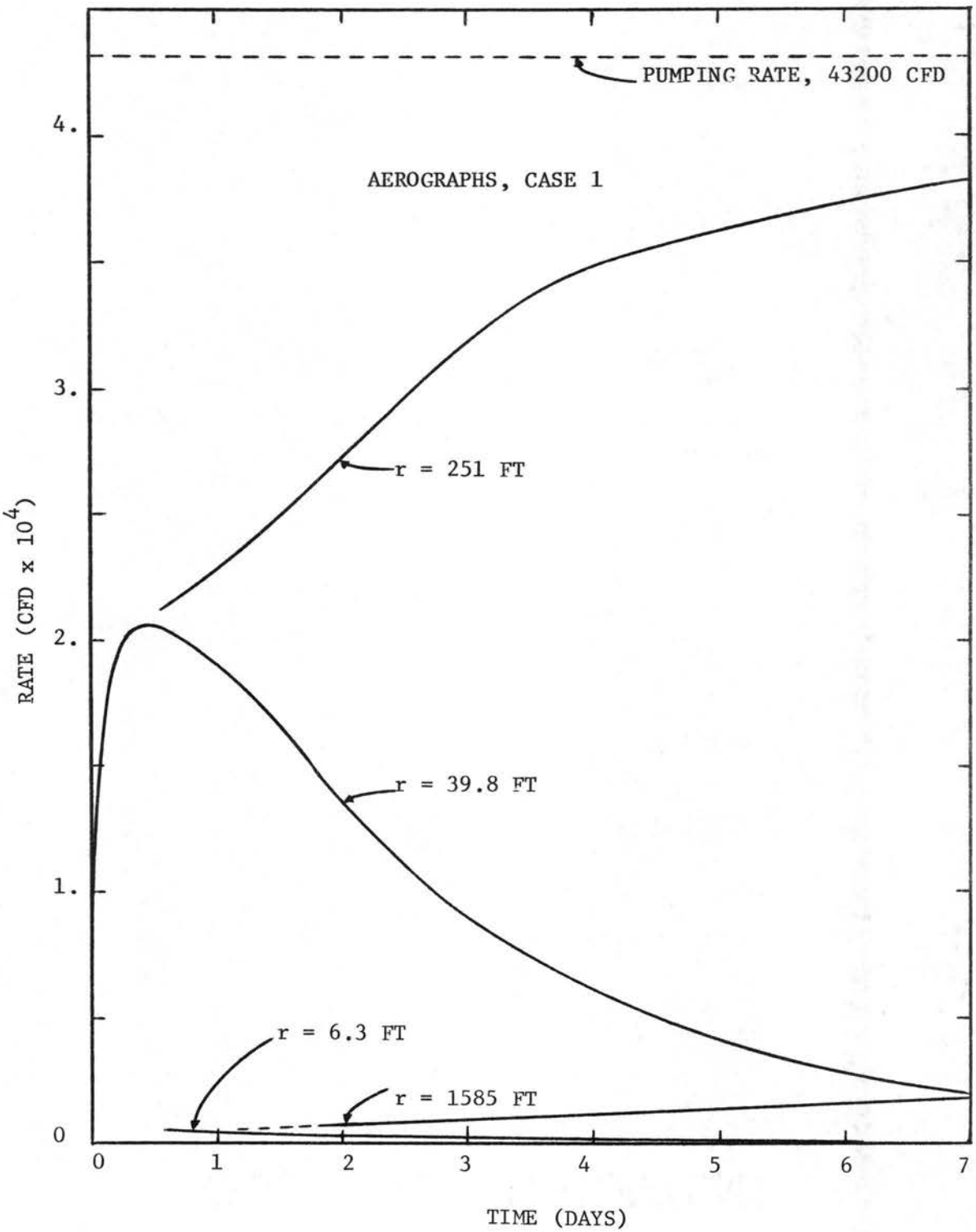

Figure 21. Aerographs of top row grid blocks at different distances from well bore; Case 1.

Varying rates of air flow into the blocks with radii of 39.8 feet, 251 feet and 1,585 feet, are shown as a function of time in Figure 21. The shape of these areographs (i.e., rate vs. time curve, cf. hydrograph) is exactly related to the behavior of the free surface, regarding the point of inflection moving away from the well bore as pumping goes on. The point of inflection of the free surface curve is 39.8 feet away from the well at about 0.35 days, which is when the peak of the aerograph occurs. At 251 feet, the air rate is increasing but would soon reach a maximum when the point of inflection of the free surface curve reaches that distance, and then decrease. At 1,585 feet, the effect of pumping is gradually being felt.

The above result is rather pleasing from a numerical solution point of view, since it is more or less a balance of materials on a macroscale, and an argument in favor of the correct mathematical treatment of the free surface boundary condition.

5.4 Analysis of Case 2

5.4.1 Results of Case 2, compared with Case 1 - The results of Case 2, the high permeability case, do not reveal any new striking features of two-phase, free surface, compressible fluid, gravity flow. The results of course, are different from Case 1, in that the same phenomena are interacting but at different times than in Case 1. For this reason, the discussion of Case 2 will consist of a brief enumeration pointing out similarities and important differences with Case 1

(1) The flow pattern as shown on the potentiometric map of Figure 22 is analogous to the flow pattern of Case 1.

(2) The potential decline toward the well bore along the bottom of the aquifer at any time is much less steep than in Case 1; an example after two days of pumping is shown in Figure 23. The effect of pumping, however, extends much farther for the same period of analysis.

CASE 2. POTENTIOMETRIC MAP AT 6.675 DAYS

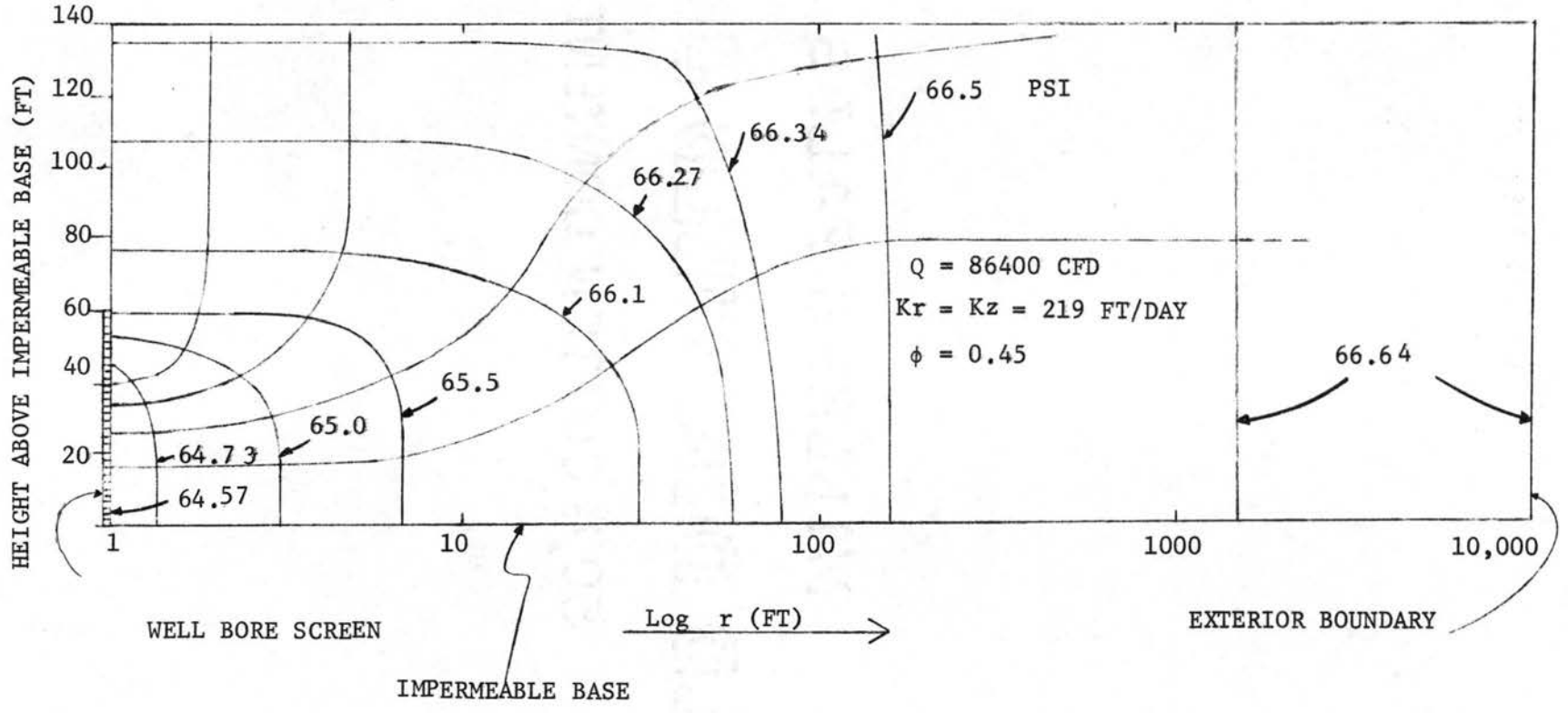

Figure 22. Potentiometric map and flow lines of Case 2: logarithmic distance scale.

(3) Again, there is no agreement between the free surface curve and the curve of potential drop along the bottom of the aquifer. Both show a drawdown of the same order of magnitude though (Figure 23), close to where the curves intersect.

(4) When the potential decline toward the well bore along the bottom of the aquifer is compared with the piezometric head of analytic solutions along the bottom of the aquifer at any time then again these solutions are analogous in behavior; the two solutions compared are parallel in space and close together for a short while after pumping starts. As time grows large, the two solutions remain parallel in space but get further and further apart in time; as in Case 1 the analytical solution lies below the numerical solution. An example after two days of pumping is shown in Figure 23. There is no reason, however, for these two solutions to remain close together, since two different flow phenomena are solved for. Permeability seems to influence the rate of divergence of the two solutions (compare Case 2 with Case 1).

(5) The potential distribution in time at the bottom of the aquifer again shows a minor inflection of the curves at about 0.02 - 0.03 days (Figures 24, 25 and 26) instead of at 0.7 days for Case 1. Hence, the higher the permeability, the sooner the effect of storage release by expansion of water diminishes.

(6) The behavior of the potential distribution in time at the bottom of the aquifer, when compared with the analytical solution for piezometric head, is analogous to Case 1. The potential drop of the numerical solution is larger at first, but then the curve proceeds with a less steeper slope than the slope of the curve of the analytical solution. Both solutions cross each other at about 0.03 days (0.7 days for Case 1). Again, there is no reason to obtain agreement between numerical and analytical results.

(7) Aerographs are shown in Figure 27. The point of inflection of the free surface curve is at a radial distance from the well bore of 251 feet after 5.5 days of pumping. The total air inflow rate along the upper row of blocks nearly adds up again to the pumping rate (86,400 CF/DAY).

(8) Air coming out of solution near the well bore is not nearly as spectacular as in Case 1. This is understandable because the larger permeability results in a much smaller pressure drop toward the well bore. Air saturation reached its residual (critical) value of 0.05 at 1.715 days of pumping in the upper block of the two blocks facing the well screen. In the lower block, the air saturation reached its residual value at 6.68 days of pumping. The relative permeability of water at residual air saturation is 0.92.

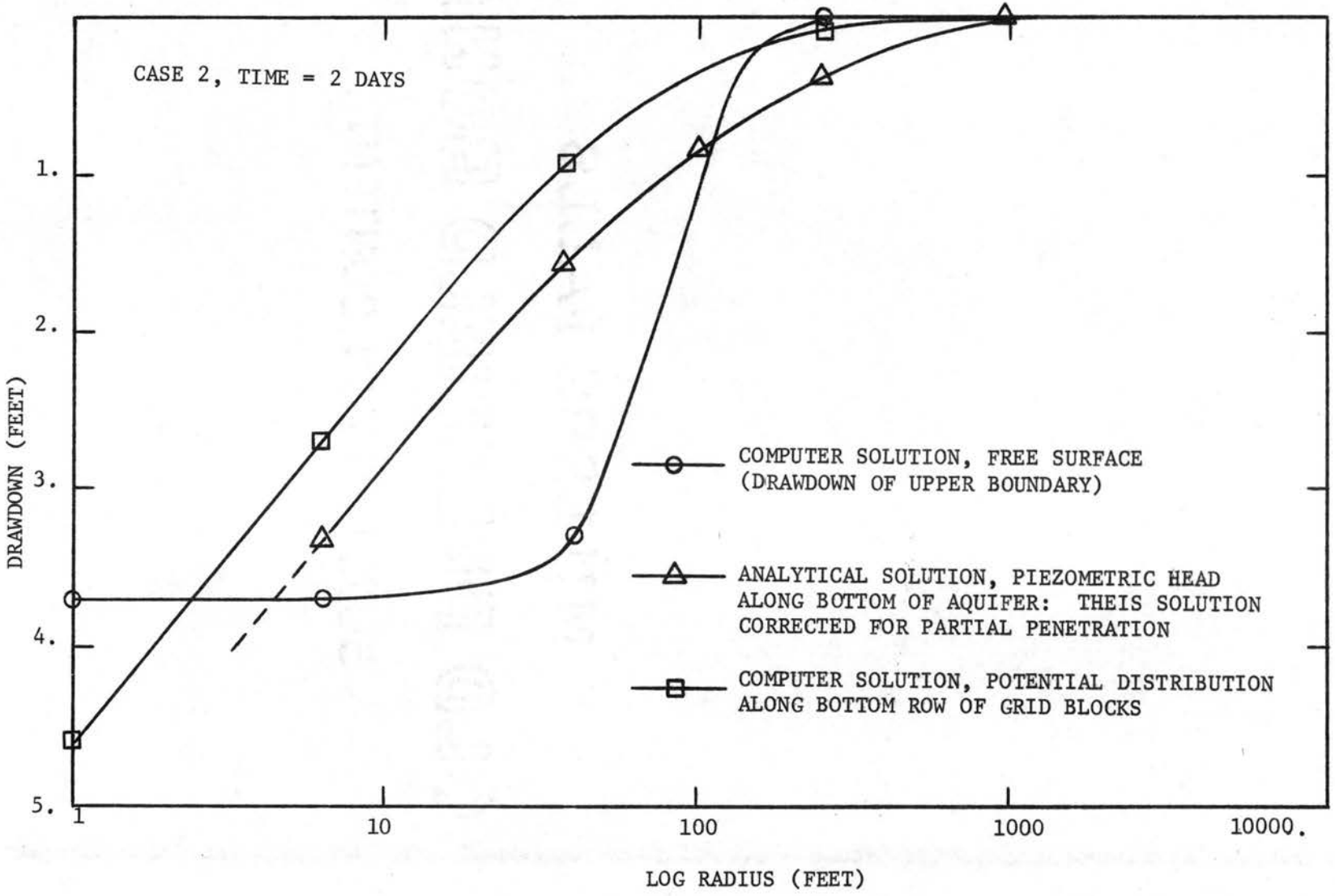

Figure 23. Potential distribution along bottom of aquifer compared with Theis solution corrected for partial penetration at 2 days; Case 2.

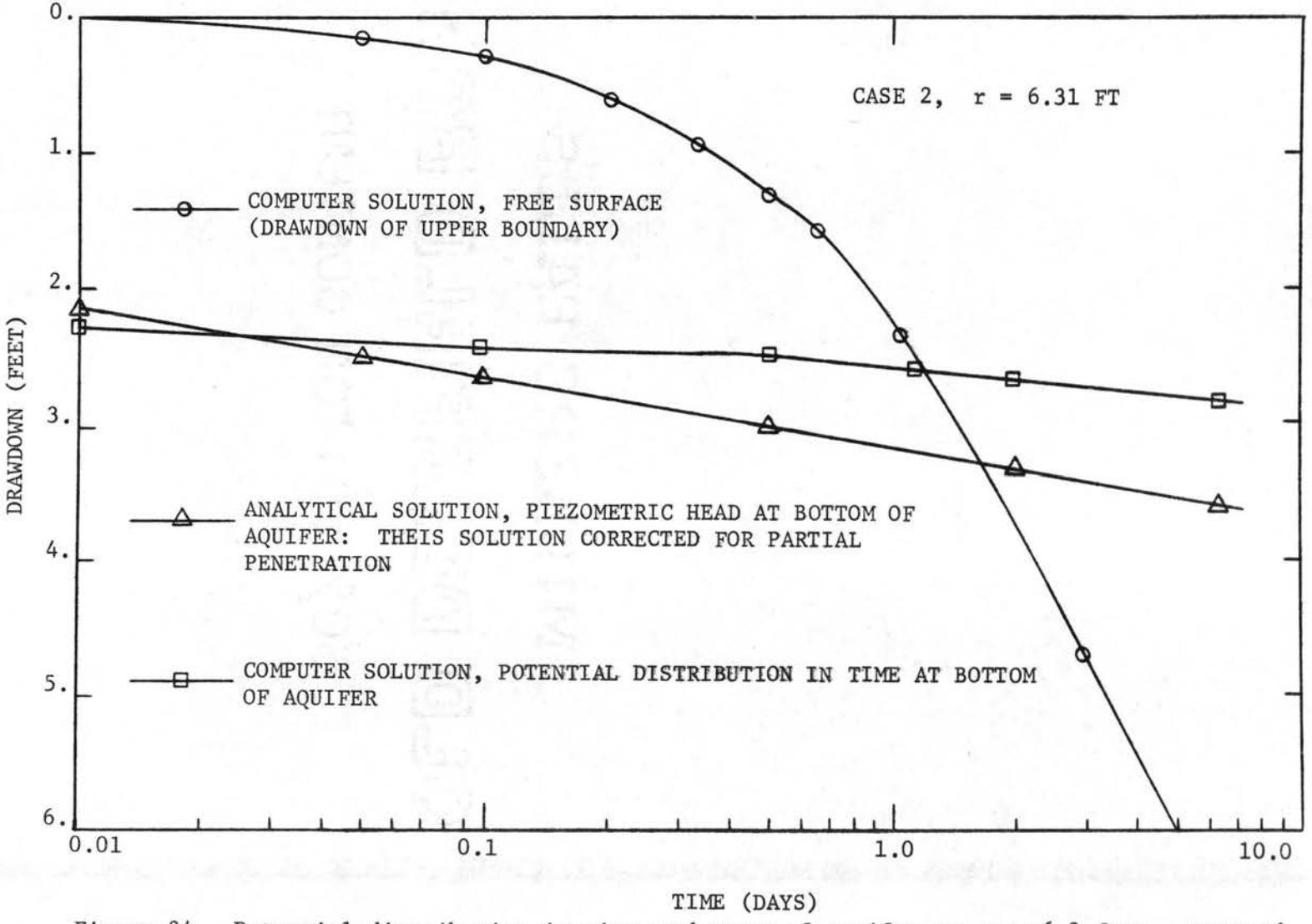

Figure 24. Potential distribution in time at bottom of aquifer at r = 6.3 feet, compared with analytic solution; Case 2.

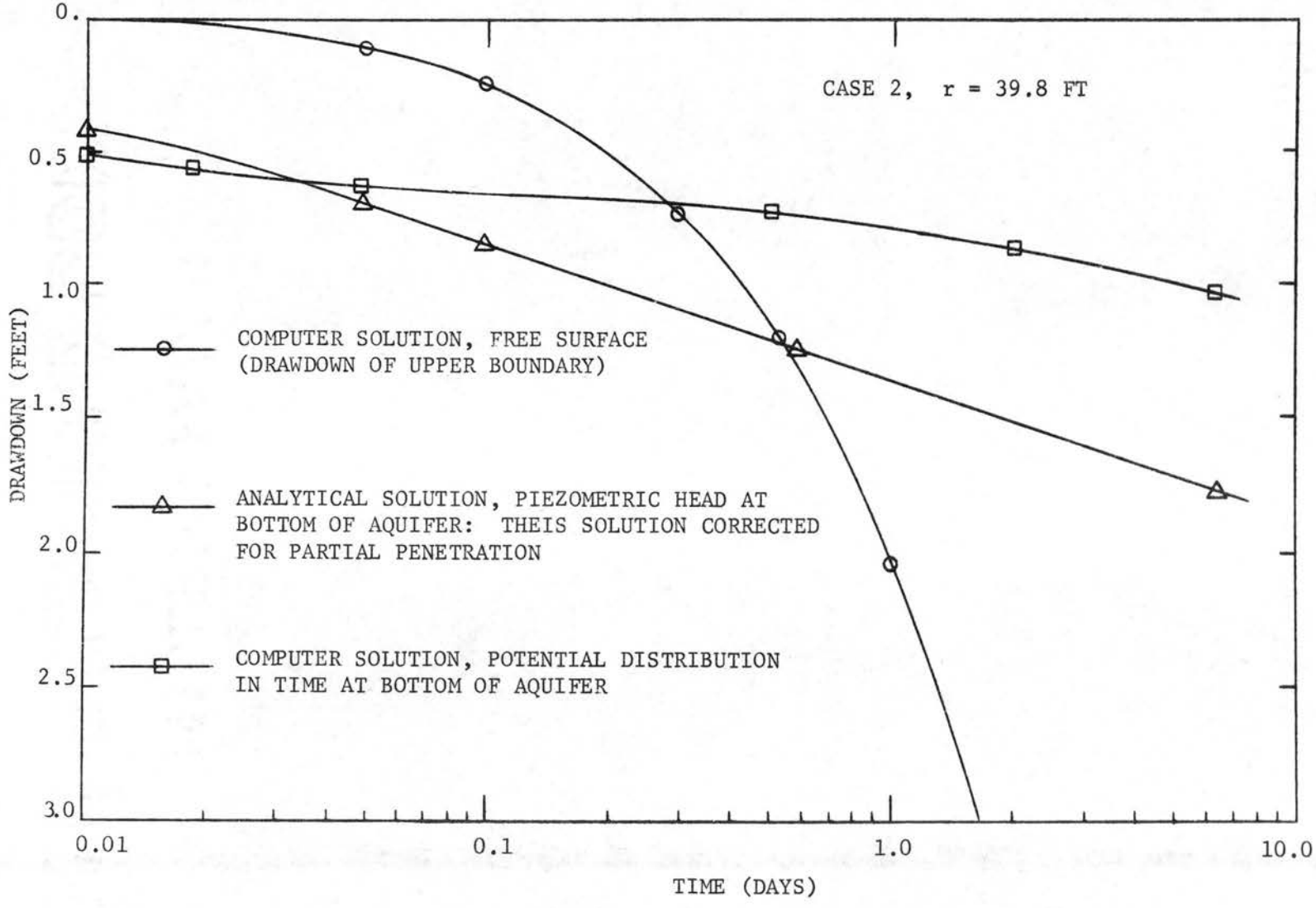

Figure 25. Potential distribution in time at bottom of aquifer at r = 39.8 feet, compared with analytic solution; Case 2.

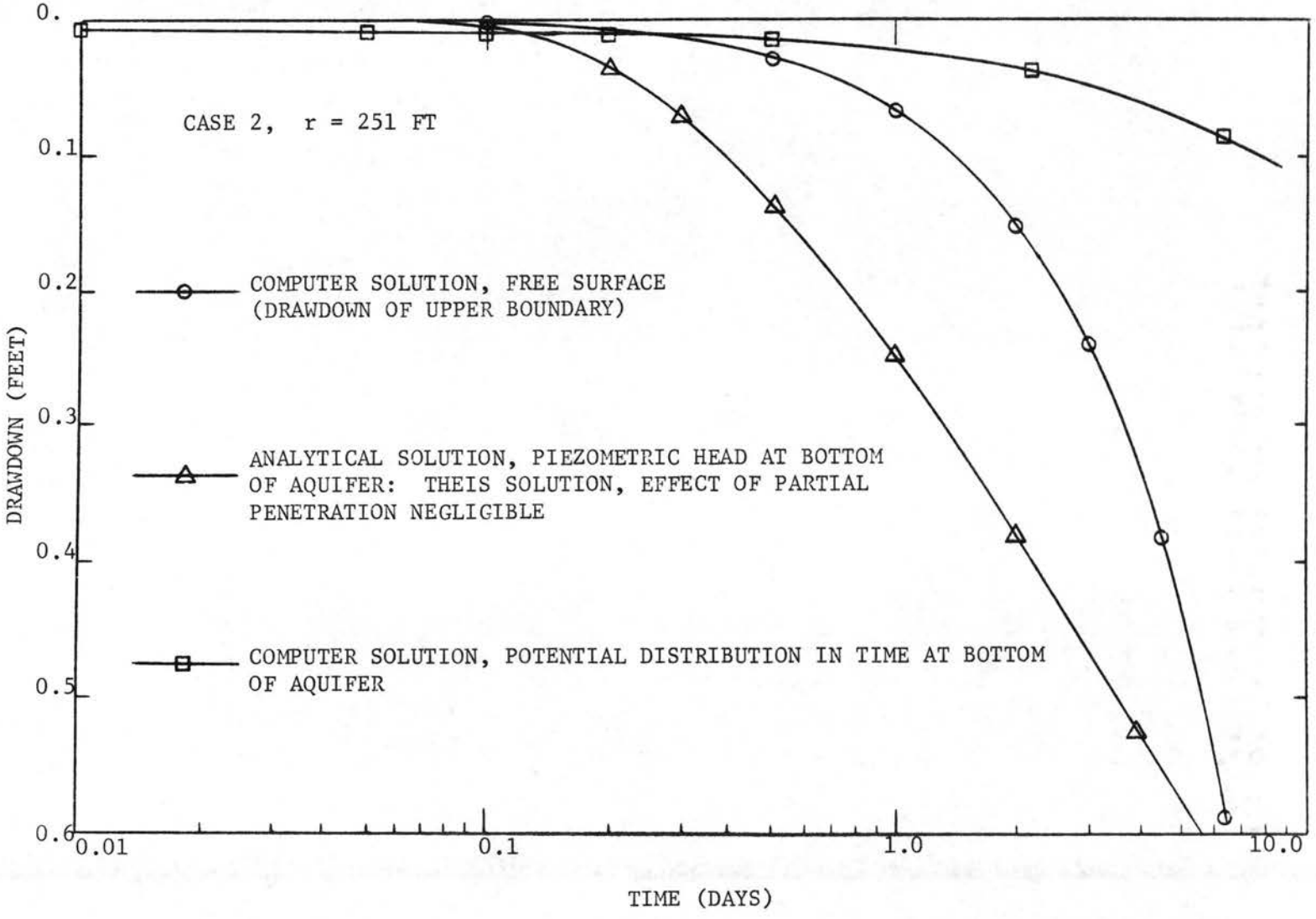

Figure 26. Potential distribution in time at bottom of aquifer at r = 251 feet, compared with analytic solution; Case 2.

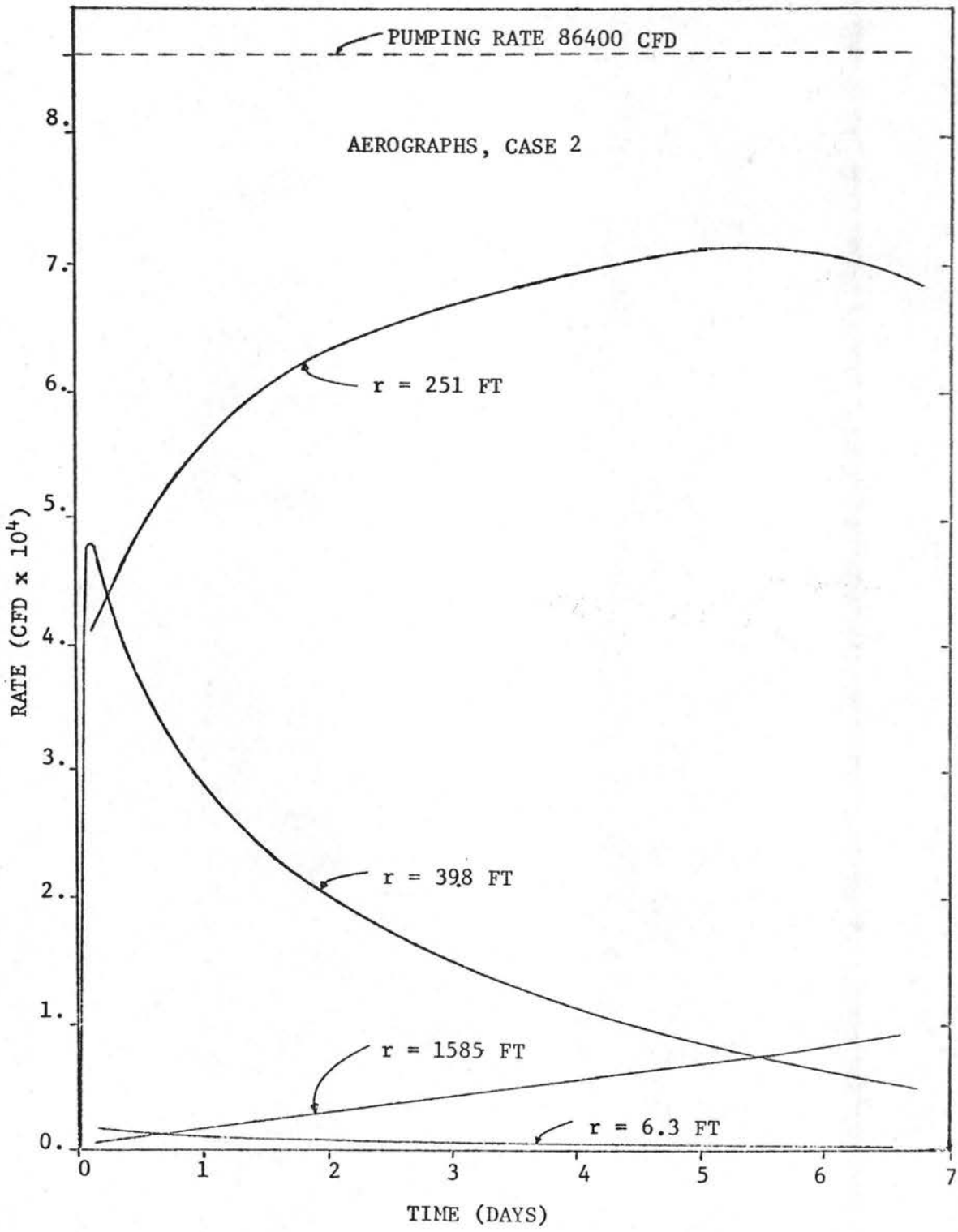

Figure 27. Aerographs of top row grid blocks at different distances from well bore; Case 2.

5.5 Aquifer Test Analysis and Unconfined Free Surface Flow

In this study, two-phase, free surface compressible fluid gravity flow was modeled. The results were shown to be quite different from confined flow analysis. In fact, it is shown that the confined flow analysis does not apply to unconfined flow.

From the literature it appears that obtaining reasonable aquifer constants is a matter of luck. Accounts of contradictory results, meaningless results, and inconsistencies are more numerous than accounts of successful aquifer tests. The chance of obtaining reasonable unconfined aquifer constants with confined flow analyses seems to depend upon the nature of the observation well, or on the depth of penetration of the piezometer tube, or on the time during which the data were taken. Some researchers will recommend that drawdown measurements be made only after several days of pumping and at large distances away from the well bore. Others will advocate the measurements to be made during the first day of pumping or even the first hours. Observation wells are either screened throughout or only partially. In other instances, piezometer tubes are recommended either open in the upper portion of the saturated thickness or open in the lower portion.

This variety of opinions and guidelines is understandable in the light of the results of this study. Depending upon what, where, and when measurements are made it is possible to obtain reasonable results. Consider for example Case 1, the low permeability case. If drawdown measurements were obtained from a piezometer open at the bottom of the aquifer and located near the well bore, there is a fair chance for the analyst to obtain acceptable aquifer constants, if he made his measurements beyond one day of pumping (Figure 17). If for the same case, the

piezometer tube were only open at the top, he would not get any reasonable results at all. Although the data may be perfect, they are not apt to fit exactly a confined flow analytical solution. His conclusion will be wrongly that his data are not reliable.

Figures 28 and 29 are examples of what can happen in actual aquifer test analyses. The drawdown data in this simulated aquifer test come from the numerical solution of Case 2 at a distance of 251 feet away from the well bore. In Figure 28 the data would correspond to piezometer measurements at the bottom of the aquifer, whereas in Figure 29, the data would correspond to piezometer measurements at the top of the aquifer. A "type" curve of $W(u)$ versus u (1,26,32) is superimposed upon the curve of drawdown versus r^2/t. The inflection of the latter curve in Figure 28 was explained earlier in terms of storage release by expansion of water. A portion of the type curve covers the data curve only beyond the effect of storage release by expansion. The permeability computed from the Theis solution was four times too large. The computation of specific yield was meaningless. In Figure 29, curves could not be matched over a certain length of the type curve and no computations were made.

To conclude this section, the following example, drawn from the literature, is discussed. Weeks (70) and Dagan (19) analyzed data obtained from the same unconfined aquifers. Weeks used the Hantush (30) analysis for partially penetrating wells. Dagan, on the other hand, analyzed the data with an analytical solution which includes the vertical flow component. In short, Dagan described the free surface boundary condition with a non-linear time dependent partial differential equation to account for the flux across the free surface; this flux in its turn

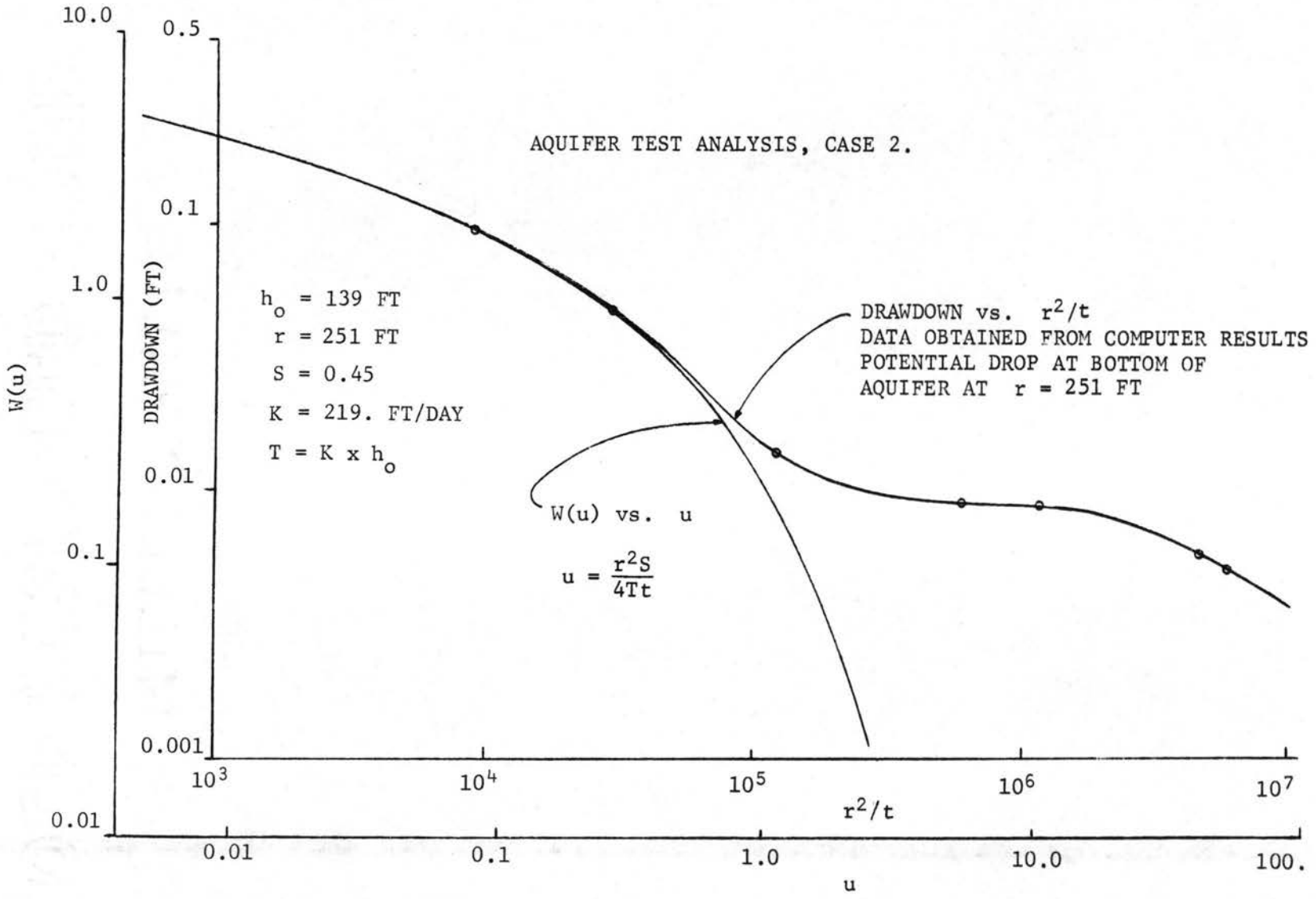

Figure 28. Aquifer test analysis: fitting the drawdown data obtained from the potential at bottom of numerical model with the Theis solution, r = 251 feet, Case 2.

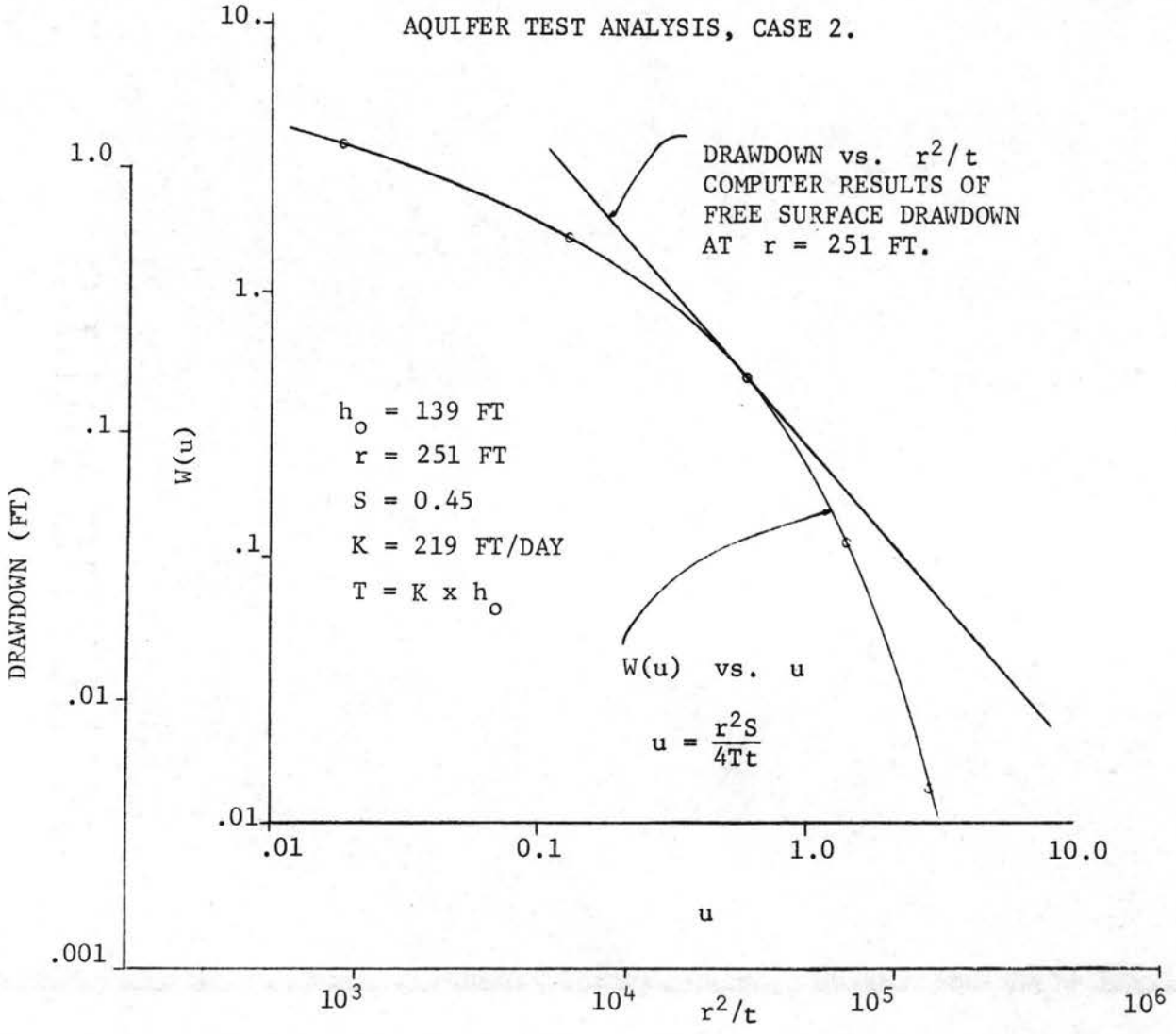

Figure 29. Aquifer test analysis: fitting the free surface drawdown data obtained from the numerical model with the Theis solution, r = 251 feet, Case 2.

depends upon the potential distribution inside the solution region, given by Laplace's equation. Dagan succeeded in solving this system of two equations analytically after first linearizing the condition at the free surface. His solution shows analogous shapes of the free surface as obtained by the author of this study (Dagan, Fig. 1, p. 1060). However, his solution adopts the usual assumptions of constant effective porosity, small drawdowns and fully saturated flow. The field data were obtained from piezometers, open at approximately 12 feet below the watertable. To fit his analytical solution with the field data, Weeks concluded that the aquifer had a horizontal to vertical permeability ratio of 20 to 1. Dagan contradicts this result completely by obtaining a horizontal to vertical permeability ratio of 2 to 1.

The author of this study would tend to believe Dagan's result and would like to point out the value of Dagan's solution, which has not drawn much attention in the literature. His solution is obtained under unconfined aquifer conditions, including the vertical velocity components; tabular results, however, could be easily obtained by computer for a broad range of parameters.

5.6 Computational Aspects of the Model

Time step sizes in Case 1 as well as in Case 2 ranged from 0.01 days in the beginning of the analysis to 0.15 days toward the end of the analysis, with a throughput of 10 in the blocks adjacent to the well screen. By a throughput of 10 is meant that during a time step 10 times the amount of the pore volume flows through a block.

A criterion for time step size was not developed. A solution obtained by Newton iteration depends upon the goodness of an initial

guess to start the iteration process (see Appendix A). This initial guess should be sufficiently close to the new solution. Much depends upon the interpretation of "sufficiently close". Hence, time step size with the Newton iteration technique is most likely a process of trial. In this study, time step sizes were gradually increased until the solution "blew". Punched output, however, of pressure and saturation results of the last running timestep were obtained. This punched output could then be used to restart the run from the last punched output on, using smaller time steps. Loading and compiling of the punched card deck each time was eliminated by keeping the program on tape in binary form. Normally, loading and compiling time for this nearly 3,000 punched card model consisted of 58 seconds central processor time and 108 seconds peripheral processor time (CDC 6400 computer, SCOPE system with FORTRAN EXTENDED, VERSION 3.2).

The Newton iteration process is said to be particularly suitable for "physically oriented" problems. It seems, however, that the inflection in the solution does not quite correspond to this idea of "physically oriented problems", and that this is most likely the reason why these rather small time step sizes had to be used. Indeed, divergence problems always originated in the region of inflection of the solution.

With convergence criteria on S^* of 0.0001 and on p^* of 0.001 the computer time required to solve for 1 time step was 4.0 seconds on an average for this 6 x 8 grid system. Convergence criteria were normally satisfied after the second or third pressure iterate. The first pressure iterate was usually followed by three saturation iterates, the second pressure iterate by two saturation iterates, and the third, if any, by one.

An evaluation of this fully implicit Newton iteration solution procedure with respect to implicit-explicit methods cannot be made for this unconfined flow case. It is believed though, that the implicit-explicit methods would be restricted in time step size for the same reason as is the Newton iteration method, i.e., the inflection of the flow field. Therefore, a comparision of performance of both methods should be very similar to comparisons published by Blair and Weinaug (3) for confined flow coning models. Limited funds did not permit further experimentation.

6. CONCLUSIONS

A continuous mathematical analogue of multiphase flow was derived; a well flow computer simulator was developed by discretizing the mathematical analogue with fully implicit finite differences. A positive answer to the question of concern in this study whether unconfined well flow is a multiphase flow phenomenon affecting aquifer response is obtained. The following conclusions were drawn:

(1) Solving the multiphase radial flow equations with fully implicit finite differences and Newton iteration to solve the system of non-linear difference equations is practical in ground water hydrology.

(2) An original solution is obtained for free surface gravity well flow which is shown to be a multiphase flow phenomenon affecting aquifer response.

(3) Gravity combined with the radial nature of flow seem to be the governing factors in determining the flow configuration, which deviates entirely from confined horizontal flow concepts.

(4) The free surface profile shows a point of inflection which moves away from the well bore as pumping continues. The free surface profile is nearly horizontal near the well bore in case of partially penetrating wells, open to a lower portion of the saturated thickness. It is concluded by deduction that so-called fully penetrating wells nearly operate as partially penetrating wells; a second inflection in the free surface (atmospheric pressure) curve would exist near the well bore, very little affecting the overall radial gravity flow phenomenon.

(5) An analogous behavior of the Theis solution, corrected for the effect of partial penetration, and the multiphase flow model is observed only along the bottom of the aquifer, where flow is horizontal.

(6) Storage release by expansion of water is considerable during the first few hours of pumping and explains the inflection in the curves of drawdown vs. log r^2/t, commonly observed in field data. Permeability affects the extent of this storage release. In a real field situation aquifer compressibility may be considerable. It is quite understandable that aquifer compressibility then will play a role in a sense that it may accentuate the inflecting behavior of these curves.

(7) The nature of the behavior of the drawdown curve in time and space reveals that flow in the so called cone of depression is insignificant with respect to the total flow phenomenon and hence, that delayed yield from storage, as explained by capillarity in this model, has very little bearing upon the solution. The overall drawdown in radial flow is too slow for capillarity to be a critical factor.

(8) Air dissolved in the water is an important part of the flow phenomenon affecting the effective permeability near the well bore. The lower permeability the faster the air phase reaches its residual saturation near the well bore.

(9) The confined flow analysis does not apply to unconfined gravity flow; in other words, confined flow and unconfined gravity flow are two different flow phenomena. There is a variety of undetermined factors involved when confined flow analysis is applied to unconfined flow, and adjusting the confined flow solutions to fit unconfined flow data is highly questionable. A good example is trying to explain discrepancies between unconfined flow data and confined analysis by "delayed yield from storage".

(10) The Newton iteration method for solving multiphase free surface gravity well flow problems seems to be affected by the inflecting behavior of the solution which does not seem to correspond to the concept of "physically oriented problems"; this probably explains the rather small time step sizes.

Finally, it is concluded that, regarding recommendations, the multiphase flow approach for solving unconfined gravity flow problems is a fertile field for future work. The well flow problem of this study is a good initiative and could now be studied under a variety of factors to determine the magnitude and extent of their effect upon the solution. This could lead to some practical guidelines for unconfined aquifer test analysis.

REFERENCES

1. Bear, J., D. Zaslavsky and S. Irmay, "Physical principles of water percolation and seepage," UNESCO, Arid Zone Research XXIX, published by the UNESCO, Place de Fontenoy, Paris, 1968.

2. Blair, P. M. and D. W. Peaceman, "An experimental verification of a two-dimensional technique for computing performance of gas-drive reservoirs," Trans. AIME, 228, pp. 19-27, 1963.

3. Blair, P. M. and C. F. Weinaug, "Solution of two-phase flow problems using implicit difference equations," Paper No. SPE 2185, presented at the 43rd Annual Fall Meeting of the Society of Petroleum Engineers of AIME, Houston, Texas, September 29 - October 2, 1968.

4. Boreli, M., "Free-surface flow toward partially penetrating wells," Trans. American Geophysical Union, Vol. 36, No. 4, pp. 664-672, August 1955.

5. Boreli, M., "Sur la porosité effective," C. R. Acad. Sc. Paris, t. 265, Série A, pp. 275-277, août 1967.

6. Boreli, M., et G. Vachaud, "Note sur la détermination de la teneur en eau résiduelle et sur la variation de La perméabilité relative dans les sols non saturés," C. R. Acad. Sc. Paris, t. 263, Série A, pp. 698-701, November 1966.

7. Boulton, N. S., "The drawdown of the water table under non-steady conditions near a pumped well in an unconfined formation," Inst. Civil Eng. Proc., Part 3, pp. 564-579, 1954.

8. Bouwer, H., "Limitation of the Dupuit-Forscheimer assumption in recharge and seepage," Trans. of the ASAE, Vol. 8, No. 4, pp. 512-515, 1965.

9. Breitenbach, E. A., D. H. Thurnau and H. K. van Poollen, "Immiscible fluid flow simulator," Paper No. SPE 2019, Presented at the Symposium on Numerical Simulation of Reservoir Performance, Society of Petroleum Engineers of AIME, Dallas, Texas, April 22-23, 1968.

10. Breitenbach, E. A., D. H. Thurnau and H. K. van Poollen, "The fluid flow simulation equations," Paper No. SPE 2020, Presented at the Symposium on Numerical Simulation of Reservoir Performance, Society of Petroleum Engineers of AIME, Dallas, Texas, April 22-23, 1968.

REFERENCES (Continued)

11. Breitenbach, E. A., D. H. Thurnau and H. K. van Poollen, "Solution of the immiscible fluid flow simulation equations," Paper No. SPE 2021, Presented at the Symposium on Numerical Simulation of Reservoir Performance, Society of Petroleum Engineers of AIME, Dallas, Texas, April 22-23, 1968.

12. Brooks, R. H. and A. T. Corey, "Hydraulic properties of porous media," Hydrology Paper No. 3, Colorado State University, Fort Collins, Colorado, March 1964.

13. Cazal, A. "Evolution de l'humidité dans Le cône de dépression d'une nappe autour d'un puits, au cours d'un pompage," C. R. Acad. Sc. Paris, t. 264, Serie A, pp. 474-476, Mars 1967.

14. Childs, E. C., "Soil moisture theory," in: Advances in Hydroscience, Vol. 4, pp. 73-117, Ed. V. T. Chow, 1967.

15. Childs, E. C., An introduction to the physical basis of soil water phenomena, Wiley-Interscience Publications, John Wiley and Sons, LTD., London, 1969.

16. Coats, K. H., "Computer simulation of three-dimensional three-phase flow in reservoirs," Unpublished paper, Dept. of Petroleum Engineering, The University of Texas, November 1968.

17. Coats, K. H., "Use and misuse of reservoir simulation models," Journal of Petroleum Technology of the AIME, pp. 1391-1398, November 1969.

18. Corey, A. T., "Flow in porous media," Course outline for AE-728 and AE-730, Dept. of Agricultural Engineering, Colorado State University, Fort Collins, Colorado, 259 pages, 1969.

19. Dagan, G. "A method of determining the permeability and effective porosity of unconfined anisotropic aquifers," Water Resources Research, Journal published by the American Geophysical Union, Vol. 3, No. 4, pp. 1059-1071, 1967.

20. Dodson, C. R. and M. B. Standing, "Pressure-volume-temperature and solubility relations for natural gas-water mixtures," American Petroleum Institute, Drilling and Production Practice, pp. 173-179, 1944.

REFERENCES (Continued

21. Dougherty, E. L., and H. C. Mitchell, "Simulation of oil reservoirs on a digital computer," in: Computers in the mineral industries, Part 2, School of Earth Science, Stanford University, Stanford, California, pp. 787-822, 1964.

22. Douglas, J., Jr., "A survey of numerical methods for parabolic differential equations," Advances in Computers, 2, editor, F. L. Alt, Academic Press, New York, pp. 1-54, 1961.

23. Douglas, J., Jr., D. W. Peaceman and H. H. Rachford, Jr., "A method for calculating multidimensional immiscible displacement," Trans. AIME, Vol. 216, pp. 297-308, 1959.

24. Earlougher, R. C., Jr., "Behavior of transient reservoir pressures considering two-phase flow," Ph.D. Dissertation, Dept. of Petroleum Engineering, Stanford University, California, May 1966.

25. Fagin, R. G., and C. H. Stewart, Jr., "A new approach to the two-dimensional multiphase reservoir simulator," JPT Journal of the Society of Petroleum Engineers, Vol. 6, pp. 175-182, 1966.

26. Ferris, J. G. D. B. Knowles, R. H. Brown, and R. W. Stallman, "Theory of aquifer tests," USGS Water Supply Paper 1536-E, 1962.

27. Forsythe, G. and C. B. Moler, Computer solution of linear algebraic systems, Chapter 25: "Nonlinear systems of equations," Prentice-Hall, Inc., Series in Automatic Computation, G. Forsythe editor, Englewood Cliffs, New Jersey, 1967.

28. Freudenstein, F. and B. Roth, "Numerical solution of systems of nonlinear equations," Trans. ASME, October 1963, pp. 550-556, 1963.

29. Glover, R. E., "Application of the Dupuit-Forchheimer assumption in groundwater hydraulics," Trans. of the ASAE, Vol. 8, No. 4, pp. 510-512, 1965.

30. Hantush, M. S., "Drawdown around a partially penetrating well," Journal of the Hydraulics Division, Proceedings of the ASCE, Vol. 87, No. HY4, pp. 83-98, July 1961.

REFERENCES (Continued)

31. Hantush, M. S., "On the validity of the Dupuit-Forchheimer well-discharge formula," Journal of Geophysical Research, Vol. 67, No. 6, pp. 2417-2420, June 1962.

32. Hantush, M. S., "Hydraulics of wells," in: Advances in Hydroscience, Vol. 1, pp. 281-432, editor, V. T. Chow, 1964.

33. Hayden, J. W., "Unsaturated flow through porous media - Experimental investigation," Proc. Second Annual American Water Resources Conference, sponsored by AWWR, Held at the University of Chicago, November 22, 1966.

34. Jacob, C. E. and S. W. Lohman, "Nonsteady flow to a well of constant drawdown in an extensive aquifer," Trans. American Geophysical Union, Vol. 33, No. 4, pp. 559-569, 1952.

35. Kantorovich, L. V. and G. P. Akilov, "Application of Newton's method to concrete functional equations," in: Functional Analysis in Normed Spaces, pp. 723-749, International Series of Monographs in Pure and Applied Mathematics, Vol. 46, The Macmillan Company, New York, 1964.

36. Kashef, A. I., "Exact free surface of gravity wells," Journal of the Hydraulics Division, Proceedings of the ASGE, Vol. 91, No. HY4, pp. 167-185, July 1965.

37. Kawabata, H., "Free surface and interface of two layers' liquids through porous media by pumping up," J. Sci., Hiroshima University, Ser. A., Vol. 24, No. 2, pp. 417-442, October 1960.

38. Kirkham, D., "Exact theory for the shape of the free water surface about a well in a semi-confined aquifer," Journal of Geophysical Research, Vol. 69, No. 12, pp. 2537-2549, June 15, 1964.

39. Laliberte, G. E., A. T. Corey and R. H. Brooks, "Properties of unsaturated porous media," Hydrology Paper No. 17, Colorado State University, Fort Collins, Colorado, November 1966.

40. Lees, M., "Alternating direction and semi-explicit difference methods for parabolic differential equations," Numerische Math., 3, pp. 398-412, 1961.

41. Matthews, C. S. and D. G. Russell, Pressure buildup and flow tests in wells, Society of Petroleum Engineers of AIME Monograph, Vol. 1, H. L. Doherty Series, Storm Printing Corporation, Dallas Texas, 1967.

REFERENCES (Continued

42. Morel-Seytoux, H. J., "Introduction to flow of immiscible liquids in porous media," Chapter 11 in: Flow Through Porous Media, edited by R. De Wiest, Academic Press, New York and London, 1969.

43. Muskat, M., Physical principles of oil production, McGraw-Hill Publishing Company, New York, 1949.

44. Nelson, R. W., "Flow in heterogeneous porous mediums. 1. Darcian-type description of two-phase systems," Water Resources Research, Vol. 2, No. 3, Third Quarter, 1966.

45. Odeh, A. S., "Reservoir simulation- What is it?," Journal of Petroleum Technology of the AIME, pp. 1383-1388, November 1969.

46. Remson, I., S. S. McNeary and J. R. Randolph, "Water levels near a well discharging from an unconfined aquifer," U.S. Geol. Surv. Water Supply Paper 1536-B, 1961.

47. Richards, L. A., "Capillary conduction of liquids through porous mediums," Physics, Vol. 1, November 1931.

48. Rose, M., "On the integration of non-linear parabolic equations by implicit difference methods," Quart. Appl. Math., 15, pp. 237-248, 1956.

49. Scheidegger, A. E., The Physics of Flow Through Porous Media, University of Toronto Press, Second Edition, 1959.

50. Schneebeli, G., Hydraulique Souterraine, Chapter VI, Collection du Centre de Recherches et d'Essais de Chatou, Eyrolles, 1966.

51. Sheldon, J. W. C. D. Harris, and D. Bavly, "A method for general reservoir behavior simulation on digital computers," Paper No. SPE 1521-G, Presented at the 35th Annual Fall Meeting of the Society of Petroleum Engineers, Denver, October 2-5, 1960.

52. Smith, G. D., Numerical Solution of Partial Differential Equations, Oxford University Press, London, 1965.

53. Snyder, L. J., "Two-phase reservoir flow calculations," JPT Jour. of the Society of Petroleum Engineers, Vol. 9, pp. 170-182, June 1969.

54. Soengkowo, I., "Model studies of water coning in petroleum reservoirs with natural water drives," Ph.D. Dissertation, Dept. of Petroleum Engineering, The University of Texas, Austin, Texas, May 1969.

REFERENCES (Continued)

55. Spivak, A., and K. H. Coats, "Simulation Techniques for two- and three-phase coning studies," Paper Number SPE 2595, Presented at the 44th Annual Fall Meeting of the Society of Petroleum Engineers of AIME, Denver, Colorado, September 28-October 1, 1969.

56. Stallman, R. W., "The significance of vertical flow components in the vicinity of pumping wells in unconfined aquifers," U.S. Geol. Surv., Profess. Papers, 424-B, pp. 41-43, 1961.

57. Stallman, R. W., "Electric analog of three-dimensional flow to wells and its application to unconfined aquifers," U.S. Geol. Surv. , Water Supply Papers, 1536-H, pp. 205-242, 1963.

58. Stallman, R. W., "Multiphase fluids in porous media - A review of theories pertinent to Hydrologic studies," USGS Professional Paper 411-E, 1964.

59. Stallman, R. W., "Effects of water table conditions on water level changes near pumping wells," Water Resources Research, Bulletin of the American Geophysical Union, Vol. 1, No. 2, pp. 295-312, 1965.

60. Stallman, R. W., "Flow in the zone of aeration," in: Advances in Hydroscience, Vol. 4, Editor, V. T. Chow, 1967.

61. Stone, H. L., and A. O. Garder, Jr., "Analysis of gas-cap or dissolved-gas drive reservoirs," Trans. AIME, Vol. 222, p. 92, 1961.

62. Theis, C. V., "The relation between the lowering of the piezometric surface and the rate and duration of discharge of a well using groundwater storage," Trans. American Geophysical Union, Vol. 16, pp. 519-524, 1935.

63. Theis, C. V., "The significance and nature of the cone of depression in groundwater bodies," Economic Geology, Vol. XXXIII, No. 8, pp. 889-902, December 1938.

64. Turner, L. R., "Solution of nonlinear systems," Ann. New York Acad. Sci., 86, pp. 817-827, 1960.

65. Vachaud, G., "Etude de la valeur du coefficient d'emmagasinement des nappes à surfaces Libre, considérant l'écoulement dans la zone non saturée," Symposium de Haifa, AISH, publ. No. 72, pp. 69-82, 1967.

REFERENCES (Continued)

66. Van Wingen, N., "Viscosity of air, water, natural gas, and crude oil at varying pressures and temperatures," American Petroleum Institute, Secondary Recovery of Oil in the United States, pp. 126-132, 1950.

67. Varga, R. S., Matrix Iterative Analysis, Prentice Hall, Inc., Englewood Cliffs, New Jersey, 1962.

68. Wattenbarger, R. A., "Convergence of the implicit pressure - Explicit saturation method," JPT Forum, Journal of Petroleum Technology, pp. 1220-1221, November 1968.

69. Watts, J. W., "An iterative matrix inversion method suitable for anisotropic problems," Unpublished Paper, Mobil Research and Development Corporation, Field Research Laboratory, Dallas, Texas, 1969.

70. Weeks, F. P., "Determining the ratio of horizontal to vertical permeability by aquifer-test analysis," Water Resources Research, Bulletin of the American Geophysical Union, Vol. 5, No. 1, February 1969.

71. Welge, H. J. and A. G. Weber, "Use of two dimensional methods for calculating well coning behavior," Trans. AIME, Vol. 231, pp. 345-354, 1964.

72. Wenzel, L. K., "Methods for determining permeability of water-bearing materials," U.S. Geol. Surv., Water Supply Paper, 887, 1942.

APPENDIX A

THE NEWTON ITERATION PROCESS FOR SOLVING SYSTEMS OF NON-LINEAR EQUATIONS

Because of its quadratic convergence, the Newton iteration process was selected to solve the system of non-linear equations as represented by equation 24, 25 and 26. The proof of quadratic convergence is presented in many standard textbooks on numerical analysis (27) or on functional analysis (35).

For n-dimensional systems, as is the one in this study, the process can be described as follows. Consider the following system of non-linear equations in the dependent variable p

$$F_{i,j}p_{i,j} - F_{i-1,j}p_{i-1,j} - F_{i+1,j}p_{i+1,j} - F_{i,j-1}p_{i,j-1} - F_{i,j+1}p_{i,j+1} + H_{i,j} = 0 \qquad \text{(A-1)}$$

The coefficients F and H are fucntions of p, therefore, the system is non-linear in p. In vector form equation A-1 can also be written as

$$f(\vec{p}) = 0 \qquad \text{(A-2)}$$

Suppose $\vec{p}^{k}$ is a present solution estimate of the system $f(\vec{p})$. Then, an improved estimate can be obtained by linearizing the system A-2, involving derivatives of $f(\vec{p}^{k})$ evaluated at p^{k}. This linearized problem now is a system of linear algebraic equations, which is solved for $\Delta\vec{p}$, an increment. This "correction" increment is added to $\vec{p}^{k}$ to give an improved solution $\vec{p}^{k+1}$. This process is iterated until convergence is obtained.

In mathematical terms the process can be summarized as follows. To linearize the system $f(\vec{p}^{k})$, it is represented by the first two terms of its Taylor series at $\vec{p}^{k}$

$$f(\vec{p}^{k+1}) = f(\vec{p}^{k}) + \sum_{j=1}^{M} \frac{\partial f(\vec{p}^{k})}{\partial p_j^{k}} \left(p_j^{k+1} - p_j^{k}\right) \qquad \text{(A-3)}$$

The right hand side of this equation is the linear vector function of $\vec{p}^{k}$ which best approximates the non-linear function $f(\vec{p}^{k})$. It is the tangent hyper plane to the surface $f(\vec{p}^{k})$ at $\vec{p}^{k}$. From equation A-3 the following linear system is obtained

$$\vec{p}^{k+1} = \vec{p}^{k} - \frac{f(\vec{p}^{k})}{\sum_{i,j,\ell=1} \frac{f(\vec{p}^{k})}{\vec{p}_{\ell}}} \qquad \text{(A-4)}$$

which is the general step in the iteration process.

In this Newton iteration process the convergence very much depends upon a good first guess $\vec{p}^{o}$. This often leads to time step restrictions when initial conditions are used as a first guess. Fortunately, for physically oriented problems, as is the one in this study, initial conditions are usually good enough for an initial guess without a too severe limitation on time step size. What happens if $\vec{p}^{o}$ is far away from the solution is a question impossible to answer; some solution may eventually be approached or it may jump around the space for quite a distance and quite a number of steps. Bounds set to this kind of oscillation often leads to convergence.

APPENDIX B

THE RESIDUAL APPROACH FOR SOLVING SYSTEMS OF EQUATIONS

The residual approach for solving systems of equations simultaneously proceeds as follows in matrix notation (11). Suppose the matrix equation

$$[A]\ [P] = [B] \tag{B-1}$$

is to be solved for the new vector P. If the new P vector is defined as an initial guess, P^k, at new values of P, plus an error vector, P^*, being the difference between initial guess and final answer, i.e.,

$$[P] = [P^k] + [P^*] \tag{B-2}$$

then matrix equation B-1 can be rewritten as

$$[A]\ [P^k] + [A]\ [P^*] = [B] \tag{B-3}$$

or

$$[A]\ [P^*] = [B] - [A]\ [P^k] \tag{B-4}$$

or also

$$[A]\ [P^*] = [r] \tag{B-5}$$

where the r vector is the residual error and is defined by the right hand side of equation B-4. Depending upon the computer hardware, it is sometimes advisable to compute the r vector by double precision using the latest P values. Any matrix solution technique can then be used to solve for the correction vector, P^*, by single precision. This vector is then substituted in equation B-2, using double precision, to come up with an improved new value. This process can be repeated until the desired accuracy is obtained. The residual approach is very powerful, because extreme accuracy can be obtained when desired.

APPENDIX C

INPUT DATA

1. Inpute data: Case 1

The aquifer properties selected for Case 1 correspond to a Columbia sandy loam with an average permeability of 5000 milli-darcies (13.7 FEET/DAY). The saturation dependent data were obtained from Laliberte, Corey and Brooks (39). The fluid properties were obtained from Dodson and Standing (20). The well bore is screened over the lower 45 percent of the initial saturated thickness (136 feet), with a constant pumping rate of 43,200 FT^3/DAY.

The following four pages are a computer listing of the input data and are self explanatory.

CASE 1

```
CMNT =========INPUT DATA=========
CMNT
CMNT              ALL CMNT CARDS ARE COMMENT CARDS AND ARE NOT PUT ON TAPE
IMAX               6
JMAX               8
NCOM             500
RWEL             1.0
REXT         10000.
CMNT                        IMAX = MAXIMUM I INDEX (NUMBER OF COLUMNS)
CMNT                        JMAX = MAXIMUM J INDEX (NUMBER OF ROWS)
CMNT                        NCOM = NUMBER OF COMPUTATIONS(NUMBER OF TIME STEPS)
CMNT                        RWEL = WELL RADIUS (FT)
CMNT                        REXT = EXTERIOR BOUNDARY RADIUS (FT)
NEAS               1
NWES               3
NNOR               2
CMNT      NEAS,NWES,AND NNOR DETERMINE THE TYPE OF BOUNDARY CONDITION AT THE
CMNT      EAST,WEST,AND NORTH SIDE OF THE MODEL(WEST = WELL BOUNDARY )
CMNT      1  ASSIGNS A  NO FLOW BOUNDARY CONDITION
CMNT      2  ASSIGNS A  PRESSURE BOUNDARY CONDITION
CMNT      3  ASSIGNS A  FLOW RATE
OMEG            1.30
CMNT                        OMEG = OVER RELAXATION OMEGA
SCON            .001
CMNT                        SCON = CONVERGENCE CRITERION ON SATURATIONS
PCON            .001
CMNT                        PCON = CONVERGENCE CRITERION ON PRESSURES
GRAV          32.174
CMNT                        GRAV = GRAVITY
CMNT                          GRAV = 0.0     NO GRAVITY EFFECT
CMNT                          GRAV = 32.174  DENSITY OF FLUIDS IS USED
CMNT                                         SLUG/CUBIC FOOT
CMNT                          GRAV = 1.0     SPECIFIC WEIGHT OF FLUIDS IS
CMNT                                         USED (LBS/CUBIC FOOT)
CMNT      PERF STANDS FOR PERFORATION OF THE GRIDS ALONG THE WELL BORE
CMNT      THE FIRST NUMBER IS THE SUBSCRIPT OF THE PERFORATED WELL BLOCK/
CMNT      THE SECOND NUMBER IS THE PERFORATION INDEX.
CMNT      1  =  BLOCK IS PERFORATED (OTHERWISE = 0)
CMNT      IF NO PERF CARDS ARE USED,ALL PERF INDICES ARE SET EQUAL TO ZERO
NOIL               1
NGAS               1
NWAT               0
CMNT      NOIL,NGAS,NWAT ARE THE TURN ON OR OFF SWITCHES FOR THE OIL ,
CMNT      GAS, AND WATER PHASES( E.G.  NWAT=0 MEANS NO WATER PHASE)
DEBU               0
CMNT      DEBU IS THE DEBUGGING SWITCH
ENDS
CMNT =========================================================================
CMNT ==========  ARRAY DATA  ==========
CMNT      WHEN THE ARRAY IS CONSTANT,THEN THE VALUE OF THE CONSTANT APPEARS ON
CMNT      THE ARRAY NAME CARD IN COLUMNS 11-20 .
CMNT      WHEN THE ARRAY IS VARIABLE,THEN A ZERO IS PUNCHED ON THE ARRAY NAME
CMNT      CARD IN COLUMNS 11-20, AND THE ARRAY IS PUNCHED PER ROW WHITH THE
CMNT      FORMAT  8(1X,F9.0) . FOR EACH NEW ROW,A NEW CARD IS STARTED.
PORO              .5
CMNT                        PORO = POROSITY
```

```
PRES                0.0
CMNT                                PRES = PRESSURE
 10.365300 10.365300 10.365300 10.365300 10.365300 10.365300
 13.215269 13.215269 13.215269 13.215269 13.215269 13.215269
 18.632538 18.632538 18.632538 18.632538 18.632538 18.632538
 25.134246 25.134246 25.134246 25.134246 25.134246 25.134246
 32.719941 32.719941 32.719941 32.719941 32.719941 32.719941
 41.389802 41.389802 41.389802 41.389802 41.389802 41.389802
 52.227792 52.227792 52.227792 52.227792 52.227792 52.227792
 65.234358 65.234358 65.234358 65.234358 65.234358 65.234358
SATG                0.0
CMNT                                SATG = GAS SATURATION
       .80       .80       .80       .80       .80       .80
       .40       .40       .40       .40       .40       .40
       .00       .00       .00       .00       .00       .00
       .00       .00       .00       .00       .00       .00
       .00       .00       .00       .00       .00       .00
       .00       .00       .00       .00       .00       .00
       .00       .00       .00       .00       .00       .00
       .00       .00       .00       .00       .00       .00
SATO                0.0
CMNT                                SATO = OIL SATURATION
       .20       .20       .20       .20       .20       .20
       .60       .60       .60       .60       .60       .60
      1.00      1.00      1.00      1.00      1.00      1.00
      1.00      1.00      1.00      1.00      1.00      1.00
      1.00      1.00      1.00      1.00      1.00      1.00
      1.00      1.00      1.00      1.00      1.00      1.00
      1.00      1.00      1.00      1.00      1.00      1.00
      1.00      1.00      1.00      1.00      1.00      1.00
SATW                0.0
CMNT                                SATW = WATER SATURATION
         0         0         0         0         0         0
         0         0         0         0         0         0
         0         0         0         0         0         0
         0         0         0         0         0         0
         0         0         0         0         0         0
         0         0         0         0         0         0
         0         0         0         0         0         0
         0         0         0         0         0         0
RADI               10.
CMNT                                RAD  = RADII (NORMALLY.IF RWEL AND REXT ARE READ IN
CMNT                                       THE RADII ARE LOGARITHMICALLY DISTRIBUTED.
CMNT                                       THE OTHER OPTION IS TO ASSIGN RADII BY
CMNT                                       MAKING USE OF THE ARRAY CARD
DELZ                0.0
CMNT                                DELZ = DELTA Z ARRAY
        50         10         15         15         20         20         30         30
KR                5000.
CMNT                                KR   = PERMEABILITY ARRAY IN R-DIRECTION (M.D.)
KZ                5000.
CMNT                                KZ   = PERMEABILITY ARRAY IN Z-DIRECTION (M.D.)
ENDA
CMNT ==========================================================================================
QO                 10.       0.0
```

```
QG                0.0         0.0
          0.        0.          0.          0.          0.          0.
          0.        0.          0.          0.          0.          0.
          0.        0.          0.          0.          0.          0.
          0.        0.          0.          0.          0.          0.
          0.        0.          0.          0.          0.          0.
          0.        0.          0.          0.          0.          0.
          0.        0.          0.          0.          0.          0.
          0.        0.          0.          0.          0.          0.
QW                10.         0.0
CMNT        QO,QG,AND QW ARE THE OIL ,GAS,AND WATER PRODUCTION TERMS
CMNT    IN CASE OF A CONSTANT ARRAY ,THE FIRST VALUE IS A DUMMY,GREATER THAN 1
CMNT    AND THE SECOND DESIGNATES THE VALUE OF THE CONSTANT ARRAY
CMNT    IN CASE OF A VARIABLE ARRAY , THE FIRST VALUE SHOULD BE A ZERO AND THE
CMNT    SECOND BECOMES IMMATERIAL.
ENDQ
CMNT    ================================================================================
CMNT    ============== PRESSURE-VOLUME-TEMPERATURE INTERPOLATION TABLES=========
CMNT                              BO    = OIL FORMATION VOLUME FACTOR
CMNT                              BG    = GAS FORMATION VOLUME FACTOR
CMNT                              BW    = WATER FORMATION VOLUME FACTOR
CMNT                              VISO = OIL VISCOSITY (CENTIPOISE)
CMNT                              VISG = GAS VISCOSITY (CENTIPOISE)
CMNT                              VISW = WATER VISCOSITY (CENTIPOISE)
CMNT                              DENO = OIL DENSITY (SEE GRAV)
CMNT                              DENG = GAS DENSITY (SEE GRAV)
CMNT                              DENW = WATER DENSITY (SEE GRAV)
CMNT                PRES       VISO          BO         DENO          RS
CMNT                ----       ----          --         ----          --
PVTO                 0.0        1.0           1.0        1.94         0.0
PVTO                 10.                  1.0000060                 .0230
PVTO                 14.7                 1.0                       .0338
PVTO                 20.                  .99999258                 .0460
PVTO                 60.                  .99993658                 .1380
PVTO                 80.                  .99990858                 .1840
PVTO    FLAG                    9999.                    9999.        0.0
CMNT                PRES       VISG          BG         DENG
CMNT                ----       ----          --         ----
PVTG                 0.0        .018          1.25      .00237
PVTG                10.0                     1.08
PVTG                14.7                     1.0
PVTG                 20.                     0.92
PVTG                60.0                     0.25
PVTG                 80.                     0.01
PVTG    FLAG                    9999.                    9999.
CMNT                PRES       VISW          BW         DENW
CMNT                ----       ----          --         ----
PVTW                 0.          1.0           1.0        1.9
PVTW                 10.                      1.01
PVTW                14.7                     1.02
PVTW                 20.                     1.030
PVTW                 50.                     1.05
PVTW                 80.                     1.06
PVTW    FLAG                    9999.                    9999.
CMNT    DENSITIES ARE EITHER READ IN AS A FUNCTION OF PRES,OR COMPUTED WITH F.V.F.
CMNT    FROM DENSITIES AT ATMOSPHERIC CONDITIONS (OR STOCK TANK)
CMNT    ================================================================================
```

```
CMNT ==========SATURATION DATA INTERPOLATION TABLE ==========
CMNT                    RK   = RELATIVE PERMEABILITY
CMNT                    PCOG = OIL-GAS CAPILLARY PRESSURE
CMNT                    PCOW = WATER-OIL CAPILLARY PRESSURE
CMNT          SAT     RK.OIL     RK.GAS     RK.WAT      PCOG       PCOW
CMNT          ---     ------     ------     ------      ----       ----
SATD          0.0       0.0        0.0        0.0       0.0        0.0
SATD           .1       0.0        0.00       0.0       5.0
SATD          0.2       0.0        0.11       0.0     4.3347
SATD          0.3     0.125      0.222      0.125      3.40
SATD         0.35     0.190       0.28      0.190      2.95
SATD         0.45     0.315       0.39      0.315       2.0
SATD         0.90     0.875      0.895      0.875       0.5
SATD          1.0       1.0        1.0        1.0       0.0
SATD FLAG                0.0        0.0        0.0       0.0      9999.
CMNT  THE LAST VALUE OF EACH ARRAY IS AN INDICATOR FOR WHETHER OR NOT A PARTICU-
CMNT  LAR FUNCTION IS CONSTANT.(INDICATOR VALUE = 9999. ,THEN THE FIRST VALUE
CMNT  OF THE ARRAY IS THE CONSTANT)
ENDT
CMNT ==========================================================================
CMNT ==========NEW TIME STEP DATA==========
CMNT      DELT IS ALWAYS THE LAST CARD IN A SET OF NEW TIME STEP CARDS
GRCO            0
QO              1          7    21600.
QO              1          8    21600.
DELT          .050
DELT          .050
DELT          .050
PUNCH
CMNT ==========END OF INPUT DATA==========
END
```

APPENDIX C (continued)

INPUT DATA

2. Input data: Case 2

The aquifer properties selected for Case 2 correspond to an unconsolidated sand with an average permeability of 80,000 milli-darcies (219 FEET/DAY). The saturation dependent data were obtained from Laliberte, Corey, and Brooks (39). The fluid properties were obtained from Dodson and Standing (20). The well bore is screened over the lower 43 percent of the initial saturated thickness (139 feet), with a constant pumping rate of 86,400 FT^3/DAY.

The following four pages are a computer listing of the input data and are self explanatory.

CASE 2

```
CMNT ==========INPUT DATA==========
CMNT
CMNT              ALL CMNT CARDS ARE COMMENT CARDS AND ARE NOT PUT ON TAPE
IMAX               6
JMAX               8
NCOM             500
RWEL             1.0
REXT         10000.
CMNT                        IMAX = MAXIMUM I INDEX (NUMBER OF COLUMNS)
CMNT                        JMAX = MAXIMUM J INDEX (NUMBER OF ROWS)
CMNT                        NCOM = NUMBER OF COMPUTATIONS(NUMBER OF TIME STEPS)
CMNT                        RWEL = WELL RADIUS (FT)
CMNT                        REXT = EXTERIOR BOUNDARY RADIUS (FT)
CMNT                        REXT = EXTERIOR BOUNDARY RADIUS
NEAS               1
NWES               3
NNOR               2
CMNT      NEAS,NWES,AND NNOR DETERMINE THE TYPE OF BOUNDARY CONDITION AT THE
CMNT      EAST,WEST,AND NORTH SIDE OF THE MODEL(WEST = WELL BOUNDARY )
CMNT      1  ASSIGNS A  NO FLOW BOUNDARY CONDITION
CMNT      2  ASSIGNS A  PRESSURE BOUNDARY CONDITION
CMNT      3  ASSIGNS A  FLOW RATE
OMEG           1.30
CMNT                        OMEG = OVER RELAXATION OMEGA
SCON           .0001
CMNT                        SCON = CONVERGENCE CRITERION ON SATURATIONS
PCON             .01
PCON           .001
CMNT                        PCON = CONVERGENCE CRITERION ON PRESSURES
GRAV          32.174
CMNT                        GRAV = GRAVITY
CMNT                               GRAV = 0.0     NO GRAVITY EFFECT
CMNT                               GRAV = 32.174  DENSITY OF FLUIDS IS USED
CMNT                                              SLUG/CUBIC FOOT
CMNT                               GRAV = 1.0     SPECIFIC WEIGHT OF FLUIDS IS
CMNT                                              USED (LBS/CUBIC FOOT)
CMNT      PERF STANDS FOR PERFORATION OF THE GRIDS ALONG THE WELL BORE
CMNT      THE FIRST NUMBER IS THE SUBSCRIPT OF THE PERFORATED WELL BLOCK/
CMNT      THE SECOND NUMBER IS THE PERFORATION INDEX.
CMNT      1  =  BLOCK IS PERFORATED (OTHERWISE = 0)
CMNT      IF NO PERF CARDS ARE USED,ALL PERF INDICES ARE SET EQUAL TO ZERO
NOIL               1
NGAS               1
NWAT               0
CMNT      NOIL,NGAS,NWAT ARE THE TURN ON OR OFF SWITCHES FOR THE OIL ,
CMNT      GAS, AND WATER PHASES( E.G.  NWAT=0 MEANS NO WATER PHASE)
DEBU               0
CMNT      DEBU IS THE DEBUGGING SWITCH
ENDS
CMNT ==========
CMNT ========== ARRAY DATA ==========
CMNT      WHEN THE ARRAY IS CONSTANT,THEN THE VALUE OF THE CONSTANT APPEARS ON
CMNT      THE ARRAY NAME CARD IN COLUMNS 11-20 .
CMNT      WHEN THE ARRAY IS VARIABLE,THEN A ZERO IS PUNCHED ON THE ARRAY NAME
CMNT      CARD IN COLUMNS 11-20, AND THE ARRAY IS PUNCHED PER ROW WITH THE
CMNT      FORMAT  8(1X,F9.0) . FOR EACH NEW ROW,A NEW CARD IS STARTED.
```

```
PORO                .5
CMNT                                PORO = POROSITY
PRES               0.0
CMNT                                PRES = PRESSURE
 14.030000 14.030000 14.030000 14.030000 14.030000 14.030000
 14.615906 14.615906 14.615906 14.615906 14.615906 14.615906
 20.034388 20.034388 20.034388 20.034388 20.034388 20.034388
 26.536728 26.536728 26.536728 26.536728 26.536728 26.536728
 34.123014 34.123014 34.123014 34.123014 34.123014 34.123014
 42.793350 42.793350 42.793350 42.793350 42.793350 42.793350
 53.631713 53.631713 53.631713 53.631713 53.631713 53.631713
 66.638396 66.638396 66.638396 66.638396 66.638396 66.638396
SATG               0.0
CMNT                                SATG = GAS SATURATION
        .9          .9          .9          .9          .9          .9
 .099989     .099989     .099989     .099989     .099989     .099989
         0           0           0           0           0           0
         0           0           0           0           0           0
         0           0           0           0           0           0
         0           0           0           0           0           0
         0           0           0           0           0           0
         0           0           0           0           0           0
SATO               0.0
CMNT                                SATO = OIL SATURATION
        .1          .1          .1          .1          .1          .1
 .900011     .900011     .900011     .900011     .900011     .900011
         1           1           1           1           1           1
         1           1           1           1           1           1
         1           1           1           1           1           1
         1           1           1           1           1           1
         1           1           1           1           1           1
         1           1           1           1           1           1
SATW               0.0
CMNT                                SATW = WATER SATURATION
         0           0           0           0           0           0
         0           0           0           0           0           0
         0           0           0           0           0           0
         0           0           0           0           0           0
         0           0           0           0           0           0
         0           0           0           0           0           0
         0           0           0           0           0           0
         0           0           0           0           0           0
RADI              10.
CMNT                                RAD  = RADII (NORMALLY, IF RWEL AND REXT ARE READ IN
CMNT                                  THE RADII ARE LOGARITHMICALLY DISTRIBUTED.
CMNT                                  THE OTHER OPTION IS TO ASSIGN RADII BY
CMNT                                  MAKING USE OF THE ARRAY CARD
DELZ               0.0
CMNT                                DELZ = DELTA Z ARRAY
        50          10          15          15          20          20          30          30
KR             80000.
CMNT                                KR   = PERMEABILITY ARRAY IN R-DIRECTION (M.D.)
KZ             80000.
CMNT                                KZ   = PERMEABILITY ARRAY IN Z-DIRECTION (M.D.)
ENDA
CMNT ==========================================================================================
```

```
QO                10.         0.0
QG                0.0         0.0
          0.        0.          0.          0.          0.          0.
          0.        0.          0.          0.          0.          0.
          0.        0.          0.          0.          0.          0.
          0.        0.          0.          0.          0.          0.
          0.        0.          0.          0.          0.          0.
          0.        0.          0.          0.          0.          0.
          0.        0.          0.          0.          0.          0.
          0.        0.          0.          0.          0.          0.
QW                10.         0.0
CMNT        QO,QG,AND QW ARE THE OIL ,GAS,AND WATER PRODUCTION TERMS
CMNT    IN CASE OF A CONSTANT ARRAY ,THE FIRST VALUE IS A DUMMY,GREATER THAN 1
CMNT    AND THE SECOND DESIGNATES THE VALUE OF THE CONSTANT ARRAY
CMNT    IN CASE OF A VARIABLE ARRAY , THE FIRST VALUE SHOULD BE A ZERO AND THE
CMNT    SECOND BECOMES IMMATERIAL.
ENDQ
CMNT ==========================================================================
CMNT ================ PRESSURE-VOLUME-TEMPERATURE INTERPOLATION TABLES=========
CMNT                              BO    = OIL FORMATION VOLUME FACTOR
CMNT                              BG    = GAS FORMATION VOLUME FACTOR
CMNT                              BW    = WATER FORMATION VOLUME FACTOR
CMNT                              VISO  = OIL VISCOSITY (CENTIPOISE)
CMNT                              VISG  = GAS VISCOSITY (CENTIPOISE)
CMNT                              VISW  = WATER VISCOSITY (CENTIPOISE)
CMNT                              DENO  = OIL DENSITY (SEE GRAV)
CMNT                              DENG  = GAS DENSITY (SEE GRAV)
CMNT                              DENW  = WATER DENSITY (SEE GRAV)
CMNT            PRES       VISO          BO        DENO          RS
CMNT            ----       ----          --        ----          --
PVTO             0.0        1.0           1.0       1.94          0.0
PVTO             10.                   1.0000066                 .0230
PVTO            14.7                   1.0                       .0338
PVTO             20.                   .99999258                 .0460
PVTO             60.                   .99993658                 .1380
PVTO             80.                   .99990858                 .1840
PVTO  FLAG                  9999.                     9999.         0.0
CMNT            PRES       VISG          BG        DENG
CMNT            ----       ----          --        ----
PVTG             0.0        .018          1.25     .00237
PVTG            10.0                      1.08
PVTG            14.7                       1.0
PVTG             20.                      0.92
PVTG            60.0                      0.25
PVTG             80.                      0.01
PVTG  FLAG                  9999.                     9999.
CMNT            PRES       VISW          BW        DENW
CMNT            ----       ----          --        ----
PVTW              0.        1.0           1.0        1.9
PVTW             10.                     1.01
PVTW            14.7                     1.02
PVTW             20.                    1.035
PVTW             60.                     1.05
PVTW             80.                     1.06
PVTW  FLAG                  9999.                     9999.
CMNT  DENSITIES ARE EITHER READ IN AS A FUNCTION OF PRES.OR COMPUTED WITH F.V.F.
CMNT  FROM DENSITIES AT ATMOSPHERIC CONDITIONS (OR STOCK TANK)
CMNT ==========================================================================
```

```
CMNT ==========SATURATION DATA INTERPOLATION TABLE ==========
CMNT                    RK   = RELATIVE PERMEABILITY
CMNT                    PCOG = OIL-GAS CAPILLARY PRESSURE
CMNT                    PCOW = WATER-OIL CAPILLARY PRESSURE
CMNT          SAT     RK.OIL     RK.GAS     RK.WAT      PCOG      PCOW
CMNT          ---     ------     ------     ------      ----      ----
SATD         0.00       0.00       0.00       0.00
SATD         0.05       0.00       0.00       0.00       .75
SATD         0.10       0.00       0.05       0.00      0.67
SATD         0.30       0.08       0.23       0.08      0.40
SATD         0.50       0.24       0.41       0.24      0.30
SATD         0.70       0.46       0.60       0.46      0.23
SATD         0.90       0.80      .86666      0.80      0.10
SATD         1.00       1.00       1.00       1.00      0.00
SATD  FLAG                                                      9999.
CMNT  THE LAST VALUE OF EACH ARRAY IS AN INDICATOR FOR WHETHER OR NOT A PARTICU-
CMNT  LAR FUNCTION IS CONSTANT.(INDICATOR VALUE = 9999. .THEN THE FIRST VALUE
CMNT  OF THE ARRAY IS THE CONSTANT)
ENDT
CMNT ==========NEW TIME STEP DATA==========
CMNT      DELT IS ALWAYS THE LAST CARD IN A SET OF NEW TIME STEP CARDS
GRCO            0
QO              1          7    43200.
QO              1          8    43200.
DELT          .045
DELT          .045
DELT          .045
PUNCH
CMNT ==========END OF INPUT DATA==========
END
```

APPENDIX D

SAMPLE TIME STEP OUTPUT

A sample time step output is given for Case 1 and Case 2 toward the end of the analysis. The left column of each map represents the values of the grid blocks adjacent to the well bore. The right column represents the exterior boundary grid blocks.

CASE 1 TIME STEP 138
CUMULATIVE TIME 7.360 DAYS
DELTA-T .120 DAYS

PRESSURE MAP

	1	2	3	4	5	6
1	.10365E+02	.10365E+02	.10365E+02	.10365E+02	.10365E+02	.10365E+02
2	.10906E+02	.10910E+02	.11053E+02	.13119E+02	.13216E+02	.13216E+02
3	.15954E+02	.15958E+02	.16144E+02	.18517E+02	.18634E+02	.18634E+02
4	.22286E+02	.22292E+02	.22569E+02	.25009E+02	.25137E+02	.25137E+02
5	.29429E+02	.29443E+02	.30018E+02	.32585E+02	.32723E+02	.32723E+02
6	.36739E+02	.36862E+02	.38465E+02	.41245E+02	.41393E+02	.41393E+02
7	.36687E+02	.43648E+02	.48974E+02	.52074E+02	.52231E+02	.52232E+02
8	.48419E+02	.55481E+02	.61756E+02	.65075E+02	.65238E+02	.65238E+02

POTENTIAL MAP

	1	2	3	4	5	6
1	.75390E+02	.75390E+02	.75391E+02	.75391E+02	.75391E+02	.75391E+02
2	.62927E+02	.62931E+02	.63075E+02	.65141E+02	.65238E+02	.65238E+02
3	.62556E+02	.62560E+02	.62747E+02	.65121E+02	.65238E+02	.65238E+02
4	.62385E+02	.62392E+02	.62670E+02	.65111E+02	.65238E+02	.65238E+02
5	.61942E+02	.61957E+02	.62532E+02	.65100E+02	.65238E+02	.65238E+02
6	.60582E+02	.60706E+02	.62309E+02	.65090E+02	.65238E+02	.65238E+02
7	.49693E+02	.56654E+02	.61981E+02	.65081E+02	.65238E+02	.65238E+02
8	.48419E+02	.55481E+02	.61756E+02	.65075E+02	.65238E+02	.65238E+02

OIL SAT. MAP

	1	2	3	4	5	6
1	.20000E+00	.20000E+00	.20000E+00	.20000E+00	.20000E+00	.20000E+00
2	.25628E+00	.25669E+00	.27202E+00	.57096E+00	.60001E+00	.60003E+00
3	.99887E+00	.99880E+00	.99769E+00	.99998E+00	.10000E+01	.10000E+01
4	.10000E+01	.10000E+01	.99932E+00	.99998E+00	.10000E+01	.10000E+01
5	.10000E+01	.10000E+01	.99945E+00	.99994E+00	.10000E+01	.10000E+01
6	.99988E+00	.10000E+01	.10000E+01	.99995E+00	.10000E+01	.10000E+01
7	.89978E+00	.95644E+00	.99865E+00	.99993E+00	.10000E+01	.10000E+01
8	.89981E+00	.95669E+00	.99934E+00	.99999E+00	.10000E+01	.10000E+01

GAS SAT. MAP

	1	2	3	4	5	6
1	.80000E+00	.80000E+00	.80000E+00	.80000E+00	.80000E+00	.80000E+00
2	.74336E+00	.74331E+00	.72797E+00	.42902E+00	.39999E+00	.39997E+00
3	.11315E-02	.11996E-02	.23119E-02	.20338E-04	.26064E-05	.25566E-05
4	0.	0.	.68283E-03	.17209E-04	.35058E-05	.34589E-05
5	0.	0.	.55173E-03	.56744E-04	.35653E-05	.35015E-05
6	.12362E-03	0.	0.	.54002E-04	.33139E-05	.32637E-05
7	.10005E+00	.43560E-01	.13508E-02	.74684E-04	.28791E-05	.28304E-05
8	.10004E+00	.45318E-01	.66081E-03	.11812E-04	.34455E-06	.33713E-06

OIL PROD. MAP

	1	2	3	4	5	6
1	0.	0.	0.	0.	0.	0.
2	0.	0.	0.	0.	0.	0.
3	0.	0.	0.	0.	0.	0.
4	0.	0.	0.	0.	0.	0.
5	0.	0.	0.	0.	0.	0.
6	0.	0.	0.	0.	0.	0.
7	.21600E+05	0.	0.	0.	0.	0.
8	.21600E+05	0.	0.	0.	0.	0.

GAS PROD. MAP

	1	2	3	4	5	6
1	-.11732E+01	-.51711E+02	-.19754E+04	-.38425E+05	-.20517E+04	-.21469E+01
2	0.	0.	0.	0.	0.	0.
3	0.	0.	0.	0.	0.	0.
4	0.	0.	0.	0.	0.	0.
5	0.	0.	0.	0.	0.	0.
6	0.	0.	0.	0.	0.	0.
7	.19952E+04	0.	0.	0.	0.	0.
8	.25793E+04	0.	0.	0.	0.	0.

CASE 2

TIME STEP 243
CUMULATIVE TIME 6.320 DAYS
DELTA-T .100 DAYS

PRESSURE MAP

	1	2	3	4	5	6
1	.14030E+02	.14030E+02	.14030E+02	.14030E+02	.14030E+02	.14030E+02
2	.14326E+02	.14326E+02	.14344E+02	.14583E+02	.14616E+02	.14616E+02
3	.19697E+02	.19697E+02	.19720E+02	.20000E+02	.20034E+02	.20034E+02
4	.26176E+02	.26177E+02	.26211E+02	.26501E+02	.26537E+02	.26537E+02
5	.33705E+02	.33707E+02	.33779E+02	.34066E+02	.34123E+02	.34123E+02
6	.42204E+02	.42219E+02	.42420E+02	.42755E+02	.42793E+02	.42793E+02
7	.51724E+02	.52547E+02	.53215E+02	.53593E+02	.53632E+02	.53632E+02
8	.64575E+02	.65408E+02	.66193E+02	.66599E+02	.66636E+02	.66638E+02

POTENTIAL MAP

	1	2	3	4	5	6
1	.79056E+02	.79056E+02	.79057E+02	.79057E+02	.79057E+02	.79057E+02
2	.66349E+02	.66348E+02	.66366E+02	.66606E+02	.66638E+02	.66638E+02
3	.66300E+02	.66301E+02	.66324E+02	.66604E+02	.66638E+02	.66638E+02
4	.66277E+02	.66278E+02	.66313E+02	.66603E+02	.66638E+02	.66638E+02
5	.66220E+02	.66222E+02	.66294E+02	.66602E+02	.66638E+02	.66638E+02
6	.66049E+02	.66064E+02	.66265E+02	.66601E+02	.66638E+02	.66638E+02
7	.64730E+02	.65353E+02	.66222E+02	.66599E+02	.66638E+02	.66638E+02
8	.64575E+02	.65408E+02	.66193E+02	.66599E+02	.66638E+02	.66638E+02

OIL SAT. MAP

	1	2	3	4	5	6
1	.10000E+00	.10000E+00	.10000E+00	.10000E+00	.10000E+00	.10000E+00
2	.31965E+00	.32063E+00	.35645E+00	.84962E+00	.89992E+00	.90001E+00
3	.10000E+01	.10000E+01	.10000E+01	.10000E+01	.10000E+01	.10000E+01
4	.10000E+01	.10000E+01	.10000E+01	.10000E+01	.10000E+01	.10000E+01
5	.10000E+01	.10000E+01	.10000E+01	.10000E+01	.10000E+01	.10000E+01
6	.10000E+01	.10000E+01	.10000E+01	.10000E+01	.10000E+01	.10000E+01
7	.95000E+00	.10000E+01	.10000E+01	.10000E+01	.10000E+01	.10000E+01
8	.97109E+00	.99935E+00	.10000E+01	.10000E+01	.10000E+01	.10000E+01

GAS SAT. MAP

	1	2	3	4	5	6
1	.90000E+00	.90000E+00	.90000E+00	.90000E+00	.90000E+00	.90000E+00
2	.67965E+00	.67949E+00	.64369E+00	.15017E+00	.10008E+00	.99989E-01
3	0.	0.	0.	0.	0.	.11862E-09
4	0.	0.	0.	0.	0.	.48396E-09
5	0.	0.	0.	0.	0.	0.
6	0.	0.	0.	0.	0.	0.
7	.56003E-01	0.	0.	0.	0.	.26871E-09
8	.28892E-01	.65512E-03	0.	.81669E-06	.79595E-09	.23542E-11

OIL PROD. MAP

	1	2	3	4	5	6
1	0.	0.	0.	0.	0.	0.
2	0.	0.	0.	0.	0.	0.
3	0.	0.	0.	0.	0.	0.
4	0.	0.	0.	0.	0.	0.
5	0.	0.	0.	0.	0.	0.
6	0.	0.	0.	0.	0.	0.
7	.43200E+05	0.	0.	0.	0.	0.
8	.43200E+05	0.	0.	0.	0.	0.

GAS PROD. MAP

	1	2	3	4	5	6
1	-.33794E+01	-.14922E+03	-.57975E+04	-.70713E+05	-.89158E+06	-.18414E+02
2	0.	0.	0.	0.	0.	0.
3	0.	0.	0.	0.	0.	0.
4	0.	0.	0.	0.	0.	0.
5	0.	0.	0.	0.	0.	0.
6	0.	0.	0.	0.	0.	0.
7	.51697E+04	0.	0.	0.	0.	0.
8	.64161E+04	0.	0.	0.	0.	0.

APPENDIX E

LIST OF SYMBOLS

A	=	Cross sectional area of flow (FT^2)
B	=	Formation volume factor
b	=	$\frac{1}{B}$
c	=	Conversion factor: for units of psi, centipoise, milli-darcy, and feet, c = 0.00633
g	=	Acceleration due to gravity
h	=	elevation above reference plane (FEET)
k	=	Saturated permeability (intrinsic): md.
kr	=	Relative permeability
MROD	=	Mass rate of depletion
p	=	Pressure (psi)
p*	=	$p^{n+1} - p^k$
p_c	=	Capillary pressure
p_{nw}	=	Pressure in the non-wetting phase
p_w	=	Pressure in the wetting phase
Pcog	=	Capillary pressure between oil and gas phase
Pcow	=	Capillary pressure between oil and water phase
q	=	Flow rate (FT^3/DAY)
q_p	=	Flow rate, sink (+), or source (-)
r_o, r_g, r_w	=	Oil, gas and water residual terms
Rs	=	Solution gas-oil ratio
S	=	Fluid saturation
S*	=	$S^{n+1} - S^k$
V_b	=	Bulk volume of differential element
x_o	=	Center of mass of differential element in x-direction

APPENDIX E (continued)

LIST OF SYMBOLS

Subscript	A	=	Aquifer conditions
	i	=	Number of columns in grid system
	j	=	Number of rows in grid system
	g	=	Gas phase
	o	=	Oil phase
	w	=	Water phase
	U	=	Upstream
	E,W,N,S	=	East, West, North, South
Superscript	n	=	Present time level
	n+1	=	New time level
	k	=	k-th level of iteration
$\Delta x, \Delta y, \Delta z, \Delta r$		=	Finite spatial increments
Δt		=	Finite time increment
∇		=	Gradient
Δ		=	Difference operator (equation 23)
μ		=	Fluid viscosity (centipoise)
ρ		=	Fluid density
ϕ		=	Porosity
Φ		=	Potential
ℓn		=	Napierian logarithm